NEL/REPORT 1452

NEL/REPORT 1452

PROBLEM

Investigate theoretically the dynamic characteristics of underwater bodies towed at speeds of about 45 knots. Specifically:

1. Devise a general procedure for designing towed underwater bodies of optimum dynamic performance.
2. Present a practical design fulfilling the design requirements.
3. Design systems for automatic control of both longitudinal and lateral motion.

RESULTS

1. General guidelines for the design of an underwater towed body were derived from an analysis of the pertinent hydrodynamics.
2. A practical tow body was designed. For a speed of 45 knots, the maximum diameter is 30 inches and the main-body length/diameter ratio is 2.7.
3. The cable tie-point location has a great influence on the body's stability, and it should be forward and above the body's center of gravity.
4. The hydrodynamic coefficients can be predetermined by means of a mathematical model which can be checked on analog or digital computers.
5. Important parameters determining the dominant characteristic equation roots for longitudinal and lateral motion are the cable tension and the damping coefficients.
6. Tow bodies can be easily designed to have longitudinal and lateral dynamic stability.
7. Automatic control systems are desirable, and proposed systems are described herein. An automatic longitudinal system can hold the tow body at a commanded depth and improve the stability and damping. An automatic lateral system can improve the stability and damping, coordinate the rudder and ailerons, and provide a yaw-rate directional control.
8. The attainable depth and required horsepower depend primarily on the towing cable and on the body drag. Small-cross-section, laminar-type streamlined cables are required to achieve low drag and to prevent cavitation.

RECOMMENDATIONS

1. Consider the use of the body designated Body A'' in this report, as a practical tow body.
2. Use the design procedure outlined herein to design additional tow bodies.
3. Consider incorporation of the automatic control systems proposed in this report in tow body designs, and consider development of the necessary hardware.

ADMINISTRATIVE INFORMATION

This analysis was performed under Subproject S 46-06, Task 1723 (NEL J60172) by the author, a staff member of the Underseas Technology Department. The work was done during the period from September 1965 to December 1966. The report was approved for publication 17 April 1967.

CONTENTS

TABLES

ILLUSTRATIONS

INTRODUCTION

This report covers a study made to originate (1) a general design procedure for towed underwater bodies, and (2) a practical body and cable design. The body and cable should be such as to enable a high-speed surface craft to drag a specified load at a specified depth. If a sufficiently large horsepower were available at the surface craft, the load could be towed at the specified depth and speed by any stable cable of adequate length. In actual practice, it becomes necessary to optimize the cable and body design so that (1) the power requirements are minimum, (2) the system is stable so that the body stays down at the prescribed depth, and (3) the transient characteristics are satisfactory.

The cable design has to be closely related to the towed-body design. The cable influences the body dynamics, changing the motion modes from those of a self-propelled body; and the dynamics are also significantly dependent on the location at which the cable is attached to the body. Cable requirements are statistical and dynamic stability, minimum drag, no cavitation effects, low vibration, and low transmission of random energy such as noise.

The dynamics of the body control its stability and transient characteristics. The dynamics can be treated by application of Newton's second law of motion, since the acceleration of the body is resisted by hydrodynamic forces, body weight, buoyancy, and cable tension. The hydrodynamic forces can be defined in terms of hydrodynamic coefficients that depend on the shape and proportions of the body. These coefficients can be approximated for a given body, and thus be used to form the basis of a design procedure. The coefficients and the effect of varying them are examined in detail in this report.

One of the most critical design requirements is minimum drag. The ratio of the depression-force-needed-to-hold-the-body-down to the drag has to be made larger as the depth increases and as the towing horsepower decreases.

The maneuverability of the surface ship with its towed load probably is determined principally by the ship's characteristics. In this report we examine the desirability of automatic controls, and propose both longitudinal and lateral control systems. The longitudinal system tends to hold the towed body at commanded depths. The lateral system coordinates the rudder and ailerons and controls the yaw-rate orientation. These systems improve the stability and damping of the towed body.

Structural vibrations of the cable and body are mainly randomly excited. One major source of vibration is the turbulent boundary-layer energy around the body produced by its high-speed motion through the water. An elastic cable, and a compliant surface on the body, can act as filters and attenuate this random energy.

DYNAMICS ANALYSIS

The dynamical properties of the tow body can be explained by the six equations of motion that express Newton's second law. Three of these equations

equate applied force to the rate of change of linear momentum with time in the three space directions. The other three equations equate applied moment to the rate of change of angular momentum with time in the three space directions. Although these equations apply to a body moving with respect to fixed inertial coordinates, the mathematical solutions can be simplified by a transformation to a system of moving coordinates that are instantaneously related to the body. In such a system, the moments of inertia become independent of time. The relationship between time derivatives referred to fixed inertial axes and those referred to moving axes is given by the equation

$$\frac{dV}{dt}_{\text{fixed}} = \frac{dV}{dt}_{\text{moving}} + \omega X V_{\text{rotation}}$$

where V is a linear velocity
ω is an angular velocity

The moving axes consist of the Cartesian body axes instantaneously fixed in space according to instantaneous body position. The derivative term is position-fixed, and then the rotation term is orientation-fixed. The time derivative of the body velocity referred to the moving axes appears as two terms, one accounting for translation and the other for rotation. The equations of motion when written in the Eulerian moving-coordinate form are given by the matrix equations

$$\{F\} = m\left\{\frac{dV}{dt} + \omega X V\right\}$$

$$\{M\} = \left\{\frac{dH}{dt} + \omega X H\right\}$$

where F is the applied force column matrix
M is the applied moment column matrix
H is the moment-of-momentum matrix, $I\omega$
I is the moment-of-inertia matrix
ω is the angular velocity of the body

Six Eulerian coordinate transformations relate the space orientation of the moving-body set of axes to the orientation of the fixed inertial set of axes, through three angular rotations. For our purpose, the standard aircraft transformations of yawing, pitching, and rolling have been chosen (fig. 1). These transformations are given by the equation

$$\begin{Bmatrix} x \\ y \\ z \end{Bmatrix}_{(Body)} = \begin{bmatrix} \cos\theta\cos\Psi & \cos\theta\sin\Psi & -\sin\theta \\ \sin\varphi\sin\theta\cos\Psi - \cos\varphi\sin\Psi & \sin\varphi\sin\theta\sin\Psi + \cos\varphi\cos\Psi & \sin\varphi\cos\theta \\ \cos\varphi\sin\theta\cos\Psi + \sin\varphi\sin\Psi & \cos\varphi\sin\theta\sin\Psi - \sin\varphi\cos\Psi & \cos\varphi\cos\theta \end{bmatrix} \cdot \begin{Bmatrix} x' \\ y' \\ z' \end{Bmatrix}_{(Inertial)}$$

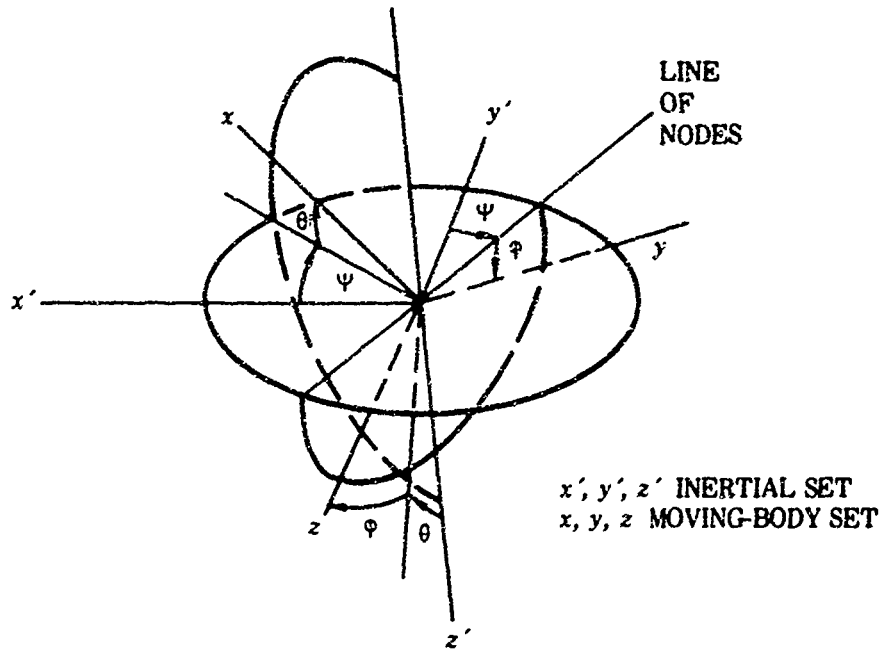

Figure 1. Coordinate transformation from inertial Cartesian set to moving-body Cartesian set.

where x, y, z are the moving-body set of coordinates
x', y', z' are the inertial set of coordinates
Ψ is the Eulerian angle through which the inertial set is yawed
θ is the Eulerian angle of pitch following yawing
φ is the Eulerian angle of roll following pitching

The vector angular velocity of the moving body is the sum of the Eulerian angular velocities. The yaw rate has components referred to the moving axes x, y, and z equal to $-\dot{\Psi}\sin\theta$, $\dot{\Psi}\cos\theta\sin\varphi$, and $\dot{\Psi}\cos\theta\cos\varphi$, respectively. The pitch rate has components referred to the y and z axes and equal to $\dot{\theta}\cos\varphi$ and $-\dot{\theta}\sin\varphi$, respectively. The roll rate occurs about the moving x-axis and has only an x component. Thus, the vector angular velocity ω has x, y, and z components designated p, q, and r, which are, respectively:

$$p = \dot{\varphi} - \dot{\Psi}\sin\theta$$

$$q = \dot{\theta}\cos + \dot{\Psi}\cos\theta\sin\varphi$$

$$r = \dot{\Psi}\cos\theta\cos\varphi - \dot{\theta}\sin\varphi$$

The geometry of a moving submerged body can be described by the use of the two sets of Cartesian axes. The inertial set is chosen so that the x- and z-axes are horizontal and the positive z-axis points downward. The moving-body set is chosen so that the positive x-axis points longitudinally toward the nose,

the positive y-axis to the right-hand side in the direction of motion, and the positive z-axis downward as in a right-handed set of Cartesian axes (fig. 1).

The six equations of motion can be separated into two sets of three equations each, one set defining the longitudinal motion and the other the lateral motion. Longitudinal motion consists of motion in the x-z plane and pitching about the y-axis without coupling energy into side motion, yawing motion, or rolling motion. Longitudinal motion is defined by the force equations in F_x and F_z, and the moment equation about the y-axis in M. The yaw and roll rates, and the side-slip velocity, are assumed to be zero. The lateral motion is defined by the side-force equation in F_y, and the yawing and rolling moment equations in N and L. The pitching moment about the y-axis is assumed to be zero. The longitudinal and lateral sets of equations are:

Longitudinal

$$\Sigma\Delta F_x = m(\dot{u} + wq)$$

$$\Sigma\Delta F_z = m(\dot{w} - U_0 q)$$

$$\Sigma\Delta M = I_{yy}\dot{q} = I_{yy}\ddot{\theta}$$

where $\Sigma\Delta F_x$ is the sum of the differential forces from the equilibrium condition in the x-axis direction

$\Sigma\Delta F_z$ is the sum of the differential forces from the equilibrium condition in the z-axis direction

m is the body mass

I_{yy} is the body moment of inertia about the y-y axis

u is the velocity change from the equilibrium condition in the x-axis direction

w is the velocity change from the equilibrium condition in the z-axis direction

U_0 is the equilibrium velocity in the x-axis direction

q is the angular velocity change from the equilibrium condition about the y-axis of the body, $\dot{\theta}$

$\Sigma\Delta M$ is the total differential of moments about the y-y axis

Lateral

$$\Sigma\Delta F_y = m(\dot{v} + U_0 r)$$

$$\Sigma\Delta L = \dot{p}I_{xx} - \dot{r}J_{xz}$$

$$\Sigma\Delta N = \dot{r}I_{zz} - \dot{p}J_{xz}$$

where $\Sigma\Delta F_y$ is the total differential of side forces from the equilibrium condition

$\Sigma\Delta L$ is the total differential of rolling moments from the equilibrium condition

$\Sigma\Delta N$ is the total differential of yawing moments from the equilibrium condition

p is the rolling angular-velocity change from equilibrium
r is the yawing angular-velocity change from equilibrium
I_{xx} is the moment of inertia about the x-x body axis
I_{zz} is the moment of inertia about the z-z body axis
J_{xz} is the product of inertia about the x and z body axes

The above equations have been written for small perturbations from the equilibrium condition of straight-line, constant-speed, level motion. The total differential of the forces and moments from the equilibrium condition balances the change in momenta from their steady-state condition (following the treatment used by Bryan and Williams in their 1904 aircraft stability analysis). The steady-state terms which balance one another across the sides of the equations have been eliminated.

Figure 2 shows the geometry of a cable-towed underwater body in longitudinal motion in the x-z plane. The cable tow point is above and ahead of the

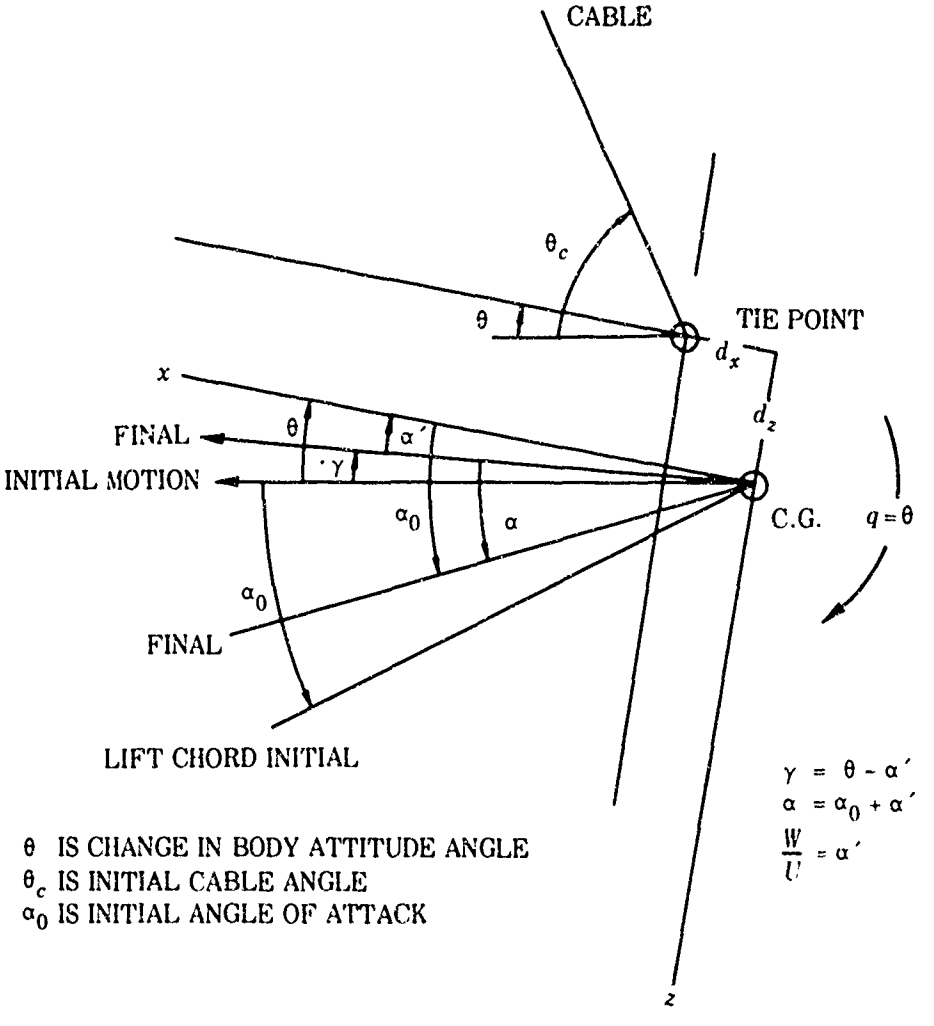

Figure 2. Motion in the x-z longitudinal plane

body's center of gravity. The equilibrium condition is taken to be horizontal motion. The body's center of gravity and center of buoyancy are assumed to be at the same point. The longitudinal equations of motion written in terms of the hydrodynamic force and moment differentials about the body's center of gravity become for the x component

$$\Sigma\Delta F_x = \frac{\partial F_x}{\partial u}u + \frac{\partial F_x}{\partial w}w + \frac{\partial F_x}{\partial \dot{w}}\dot{w} + \frac{\partial F_x}{\partial \theta}\theta + \frac{\partial F_x}{\partial \dot{\theta}}\dot{\theta} + F_{xa} = m(\dot{u} - wq)$$

where $\frac{\partial F_x}{\partial u}u$ is the force differential with forward velocity

F_{xa} is the other applied force due to the cable and the controls

$\frac{\partial F_x}{\partial w}w$ is the force differential with z-axis velocity

In the equation above, the total differential is the sum of force differentials due to forward and downward velocities, force differentials due to attitude angle and angular velocity, and force differentials due to the cable and tow-body control surface. Each term is in units of force. The terms are divided by a quantity with the dimensions of a force to make each term nondimensional. All the independent variables of the equation themselves are divided by a quantity of the same dimensions as those of the variable, and the derivative multiplier of the variable is multiplied by the same quantity. Thus, the equation can be expressed with nondimensional independent variables multiplied by nondimensional derivative multipliers:

$$\frac{U}{S\bar{q}}\frac{\partial F_x}{\partial u}\frac{u}{U} + \frac{U}{S\bar{q}}\frac{\partial F_x}{\partial w}\frac{w}{U} + \frac{U}{S\bar{q}}\frac{\partial F_x}{\partial \dot{w}}\frac{2U}{c}\frac{\dot{w}}{U}\frac{c}{2U} + \frac{1}{S\bar{q}}\frac{\partial F_x}{\partial \theta}\theta$$

$$+ \frac{1}{S\bar{q}}\frac{2U}{c}\frac{\partial F_x}{\partial \dot{\theta}}\dot{\theta}\frac{c}{2U} + \frac{F_{xa}}{S\bar{q}} = \frac{Um}{S\bar{q}}\left(\frac{\dot{u}}{U} - \frac{wq}{U}\right)$$

where $\frac{w}{U}$ is the change in angle of attack 'α

$\frac{u}{U}$ is the nondimensional forward velocity

S is the lift surface area

$\bar{q}$ is the dynamic pressure defined by $1/2\ \rho U^2$, ρ being the fluid mass per unit volume and U the forward velocity (the dimension of dynamic pressure is force per unit area)

c is a representative length, the lift surface chord

U is the disturbed forward velocity: the sum of the equilibrium velocity U_0, and the velocity variation u

The nondimensional independent variables can be written in a condensed form:

$$'u = \frac{u}{U} \qquad 'w = \frac{w}{U} \qquad 'q = \frac{qc}{U}$$

HYDRODYNAMIC COEFFICIENTS

The nondimensional derivative multipliers are known as stability derivatives or hydrodynamic coefficients for underwater bodies. They are written with a capital C, subscripts indicating the particular equation of motion and the particular independent variable. These coefficients are nearly constant over wide ranges of speeds. Their values depend on the lengths and areas used in defining them. Sometimes, the maximum cross-sectional area is used, but lengths raised to powers are usually employed with underwater bodies. The water mass density does not always feature in the definition. Here, the aircraft definition with lifting surface area and chord is adopted, because of the many experimental data available for airplanes. Coefficients for air and water agree in value, when defined by the same terms. The hydrodynamic coefficients for the x equation of longitudinal motion are as follows:

$$C_{xu} = \frac{U}{S\bar{q}} \frac{\partial F_x}{\partial u} \qquad C_{x\alpha} = \frac{U}{S\bar{q}} \frac{\partial F_x}{\partial w}$$

$$C_{x\dot{\alpha}} = \frac{U}{S\bar{q}} \frac{2U}{c} \frac{\partial F_x}{\partial \dot{w}} \qquad C_{xq} = \frac{1}{S\bar{q}} \frac{2U}{c} \frac{\partial F_x}{\partial \dot{\theta}}$$

Hydrodynamic coefficients can be ignored if they represent small differential force components that oppose the change in momentum. The hydrodynamic coefficient for the x component forward-velocity-derivative variations is small for streamlined bodies with a large enough length-to-diameter ratio. This coefficient is called the virtual mass effect and represents force due to the change in momentum of the displaced water mass.

The hydrodynamic coefficients can be estimated with reasonable accuracy, and they can be used as the basis of the design of an underwater towed body. Here, the nondimensional coefficients are given per radian angle, also a nondimensional quantity. The longitudinal coefficients whose magnitudes are large enough to affect the dynamics significantly are listed in table 1, along with their definitions, simplified formulas for evaluating them, and typical numerical values for aircraft:

TABLE 1. LONGITUDINAL HYDRODYNAMIC COEFFICIENTS

(Continued on page 13)

Coefficient	Definition	Formula	Aircraft Typical Value
C_{zu}	$\frac{U}{Sq}\frac{\partial F_z}{\partial u}$	$-2C_D - U\frac{\partial C_D}{\partial u}$	−0.05
$C_{x\alpha}$	$\frac{1}{Sq}\frac{\partial F_x}{\partial \alpha}$	$C_L - \frac{\partial C_D}{\partial \alpha}$	0.1
C_{zu}	$\frac{U}{Sq}\frac{\partial F_z}{\partial u}$	$-2C_L - U\frac{\partial C_L}{\partial u}$	−0.5
$C_{z\alpha}$	$\frac{1}{Sq}\frac{\partial F_z}{\partial \alpha}$	$-2C_D - \frac{\partial C_L}{\partial \alpha}$	−4.0
C_{zq}	$\frac{1}{Sq}2\frac{U}{c}\frac{\partial F_z}{\partial \dot{\theta}}$	$\Sigma K\frac{\partial C_m}{\partial \alpha_t} = 2\frac{\partial C_L}{\partial \alpha_t}\frac{\ell_t}{c}\frac{S_t}{S}\frac{q_t}{q}K$	−2.0
$C_{z\dot{\alpha}}$	$\frac{1}{Sq}2\frac{U}{c}\frac{\partial F_z}{\partial \dot{\alpha}}$	$2\frac{\partial C_m d\epsilon}{\partial \alpha_t d\alpha} = 2\frac{\partial C_L}{\partial \alpha_t}\frac{\ell_t}{c}\frac{S_t}{S}\frac{q_t}{q}\frac{d\epsilon}{d\alpha}$	−1.0
$C_{m\alpha}$	$\frac{1}{Sqc}\frac{\partial M}{\partial \alpha}$	$\Sigma M\left(\frac{dC_L}{d\alpha}\right) = \frac{\partial C_L x'}{\partial \alpha}$ $-\left(1-\frac{d\epsilon}{d\alpha}\right)\frac{\partial C_{Lt}}{\partial \alpha_t}\frac{\ell_t}{c}\frac{S_t}{S}\frac{q_t}{q}$	−0.3
$C_{m\dot{\alpha}}$	$\frac{1}{Sqc}\frac{2U}{c}\frac{\partial M}{\partial \dot{\alpha}}$	$2\frac{\partial C_m}{\partial \alpha_t}\frac{d\epsilon}{d\alpha}\frac{\ell_t}{c}$ $= 2\frac{\partial C_{Lt}}{\partial \alpha_t}\left(\frac{\ell_t}{c}\right)^2\frac{S_t}{S}\frac{q_t}{q}\frac{d\epsilon}{d\alpha}$	−3.0
C_{mq}	$\frac{1}{Sqc}\frac{2}{c}U\frac{\partial M}{\partial \dot{\theta}}$	$2K\frac{\partial C_m}{\partial \alpha_t}\frac{\ell_t}{c}$ $= 2K\frac{\partial C_{Lt}}{\partial \alpha_t}\left(\frac{\ell_t}{c}\right)^2\frac{S_t}{S}\frac{q_t}{q}$	−8.0
$C_{m\delta_e}$	$\frac{1}{Sqc}\frac{\partial M_a}{\partial \delta_e}$	$C_{m\alpha_t}\frac{d\alpha_t}{d\delta_e} = \frac{\partial C_{Lt}}{\partial \alpha_t}\frac{\ell_t}{c}\frac{S_t}{S}\frac{q_t}{q}\frac{d\alpha_t}{d\delta_e}$	0.8
$C_{z\delta_e}$	$\frac{1}{Sq}\frac{\partial F_{za}}{\partial \delta_e}$	$\frac{c}{\ell_t}C_{m\delta_e}$	0.3

TABLE 1. (Continued)

Symbols are as follows:

- S is the lift surface area
- K is a numerical factor that compensates for the remainder of the body, usually nearly equal to 1
- S_t is the horizontal tail area
- ℓ_t is the distance between the body's center of gravity and the quarter-chord of the tail area
- α_t is the tail surface angle of attack
- ϵ is the downwash angle at the tail*
- q is the dynamic pressure of free flow
- a is a subscript indicating the control surface

*The downwash effect can be computed from the equation

$$\frac{d\epsilon}{d\alpha} = \frac{2\partial C_L}{\pi e\, \partial\alpha\, AR}$$

where e is an efficiency factor
AR is the lifting-surface aspect ratio

The lateral hydrodynamic coefficients whose magnitudes are large enough to affect the dynamics significantly are listed in table 2, along with definitions, approximate formulas, and typical numerical values for aircraft:

TABLE 2. LATERAL HYDRODYNAMIC COEFFICIENTS
(Continued on page 14)

Coefficient	Definition	Formula	Aircraft Typical Value
$C_{\ell\beta}$	$\frac{1}{Sqb}\frac{\partial L}{\partial\beta}$	$\frac{2\Gamma\,\partial C_L y S_\Gamma}{57.3\,\partial\alpha\, bS}$	−0.05
$C_{\ell p}$	$\frac{1}{Sqb}\frac{2U}{b}\frac{\partial L}{\partial p}$	function of AR and wing shape	−0.5
$C_{\ell r}$	$\frac{1}{Sqb}\frac{2U}{b}\frac{\partial L}{\partial r}$	$\frac{C_L{}^w}{4}$	0.05
$C_{n\beta}$	$\frac{1}{Sqb}\frac{\partial N}{\partial\beta}$	$\frac{\partial C_N}{\partial\alpha_t}\frac{q_t}{q}\frac{S_{tv}}{S}\frac{\ell_{tv}}{b}$	0.1
C_{np}	$\frac{1}{Sqb}\frac{2U}{b}\frac{\partial N}{\partial p}$	$\frac{-C_L{}^w}{8}\left(1-\frac{d\epsilon}{d\alpha}\right)$	−0.01

TABLE 2. (Continued)

Coefficient	Definition	Formula	Aircraft Typical Value
C_{nr}	$\frac{1}{Sqb}\frac{2U}{b}\frac{\partial N}{\partial r}$	$\frac{-C_D{}^w}{4} - 2\eta\frac{S_{tv}}{S}\left(\frac{\ell_{tv}}{b}\right)^2\frac{\partial C_{L_{tv}}}{\partial\alpha}$	−0.1
$C_{y\beta}$	$\frac{1}{Sq}\frac{\partial F_y}{\partial\beta}$	$\frac{\partial C_N}{\partial\alpha_t}\frac{q_t}{q}\frac{S_{tv}}{S}$	−0.5
$C_{y\delta_r}$	$\frac{1}{Sq}\frac{\partial F_{ya}}{\partial\delta_r}$	$C_{y\beta}\frac{d\beta}{d\delta_r}$	0.2
$C_{n\delta_r}$	$\frac{1}{Sqb}\frac{\partial N_a}{\partial\delta_r}$	$C_{n\beta}\frac{d\beta}{d\delta_r}$	−0.1
$C_{\ell\delta_r}$	$\frac{1}{Sqb}\frac{\partial L_a}{\partial\delta_r}$	$\frac{C_L}{4}\frac{C_{n\delta_r}}{C_{nr}}$	0.01
$C_{\ell\delta_a}$	$\frac{1}{Sqb}\frac{\partial L_a}{\partial\delta_a}$	function of AR, aileron location, and chord ratio to wing chord	0.6
$C_{n\delta_a}$	$\frac{1}{Sqb}\frac{\partial N_a}{\partial\delta_a}$	$\frac{-C_L}{8}\frac{C_{\ell\delta_a}}{C_{\ell_p}}$	−0.015

Symbols are as follows:

- b is the lift surface span
- Γ is the dihedral angle in degrees
- y is the distance from body center along the wings to the center of pressure of each wing
- S_Γ is the area of a wing with a dihedral angle
- S_{tt} is the area of the vertical tail surface
- ℓ_{tv} is the moment arm from the vertical tail quarter-chord to the body's center of gravity
- C_N is the side force coefficient
- η is an efficiency factor
- F_{ya} is the side force due to the control surfaces
- N_a is the yawing moment due to the control surfaces
- L_a is the rolling moment due to the control surfaces
- δ_r is the rudder deflection; positive rudder causes positive yawing
- δ_a is the aileron deflection; a positive aileron deflection causes a positive rolling moment

Approximate equations for the lateral hydrodynamic coefficients can be formed from the approximate formulas given in table 2 if the values of the nearly constant quantities are taken as:

$$\frac{d\varepsilon}{d\alpha} \simeq 0.5,\ \eta = 1,\ \frac{q_t}{q} = 1,\ \frac{\partial C_N}{\partial \alpha_t} = 2,\ \frac{\partial C_{Lw}}{\partial \alpha} = 2$$

On the basis of these values, the lateral hydrodynamic coefficients become (approximately):

$$C_{\ell\beta} = \frac{-\Gamma}{57.3} \qquad C_{\ell p} = -0.5\ (AR = 5,\ \text{elliptic}) \qquad C_{\ell r} = \frac{C_L}{4}$$

$$C_{n\beta} = 2\frac{S_{tv}}{S}\frac{\ell_{tv}}{b} \qquad C_{np} = -\frac{C_L{}^{w}}{16} \qquad C_{nr} = -4\frac{S_{tv}}{S}\left(\frac{\ell_{tv}}{b}\right)^2$$

$$C_{y\beta} = 2\frac{S_{tv}}{S} \qquad C_{y\delta_r} = -0.5\,C_{y\beta} \qquad C_{n\delta_r} = -0.5\,C_{n\beta}$$

$$C_{\ell\delta_r} = \frac{C_L}{4}\frac{C_{n\delta_r}}{C_{nr}} \qquad C_{\ell\delta_a} = 0 \text{ to about } 0.6 \qquad C_{n\delta_a} = \frac{-C_L}{8}\frac{C_{\ell\delta_a}}{C_{\ell p}}$$

LONGITUDINAL EQUATIONS OF MOTION

The longitudinal equations are defined by the force equations in F_x and F_z, and the moment equation about the y-axis in M. The force equations are:

$$\Sigma\Delta F_x = m(\dot{u} + wq)$$

$$\Sigma\Delta F_z = m(\dot{w} - U_0 q)$$

For the towed underwater body, force differentials with the body attitude angle arise because of body weight and buoyancy and because of the tow cable. Figure 3 illustrates the resolution of the weight and the buoyancy forces in the body axes. The center of gravity (c.g.) and the center of buoyancy are assumed to be coincident. The x and z force components are then given by

$$F_{gx} = -(mg - B)\sin\theta$$

$$F_{gz} = (mg - B)\cos\theta$$

where mg is the body weight

B is the body buoyancy

The changes in these forces with attitude angle are given by the derivatives:

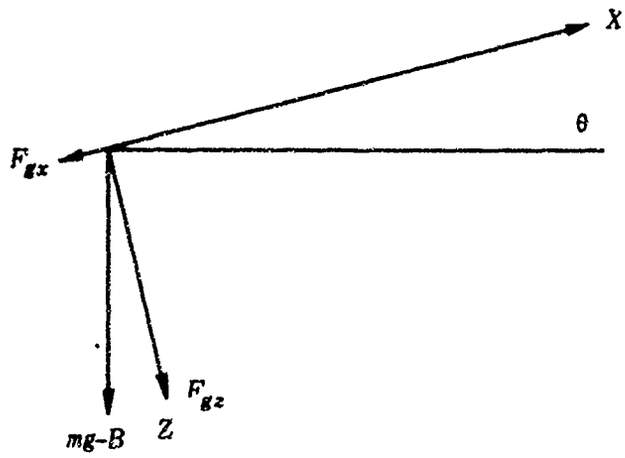

Figure 3. Weight and buoyancy resolution.

$$\frac{\partial F_{gx}}{\partial \theta} = -(mg - B)\cos\theta$$

$$\frac{\partial F_{gz}}{\partial \theta} = -(mg - B)\sin\theta$$

The tow cable produces differential forces in the x and z axes:

$$\Delta F_{xT} = T\cos\theta_c + T_0 \sin\theta_c\theta$$

$$\Delta F_{zT} = -T\sin\theta_c + T_0\cos\theta_c\theta$$

where T_0 is the undisturbed cable tension

T is the differential cable tension

θ_c is the undisturbed cable angle

θ is the change in attitude angle

A differential moment is produced about the y-y axis due to the changes in attitude angle and cable tension:

$$\Delta M = -T\cos\theta_c dz + T\sin\theta_c dx - T_0\sin\theta_c dz\theta - T_0\cos\theta_c dx\,\theta$$

where dx is the distance the tie point is ahead of the body's c.g.

dz is the distance the tie point is above the c.g.

The Laplace transformations of the small perturbation equations of motion can be written in terms of hydrodynamic coefficients that are the force and moment derivatives of changes in angle of attack, changes in attitude angle,

and changes in forward velocity. Their first-order time derivatives become for a cable-towed underwater body with elevator control:

x force equation

$$\left(\frac{mUs}{Sq} - C_{xu}\right)'u + \left(\frac{-c}{2U}C_{x\dot{\alpha}}s - C_{x\alpha}\right)'\alpha + \frac{W-B}{Sq}(\cos\theta)\theta + \left(\frac{c}{2U}C_{xq}s - \frac{T_0}{Sq}\sin\theta_c\right)\theta = \frac{T}{Sq}\cos\theta_c + \frac{1}{Sq}\frac{\partial F_{x\delta_e}}{\partial\delta_e}\delta_e$$

z force equation

$$-C_{zu}'u + \left(\left[\frac{mU}{Sq} - \frac{c}{2U}C_{z\dot{\alpha}}\right]s - C_{z\alpha}\right)'\alpha + \left(\left[\frac{-mU}{Sq} - \frac{c}{2U}C_{zq}\right]s - \frac{1}{Sq}T_0\cos\theta_c + \frac{1}{Sq}W-B\sin\theta\right)\theta = \frac{-T}{Sq}\sin\theta_c + \frac{1}{Sq}\frac{\partial F_{z\delta_e}}{\partial\delta_c}\delta_e$$

y moment equation

$$-C_{mu}'u\left(\frac{-c}{2U}C_{m\dot{\alpha}}s - C_{m\alpha}\right)'\alpha + \left(\frac{I_{yy}s^2}{Sqc} - \frac{c}{2U}C_{mq}s + \frac{T_0}{Sqc}\sin\theta_c dz + \frac{T_0}{Sqc}\cos\theta_c dx\right)\theta = \frac{1}{Sqc}\left(-T\cos\theta_c dz + T\sin\theta_c dx\right) + \frac{1}{Sqc}\frac{\partial M_{\delta_e}}{\partial\delta_e}\delta_e$$

These complete longitudinal equations of motion can be simplified if the variations with forward-velocity fluctuations are not significant, as may be the case in constant-velocity towing. The motion can then be described by the z force and the y moment equations, with $'\alpha$ and θ as the independent variables:

z force equation

$$\left(\frac{mU}{Sq} - \frac{c}{2U}C_{z\dot{\alpha}}\right)s - C_{z\alpha}'\alpha + \left[\left(\frac{-mU}{Sq} - \frac{c}{2U}C_{zq}\right)s - \frac{1}{Sq}T_0\cos\theta_c + \frac{1}{Sq}W-B\sin\theta_c\right]\theta = \frac{-T}{Sq}\sin\theta_c + \frac{1}{Sq}\frac{\partial F_{z\alpha_e}}{\partial\delta_e}\delta_e$$

y moment equation

$$\left(\frac{-c}{2U}\,C_{m\dot{\alpha}}s - C_{m\alpha}\right)\alpha + \left(\frac{I_{yy}}{Sqc}s^2 - \frac{c}{2U}\,C_{mq}s + \frac{T_0}{Sqc}\,\sin\theta_c dz + \frac{T_0}{Sqc}\,\cos\theta_c dx\right)\theta$$

$$= \frac{1}{Sqc}\left(-T\cos\theta_c dz + T\sin\theta_c dx\right) - \frac{1}{Sqc}\,\frac{\partial M_{\delta_e}}{\partial \delta_e}\,\delta_e$$

LONGITUDINAL EQUATIONS FOR SPECIFIC TOWED BODIES

For this report, three specific underwater bodies were quantitatively studied. A design parameter basic to all three bodies is a 30-inch maximum-diameter cross section Below we detail the analysis of a body designated Body A (fig. 4), using both the complete longitudinal equations and the short equations (for insignificant forward-velocity fluctuations). For the analysis, the body is assumed to be towed at 45 knots in a straight-line, level path. The numerical parameters for Body A are:

U = 76 ft/sec	S = 6 ft^2	m = 60 slugs
I_{yy} = 400 slug-ft^2	T_0 = 14,000 lb	ℓ_t = 6 ft
x' = 6.8 inches	dz = 1.167 ft	dx = 0.167 ft
S_t = 2 ft^2	θ_c = 81.85 degrees	W-B = 500 lb
$\bar{q}$ = 5776 lb/ft^2		

The hydrodynamic coefficients for longitudinal motion can be obtained from the approximate formulas given in this report. Based on the body parameters, the coefficients become:

$C_{xu} = -C_D = -0.12$

$C_{z\alpha} = -\dfrac{\partial C_L}{\partial \alpha} = -4.0$

$C_{z\dot{\alpha}} = -3\dfrac{\ell_t}{c}\dfrac{S_t}{S} = -6.0$

$C_{zq} = -6\dfrac{\ell_t}{c}\dfrac{S_t}{S} = -12.0$

$C_{m\alpha} = 4\dfrac{x'}{c} - 1.5\dfrac{\ell_t}{c}\dfrac{S_t}{S} = -0.7333$

$C_{m\dot{\alpha}} = -3\left(\dfrac{\ell_t}{c}\right)^2\dfrac{S_t}{S} = -36.0$

$C_{mq} = -6\left(\dfrac{\ell_t}{c}\right)^2\dfrac{S_t}{S} = -72.0$

$C_{m\delta_e} = -1.5\dfrac{\ell_t}{c}\dfrac{S_t}{S} = -3.0$

$C_{z\delta_e} = \dfrac{c}{\ell_t}\,C_{m\delta_e} = -0.5$

$C_{xq} = C_L = -0.4$

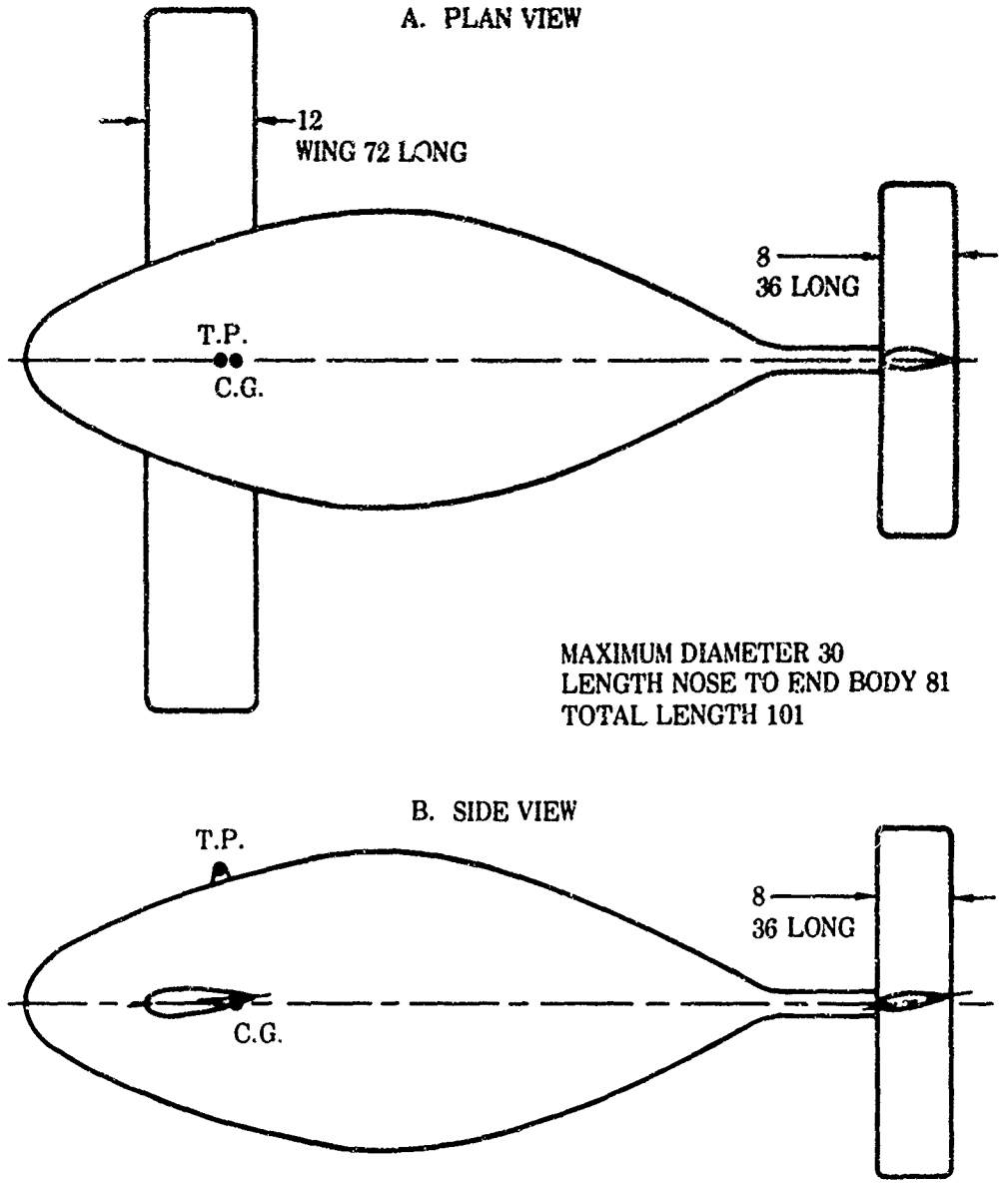

WING SECTIONS MODIFIED NACA FOUR DIGIT
0020-65
5 INDICATES MAXIMUM AT 0.5 CHORD
6 INDICATES LEADING EDGE RADIUS
00 INDICATES SYMMETRY
20 INDICATES THICKNESS 0.2 CHORD

MAIN BODY DTMB
(LANDWEBER-GERTLER) FORM

$C_p = 0.55 \quad m = \frac{X_m}{\ell} = 0.5 \quad \frac{\ell}{d} = 2.7$

$r_0 = \frac{R_0 \ell}{d^2} = 0.45 \quad r_1 = \frac{R_1 \ell}{d^2} = 0.18$

Figure 4. Form of Bodies A, A′, and A″ (dimensions in inches).

and x' is the distance by which the lift-surface quarter-chord is ahead of the c.g.

q_t is the dynamic pressure at the tail

δ_e is the angle of deflection of the elevator (taken positive for downward deflections)

SM is the static margin (or the chord ratio) by which the c.g. is ahead of the neutral point

Approximate design equations can be derived by using values near the following for some of the quantities that do not vary greatly from design to design:

$$\frac{d\epsilon}{d\alpha} = 0.5,\ K = 1.0,\ \frac{d\alpha_t}{d\delta_e} = 0.5,\ \frac{q_t}{q} = 1.0,\ \frac{\partial C_L}{\partial \alpha_t} = 3.0,\ \frac{\partial C_L}{\partial \alpha} = 4.0$$

Based on the preceding approximations, the longitudinal hydrodynamic coefficients become:

$$C_{zq} = -6\,\frac{\ell_t}{c}\,\frac{S_t}{S} \qquad C_{z\dot{\alpha}} = -3\,\frac{\ell_t}{c}\,\frac{S_t}{S} \qquad C_{xu} = -2\,C_D$$

$$C_{mq} = -6\left(\frac{\ell_t}{c}\right)^2\frac{S_t}{S} \qquad C_{m\dot{\alpha}} = -3\left(\frac{\ell_t}{c}\right)^2\frac{S_t}{S} \qquad C_{x\alpha} = C_L$$

$$C_{m\alpha} = 4\,\frac{x'}{c} - 1.5\,\frac{\ell_t}{c}\,\frac{S_t}{S} \qquad C_{z\alpha} = -\frac{\partial C_L}{\partial \alpha}$$

$$C_{z\delta_e} = \frac{c}{\ell_t}\,C_{m\delta_e} \qquad C_{m\delta_e} = -1.5\,\frac{\ell_t}{c}\,\frac{S_t}{S} \qquad C_{zu} = -2\,C_L$$

Thus, most of the longitudinal hydrodynamic coefficients are functions of the moment arm from the quarter-chord of the horizontal tail area to the body's center of gravity and of the ratio of the size of the horizontal tail area to the lifting-surface area. The magnitudes of the approximate coefficients agree fairly well with measured values. The approximate design formulas are based on assumed values such as 0.5 for the slope of the downwash angle with angle of attack, $d\epsilon/d\alpha$. This value can be diminished by raising the tail.

Below are given the complete longitudinal equations of motion for Body A, with numerical values of the coefficients inserted:

$$(0.13158s - 0.12)\,'u + \qquad (0.4)\,'\alpha + \qquad (-0.29405)\theta$$
$$= 4.0830 \times 10^{-6}\,T$$
$$(-0.8)\,'u + (0.17105s + 4.000)\,'\alpha + \qquad (-0.05263s - 0.057162)\,\theta$$
$$= -2.8564 \times 10^{-5}\,T \quad -0.5\,\delta_e$$

$$(0)\ 'u + (0.23684s + 0.73333)\ '\alpha + (0.011542s^2 + 0.47368s + 0.36943)\theta$$

$$= -3\delta_e$$

The solution of these equations of motion for the homogeneous case of no right-hand applied terms gives transients of the same exponential form for all of the independent variables $'\alpha$, u, and θ:

$$u = Ae^{s_1 t} + Be^{s_2 t} + Ce^{s_3 t} + De^{s_4 t}$$

where A, B, C, D are constants.

The quantities s_1, s_2, s_3, s_4 are the roots of the characteristic equation, which is the polynomial equation in s obtained from the determinant of the coefficients of the independent variables of the homogeneous simultaneous equations. The value of the determinant is zero if the transient solution is to exist. The roots of the characteristic equation must be negative or have negative real parts for the transient solution to be stable. Stability can be indicated by the Routh Hurwitz method without solving for the roots. Solution for the roots directly indicates the stability of the solution. Graeffe's method is an accurate and straightforward means of solving polynomial equations. It is based on raising the polynomial to higher powers so that the roots separate.

The characteristic equation for the complete longitudinal equations of motion for Body A is a quartic:

$$s^4 + 71.649\ s^3 + 1096.8\ s^2 + 2496.2\ s + 1821.1 = 0$$

The roots of this equation obtained by Graeffe's method are a pair of negative real roots and a pair of complex roots with negative real parts:

$$s_1 = -51.14$$

$$s_2 = -17.96$$

$$s_3 = -1.28 - j0.63$$

$$s_4 = -1.28 + j0.63$$

The complex roots represent a damped sinusoid. The complex pair can be written as a quadratic equation in terms of the natural frequency, ω_n, and the damping ratio, ζ:

$$s^2 + 2\zeta\omega_n s + \omega_n^2 = 0$$

For Body A, the natural frequency, ω_n, is 1.408 radians per second and the damping ratio, ζ, is 0.9055. The complex terms damp to half-amplitude in the time

$$T = \frac{0.693}{\zeta\omega_n} \text{ seconds}$$

The real root transient terms represent pure exponentials and damp to half-amplitude in the following time:

$$T = \frac{0.693}{\text{root value}} \text{ seconds}$$

The time to damp to half-magnitude for the complete longitudinal equations for Body A is determined by the smallest of the two real root times (0.0136 and 0.0386 second) and the complex root time (0.544 second).

The short solution of the longitudinal equations ignores the u velocity fluctuations and is determined by the z force equation and the y moment equation. The characteristic equation is a cubic and becomes, for Body A,

$$s^3 + 70.738\, s^2 + 1018.12\, s + 769.728 = 0$$

The roots of the cubic, obtained by Graeffe's method, are

$$s_1 = -51.18$$

$$s_2 = -18.82$$

$$s_3 = -0.80$$

The transient solution is again stable but consists of three pure exponential terms. The time to damp to half-amplitude for the three roots becomes 0.0135, 0.0368, and 0.866 second. The values of the first two are nearly those of the two large roots of the complete solution. These two are related to the short period times of aircraft. The third root, resulting from the cable, is the dominant one and determines the body damping. A study of the characteristic equation of the short solution shows that the dominant or smallest root is approximately given by

$$s = \frac{\left[\frac{T_0}{Sqc} \sin \theta_c dz + \frac{T_0}{Sqc} \cos \theta_c dx\right]}{\frac{c}{2U} C_{mq}}$$

The dominant cable root can be increased (damping time reduced) by increasing the cable tension (depression force). The cable tie point should be in the same direction as the depression force-drag ratio of the body. The tow point should be ahead and above the center of gravity of the body. The pitch-damping hydrodynamic coefficient should not be too large. Increasing the tail length increases the damping time of the dominant root.

For Body A, the time to damp to half-amplitude is larger with the short solution than with the complete solution. Introducing the x equation of motion makes a complex root of the dominant short-solution root. An approximate value of the time to damp to half-amplitude can be obtained from

$$\frac{0.693 \times 2 \times mU\, C_{za} C_{mq} c}{Sq \qquad 2U}$$

$$\frac{mU}{Sq} C_{za}\left(\frac{T_0}{Sqc}\sin\theta_c dz + \frac{T_0}{Sqc}\cos\theta_c dx\right) + C_{zu}C_{za}\frac{c}{2U}C_{mq} + C_{xa}C_{zu}\frac{c}{2U}C_{mq}$$

This formula agrees with the short-solution approximation in that it shows the desirability of decreasing the pitch-damping hydrodynamic coefficient and increasing the depression force in order to decrease the time to damp to half-amplitude. The damping time is also decreased by increasing the drag and lift coefficients of the body.

LAPLACE TRANSFORMS OF LONGITUDINAL EQUATIONS

The Laplace transform equations of motion under applied forces are simultaneous linear algebraic equations that can be expressed in terms of the independent variables by matrix inversion. They can be algebraically solved by Cramer's rule:

$$\left|i\right| = \frac{[C]^T}{|c|}\left|f\right|$$

where $\{i\}$ is the column matrix of the independent variables (u, 'α, θ)

$[C]^T$ is the transpose of the matrix of cofactors of the hydrodynamic coefficients

$|c|$ is the determinant of the hydrodynamic coefficients

$\{f\}$ is the column matrix of the applied forces

Transfer functions are the ratios between the independent variables and the applied-force variables obtained from the simultaneous transform equations. These s-plane variations of the independent variables 'u, 'α, and θ with changes in the elevator angle and the cable tension are given for Body A by the following equations:

$$\frac{'\alpha}{\delta_e} = \frac{-9.0676 \times 10^{-2}\left[\frac{s}{67.48}+1\right]\left[\frac{s}{1.00}+1\right]\left[\frac{s}{0.84}+1\right]}{\left[\frac{s}{51.14}+1\right]\left[\frac{s}{17.96}+1\right]\left[\frac{s^2}{1.9833}+1.286\,s+1\right]}$$

$$\frac{'\alpha}{T} = \frac{-1.2639 \times 10^{-7}\left[\frac{s}{40.25}+1\right]\left[\frac{s}{0.80}+1\right]\left[\frac{s}{0.04}+1\right]}{\left[\frac{s}{51.14}+1\right]\left[\frac{s}{17.96}+1\right]\left[\frac{s^2}{1.9833}+1.286\,s+1\right]}$$

$$\frac{'u}{T} = \frac{3.5055 \times 10^{-5}\left[\frac{s}{47.75} + 1\right]\left[\frac{s}{38.49} + 1\right]\left[\frac{s}{1.12} + 1\right]}{\left[\frac{s}{51.14} + 1\right]\left[\frac{s}{17.96} + 1\right]\left[\frac{s^2}{1.9833} + 1.286\,s + 1\right]}$$

$$\frac{\theta}{\delta_e} = \frac{-4.9980\left[\frac{s}{28.81} + 1\right]\left[\frac{s}{1.575} + 1\right]}{\left[\frac{s}{51.14} + 1\right]\left[\frac{s}{17.96} + 1\right]\left[\frac{s^2}{1.9833} + 1.286\,s + 1\right]}$$

$$\frac{\theta}{T} = \frac{2.5089 \times 10^{-5}\left[\frac{s}{3.096} + 1\right]\left[\frac{s}{0.043} + 1\right]}{\left[\frac{s}{51.14} + 1\right]\left[\frac{s}{17.96} + 1\right]\left[\frac{s^2}{1.9833} + 1.286\,s + 1\right]}$$

$$\frac{'u}{\delta_e} = \frac{5.5738\left[\frac{s}{44.30} + 1\right]\left[\frac{s}{25.69} - 1\right]}{\left[\frac{s}{51.14} + 1\right]\left[\frac{s}{17.96} + 1\right]\left[\frac{s^2}{1.9833} + 1.286\,s + 1\right]}$$

In the transfer functions above, the tension change T is in pounds, the velocity fluctuation u is nondimensional, and the angles are in radians. The Body A transfer functions for the complete longitudinal equations are shown in Appendix A, and those for Body A' (with the opposite dihedral angle) are shown in Appendix B.

The short-solution transfer functions for Body A are also shown in Appendix A. The s-plane variations according to the short solutions are:

$$\frac{'\alpha}{\delta_e} = \frac{-0.23440\left[\frac{s}{67.43} + 1\right]\left[\frac{s}{0.916} + 1\right]}{\left[\frac{s}{51.18} + 1\right]\left[\frac{s}{18.82} + 1\right]\left[\frac{s}{0.80} + 1\right]}$$

$$\frac{'\alpha}{T} = \frac{-0.69440 \times 10^{-5}\left[\frac{s}{40.24} + 1\right]\left[\frac{s}{0.796} + 1\right]}{\left[\frac{s}{51.18} + 1\right]\left[\frac{s}{18.82} + 1\right]\left[\frac{s}{0.80} + 1\right]}$$

$$\frac{\theta}{\delta_e} = \frac{-7.6558\left[\frac{s}{29.47} + 1\right]}{\left[\frac{s}{51.18} + 1\right]\left[\frac{s}{18.82} + 1\right]\left[\frac{s}{0.80} + 1\right]}$$

$$\frac{\theta}{T} = \frac{-1.3784 \times 10^{-5}\left[\frac{s}{3.096} + 1\right]}{\left[\frac{s}{51.18} + 1\right]\left[\frac{s}{18.82} + 1\right]\left[\frac{s}{0.80} + 1\right]}$$

Examination of the complete-solution and the short-solution transfer functions indicates that there are two basic types for each solution:

Complete Solution

$$\frac{s^2 + a_1 s + a_0}{(s+\gamma)(s+\delta)\left[(s+\alpha)^2 + \beta^2\right]}$$

$$\frac{s^3 + a_2 s + a_1 s + a_0}{(s+\gamma)(s+\delta)\left[(s+\alpha)^2 + \beta^2\right]}$$

Short Solution

$$\frac{s + a_0}{(s+\gamma)(s+\delta)(s+\lambda)}$$

$$\frac{s^2 + a_1 s + a_0}{(s+\gamma)(s+\delta)(s+\lambda)}$$

The Laplace transform of the independent variables is equal to the product of the transfer function and the transform of the applied force. Since the transforms of the impulse functions equal constants, the transforms of the independent variables are of the same form as the transfer funct s for impulse-type applied forces. For unit-step-function applied forces, the transforms of the independent variables become the product of the transfer functions and the transform of the unit step, 1 s.

The time solution of the independent variables can be obtained by using Laplace transform pairs. For the short solution, the angle-of-attack and the attitude-angle variations with either elevator angle or cable tension impulse force are of the form

$$Ae^{-\gamma t} + Be^{-\delta t} + Ce^{-\lambda t}$$

where A, B, C are constants depending on the transfer function constants

γ, δ, λ are constants (roots of the characteristic equation)

The solution consists of three transient terms that decay to zero at rates determined by the roots of the characteristic equation. The time-solution form

depends primarily on the denominator of the transforms, the numerator (which is at least one order smaller than the denominator) only influencing the constants *A, B,* and *C*. The time solution for a step-function applied force is still of the same form but adds a constant term. The steady-state response is zero for impulses and constant for step functions as can also be seen from the equation for the steady-state response:

$$f(t) = sF(s)f(s)$$
$$t \to \infty \quad s \to 0$$

where $F(s)$ is the transfer function

$f(s)$ is the transform of the applied force

The above equation is zero for impulse functions and constant for step-function applied forces.

For the complete longitudinal equations, the time solutions for the independent variables (u, 'α , and θ) for impulse applied forces are of the form

$$Ae^{-\gamma t} + Be^{-\delta t} + Ce^{-\alpha t} \cos(\beta t + \varphi)$$

where *A, B, C* are constants depending on transfer function constants

φ is a constant

α is the damping term in the complex root, $\zeta\omega_n$

β is the natural frequency term in the complex roots

γ, δ are roots of the characteristic equation

The solution for impulse forces consists of damped exponentials and a damped sinusoid. The solution for step-function forces is of the same form but adds a constant term. The steady-state response is zero for impulses and constant for step-function inputs. Thus, the towed body's longitudinal response to impulses consists of transients that decay to zero while the body follows step-function amplitudes.

LATERAL EQUATIONS OF MOTION

The lateral small perturbation equations of motion can be written in terms of the three independent angle variables of side slip, yaw, and roll:

$$\Sigma\Delta F_y = mU_0(\dot{\beta} + \dot{\Psi}) \qquad (y \text{ force equation})$$
$$\Sigma\Delta L = \ddot{\varphi}I_{xx} - \ddot{\Psi}I_{xz} \qquad (x \text{ moment equation})$$
$$\Sigma\Delta N = \ddot{\Psi}I_{zz} - \ddot{\varphi}I_{xz} \qquad (y \text{ moment equation})$$

$$\text{with } \dot{U} = \dot{\beta}U_0 \quad \text{and} \quad U = U_0$$

where v is the side-slip velocity

U_0 is the undisturbed velocity

U is the disturbed velocity along the x-x axis

β is the angle of side slip

I_{xx} is the moment of inertia about the x-x axis

I_{zz} is the moment of inertia about the z-z axis

I_{xz} is the product of inertia about the x and z axes

Control forces and moments caused by both ailerons and a rudder are assumed. The aileron control is assumed to be a differential system, the motion of the aileron on the right wing opposing that on the left wing. The aileron deflection, δ_a, is one-half the sum of the motion of the up and down ailerons. Positive rudder and aileron deflections cause positive yawing and rolling moments. The significant hydrodynamic forces and moments are functions of the independent angle variables and their first derivatives. The body weight and buoyancy, and the cable tension, produce differential forces and moments due to the changes in angles of roll and yaw. These become hydrodynamic coefficients when they are made nondimensional:

$$\Delta F_{y_{W\text{-}B}} = (mg - B)\varphi$$

$$\Delta F_{y_T} = (-T_0 \sin\theta_c)\varphi$$

$$\Delta F_{y_T} = (-T_0 \cos\theta_c)\Psi$$

$$\Delta L_T = (-T_0 \sin\theta_c dz)\varphi$$

$$\Delta N_T = (-T_0 \cos\theta_c dx)\Psi$$

Figures 5 and 6 show the geometry.

With hydrodynamic coefficients C_{yp}, C_{yr}, and C_{ya} assumed zero, the Laplace transforms of the equations of motion written in terms of the hydrodynamic coefficients and the control forces and moments become:

y Force

$$\left[\frac{-W - B}{Sq} + \frac{T_0 \sin\theta_c}{Sq}\right]\varphi + \left[\frac{mU}{Sq}s + \frac{T_0 \cos\theta_c}{Sq}\right]\Psi + \left[\frac{mU}{Sq}s - C_{y\beta}\right]\beta$$

$$= C_{y\delta_r}\delta_r$$

x Moment

$$\left[\frac{I_{xx}}{Sqb}s^2 - \frac{b}{2U}C_{\ell_p}s + \frac{T_0 \sin\theta_c dz}{Sqb}\right]\varphi + \left[\frac{-I_{xz}}{Sqb}s^2 - \frac{b}{2U}C_{\ell_r}s\right]\Psi - C_{\ell\beta}\beta = C_{\ell\delta_a}\delta_a + C_{\ell\delta_r}\delta_r$$

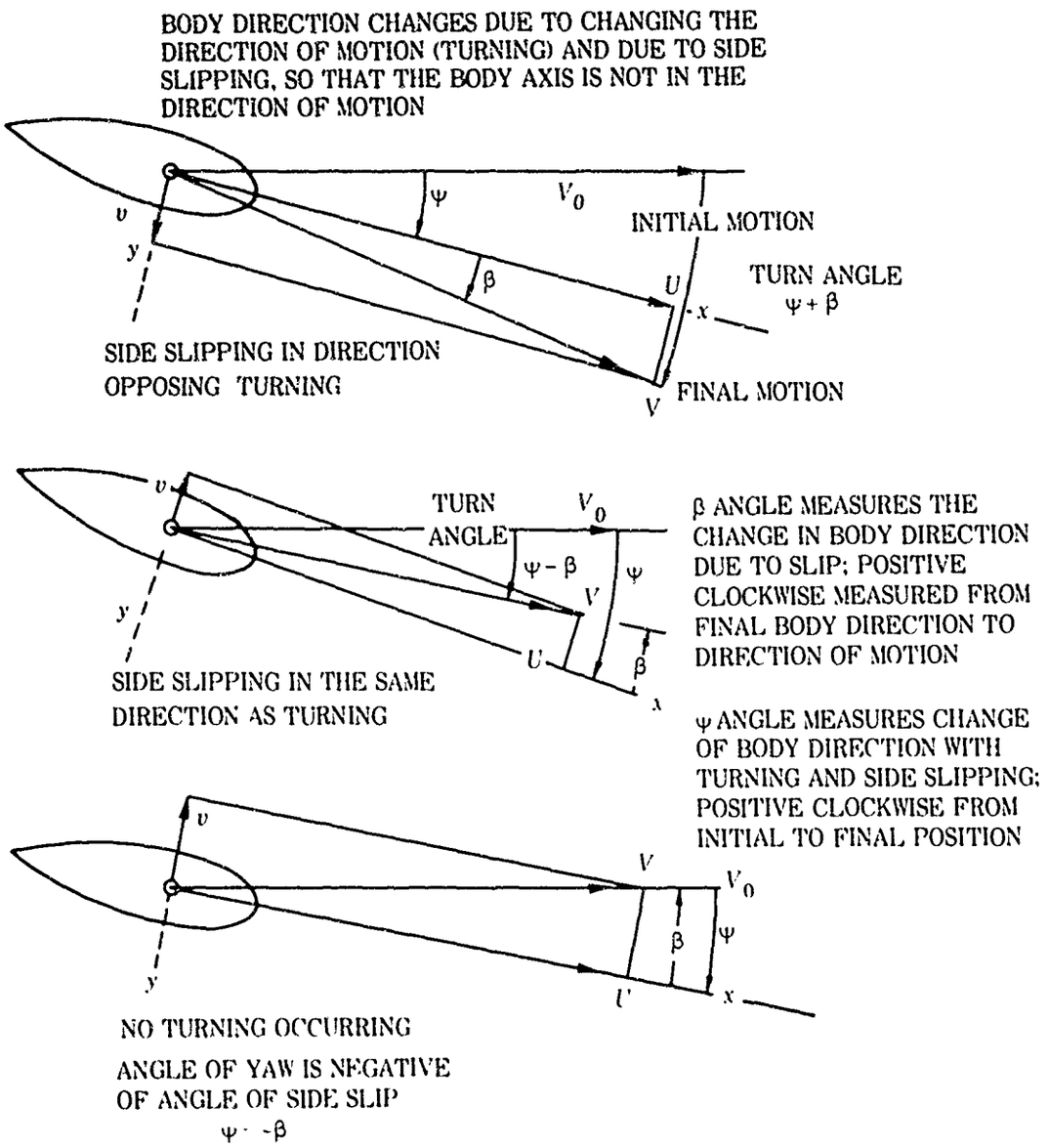

Figure 5. Motion in the x-y lateral plane

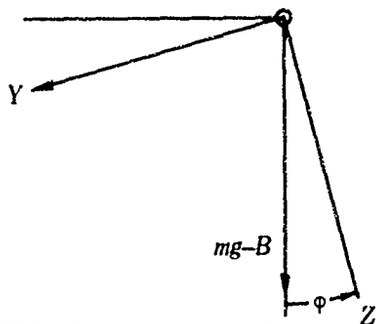

GRAVITY FORCE DUE TO ROLL

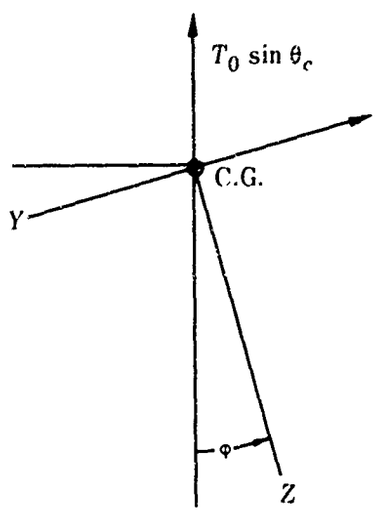

TENSION FORCE DUE TO ROLL

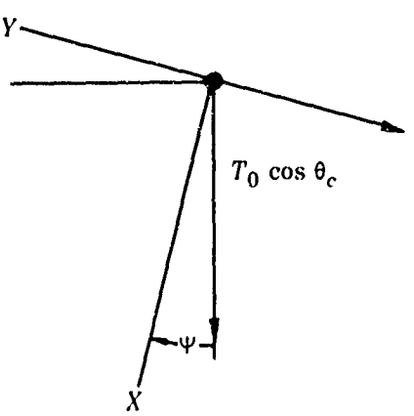

CABLE TENSION DUE TO YAW

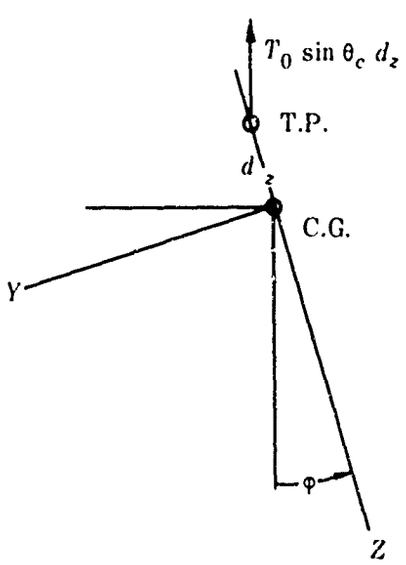

CABLE MOMENT DUE TO ROLL

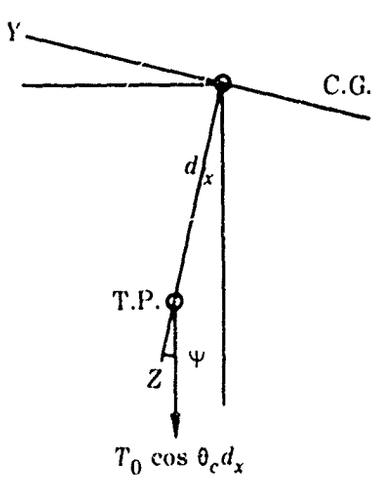

CABLE MOMENT DUE TO YAW

Figure 6. Lateral forces and moments due to roll and yaw

z Moment

$$\left[\frac{-I_{xz}}{Sqb}s^2 - \frac{b}{2U}C_{np}s\right]\varphi + \left[\frac{I_{zz}}{Sqb}s^2 - \frac{b}{2U}C_{nr}s + \frac{T_0\cos\theta_c dx}{Sqb}\right]\Psi - C_{n\beta}\beta = C_{n\delta_a}\delta_a + C_{n\delta_r}\delta_r$$

LATERAL EQUATIONS FOR SPECIFIC TOWED BODIES

The numerical analysis of the lateral equations of motion is detailed below for Body A, assuming that the body is towed at 45 knots in a straight, level path. The numerical parameters of Body A are:

U = 76 ft/sec	S = 6 ft^2	m	= 60 slugs
I_{zz} = 400 slug-ft^2	T_0 = 14,000 lb	ℓ_{tv}	= 6 ft
I_{xx} = 45 slug-ft^2	dz = 1.167 ft	dx	= 0.167 ft
I_{xz} = −100 slug-ft^2	c = 81.85 degrees	W-B	= 500 lb
S_{tv} = 1.5 ft^2	q = 5776 lb/ft^2	b	= 6 ft

Based on these parameters, the hydrodynamic coefficients are:

$C_{\ell\beta} = \frac{\Gamma}{57.3}$	= −0.0524	$C_{nr} = -4\frac{S_{tv}}{S}\left(\frac{\ell_{tv}}{b}\right)^2$	= −1.0
$C_{\ell p}$ = f (AR, Shape)	= −0.5	$C_{\ell r} = \frac{C_L}{4}$	= −0.1
$C_{n\beta} = 2\frac{S_{tv}}{S}\frac{\ell_{tv}}{b}$	= 0.5	$C_{\ell\delta_r} = \frac{C_L}{4}\frac{C_{n\delta_r}}{C_{nr}}$	= −0.025
$C_{np} = -\frac{C_L}{16}$	= 0.025	$C_{n\delta_r} = 0.5\,C_{n\beta}$	= −0.25
$C_{y\beta} = 2\frac{S_{tv}}{S}$	= −0.5	$C_{n\delta_a} = \frac{-C_L}{8}\frac{C_{\ell\delta_a}}{C_{\ell p}}$	= −0.06
$C_{y\delta_r} = 0.5\,C_{y\beta}$	= 0.25	$C_{\ell\delta_a} =$	= 0.6

The lateral equations of motion for Body A with the numerical values of the coefficients inserted are as follows:

y Force

$$0.29405\varphi + (0.13158s + 0.057162)\Psi + (0.13158s + 0.5)\beta = 0.25\delta_r$$

x Moment

$$(0.00021641s^2 + 0.019737s + 0.077781)\varphi + (0.00048092s^2 + 0.0039474s)\Psi + 0.0524\beta = -0.025\delta_r + 0.6\delta_a$$

z Moment

$$(0.00048092s^2 + 0.00098684s)\varphi + (0.0019237s^2 + 0.039474s + 0.0015910)\Psi - 0.5\beta = -0.25\delta_r - 0.06\delta_a$$

The solution of the homogeneous equations with no applied right-hand forces gives transient exponentials and a damped sinusoidal term for each of the independent variables φ, Ψ, and β. The roots of the characteristic equation obtained from the nonzero determinant of the multipliers of the independent variables determine the exponential constants of the transients. The towed-body characteristic equation is a quintic. Typical airplane characteristic equations differ from those of the towed body in that they contain no constant term. The zero root indicates that the plane is insensitive to the choice of heading, there being no moment tending to return it to the original heading. The towed body's path is determined by the cable. The characteristic equation for Body A is

$$s^5 + 247.48\,s^4 + 6689.3\ s^3 + 85{,}111\ s^2 + 246{,}333\ s + 92{,}743 = 0$$

Solution of this quintic characteristic equation by Graeffe's method indicates stability, since there are three negative real roots and a pair of complex conjugate roots with negative real parts. The roots for Body A are:

$$s_1 = -0.442$$
$$s_2 = -3.34$$
$$s_3 = -13.04 + j\,10.867$$
$$s_4 = -13.04 - j\,10.867$$
$$s_5 = -217.63$$

The transient solution for lateral motion is given for each independent variable by an equation of the form:

$$\varphi = Ae^{-0.442t} + Be^{-3.34t} + Ce^{-217.63t} + De^{-13.04t}\cos 16.97t$$

The times to damp to half-amplitude for each of the terms are 1.57, 0.2075, 0.0531, and 0.00318 seconds. The two small roots dominate the damping of the transients. Examination of the equations of motion shows that the largest damping time (smallest root) is approximated by

$$\tau = 0.693 \quad \frac{C_{y\beta}\frac{b}{2U}C_{nr} + C_{n\beta}\frac{mU}{Sq}}{\frac{T_0}{Sq}\cos\theta_c C_{n\beta}} = \frac{\frac{b^2}{2U\ell_{tv}}C_{nr} + \frac{mU}{Sq}}{\frac{T_0}{Sq}\cos\theta_c}$$

The time to damp to half-amplitude is decreased for the smallest root by increasing the cable tension and decreasing the yaw damping coefficient, C_{nr}. The time to damp to half-amplitude for the second smallest root is approximated by

$$\tau = 0.693 \frac{\frac{T_0}{Sqb}\sin\theta_c dz C_{nr}\frac{mU}{Sq}\frac{b}{2U} + C_{y\beta}C_{n\beta}\frac{b}{2U}C_{\ell p}\frac{b}{2U} + \frac{mU}{Sq}C_{\ell p}\frac{b}{2U}C_{n\beta}}{\frac{C_y}{Sqb}T_0\sin\theta_c dz\frac{b}{2U}C_{nr} + C_{n\beta}\frac{mU}{Sq}\frac{T_0}{Sqb}\sin\theta_c dz}$$

This next-to-smallest root resembles the spiral divergence root for aircraft. The cable tension replaces the rolling moment coefficients. The damping time is decreased by increasing the depression force and decreasing the roll damping coefficient, $C_{\ell p}$. The dihedral angle somewhat affects the size of the smallest root, but generally does not affect the two smallest roots as much as in the case of aircraft.

If straight-line, level motion is assumed with the side-slip angle equal to the yaw angle, and the roll angle and its derivatives being zero, the yawing moment equation becomes

$$\frac{\beta}{\delta_r} = \frac{-C_{n\delta_r}}{\frac{I_{zz}}{Sqb}s^2 - \frac{b}{2U}C_{nr}s + (C_{n\beta} + \frac{T_0}{Sqb}\cos_c dx)}$$

For Body A, the denominator is

$$0.0019237\ s^2 + 0.039474\ s + 0.5015910 = 0$$

The roots of this quadratic are

$$s_1 = -10.26 + j12.47$$
$$s_2 = -10.26 - j12.47$$

The damping coefficient ζ is 0.635, and the natural frequency ω_n is 16.15. For the complete equations of motion, the complex-pair roots give $\zeta = 0.768$ and $\omega_n = 16.97$. The complex roots represent the "Dutch Roll."

If the side-slip and the yaw angles are assumed to be zero with no applied rudder forces, the rolling moment equation can also be directly solved:

$$\frac{\varphi}{\delta_a} = \frac{C_{\ell\delta_a}}{\frac{I_{xx}}{Sqb}s^2 - \frac{b}{2U}s + \frac{T_0}{Sqb}\sin\ {}_c dz}$$

For Body A, the denominator of the transfer function is

$$0.00021641\ s^2 + 0.019737\ s + 0.077781$$

The roots of this equation are –4.13 and –87.08. The transfer function equation indicates that, for the towed body, the steady-state roll angle is zero with an impulse-type aileron deflection. The steady-state roll angle becomes a constant for a step-function aileron deflection. The ailerons act like elevators in that, for a steady-state response, the deflections must be held.

LAPLACE TRANSFORMS OF LATERAL EQUATIONS

The Laplace transform lateral equations of motion can be solved in terms of any of the independent variables φ, Ψ, or β, with either rudder or aileron applied forces, by Cramer's rule. The transfer functions which are transform ratios between the output and the input variables are numerically evaluated for Body A below:

$$\frac{\varphi}{\delta_r} = \frac{-0.01561\left[\frac{s}{0.186} - 1\right]\left[\frac{s}{0.357} - 1\right]\left[\frac{s}{7.61} + 1\right]}{\left[\frac{s}{0.442} + 1\right]\left[\frac{s}{3.34} + 1\right]\left[\frac{s}{217.63} + 1\right]\left[\frac{s^2}{288.01} + \frac{1.536}{16.97}s + 1\right]}$$

$$\frac{\varphi}{\delta_a} = \frac{7.0101\left[\frac{s}{0.34} + 1\right]\left[\frac{s^2}{176.69} + \frac{1.782}{13.29}s + 1\right]}{\left[\frac{s}{0.442} + 1\right]\left[\frac{s}{3.34} + 1\right]\left[\frac{s}{217.63} + 1\right]\left[\frac{s^2}{288.01} + \frac{1.536}{16.97}s + 1\right]}$$

$$\frac{\Psi}{\delta_r} = \frac{-0\ 18734\left[\frac{s}{0.0623} - 1\right]\left[\frac{s}{4.27} + 1\right]\left[\frac{s}{70.01} + 1\right]}{\left[\frac{s}{0.442} + 1\right]\left[\frac{s}{3.34} + 1\right]\left[\frac{s}{217.63} + 1\right]\left[\frac{s^2}{288\ 01} + \frac{1.536}{16.97}s + 1\right]}$$

$$\frac{\Psi}{\delta_a} = \frac{-39.695\left[\frac{s}{15.276}+1\right]\left[\frac{s^2}{161.81}+\frac{0.703}{12.72}s+1\right]}{\left[\frac{s}{0.442}+1\right]\left[\frac{s}{3.34}+1\right]\left[\frac{s}{217.63}+1\right]\left[\frac{s^2}{288.01}+\frac{1.536}{16.97}s+1\right]}$$

$$\frac{\beta}{\delta_r} = \frac{0.50078\left[\frac{s}{0.42}+1\right]\left[\frac{s}{4.05}+1\right]\left[\frac{s}{19.381}+1\right]\left[\frac{s}{738.82}+1\right]}{\left[\frac{s}{0.442}+1\right]\left[\frac{s}{3.34}+1\right]\left[\frac{s}{217.63}+1\right]\left[\frac{s^2}{288.01}+\frac{1.536}{16.97}s+1\right]}$$

$$\frac{\beta}{\delta_a} = \frac{0.0061729\left[\frac{s}{0.0022}+1\right]\left[\frac{s}{7.79}+1\right]\left[\frac{s}{20.662}-1\right]}{\left[\frac{s}{0.442}+1\right]\left[\frac{s}{3.34}+1\right]\left[\frac{s}{217.63}+1\right]\left[\frac{s^2}{288.01}+\frac{1.536}{16.97}s+1\right]}$$

The solution of the transforms in time can be represented by exponentials and a damped sinusoid for impulse inputs. The solution adds a constant to these transients for a step-function input. The steady-state response to an impulse-type input is zero for all the above transfer functions. The steady-state response to a step-function input is a constant for all the transfer functions.

The lateral motion analysis above was based on Body A with a dihedral coefficient of –0.0524. Consider another body, Body A', with a dihedral coefficient of + 0.0524 but with the same values as for Body A for the other coefficients. Based on this sign reversal, the roots of the quintic characteristic equation of lateral motion become

$$s_1 = -0.353$$

$$s_2 = -4.24$$

$$s_3 = -12.42 + j11.69$$

$$s_4 = -12.42 - j11.69$$

$$s_5 = -218.05$$

For these roots, the times to damp to half-amplitude are 1.96, 0.1634, 0.05580, and 0.003178 seconds, compared to 1.57, 0.2075, 0.05314, and 0.003184 seconds for Body A with the negative dihedral coefficient The dominant cable root is slightly smaller in magnitude while the other two real roots are slightly larger. The complex Dutch Roll mode has a slightly smaller real part but a slightly larger absolute magnitude than for Body A Based on the damping time of the dominant cable mode, the body with a negative value of C_{l_β} appears more desirable. (In the control-system analysis that follows, it is indicated that the body with the positive dihedral coefficient may be preferable.)

The transfer functions giving the variations of the independent variables φ, Ψ, and β in Laplace transforms, in terms of the applied rudder and aileron inputs, are for Body A':

$$\frac{\Psi}{\delta_a} = \frac{-39.611\left[\frac{s}{1.60}+1\right]\left[\frac{s^2}{162.80}+\frac{0.370}{12.76}s+1\right]}{\left[\frac{s}{0.353}+1\right]\left[\frac{s}{4.24}+1\right]\left[\frac{s}{218.05}+1\right]\left[\frac{s^2}{290.83}+\frac{1.46}{17.05}s+1\right]}$$

$$\frac{\Psi}{\delta_r} = \frac{-7.8232\left[\frac{s}{2.84}+1\right]\left[\frac{s}{4.19}+1\right]\left[\frac{s}{114.14}+1\right]}{\left[\frac{s}{0.353}+1\right]\left[\frac{s}{4.24}+1\right]\left[\frac{s}{218.05}+1\right]\left[\frac{s^2}{290.83}+\frac{1.46}{17.05}s+1\right]}$$

$$\frac{\beta}{\delta_r} = \frac{0.49975\left[\frac{s}{0.35}+1\right]\left[\frac{s}{3.75}+1\right]\left[\frac{s^2}{19.122}+\frac{0.539}{138.28}s+1\right]}{\left[\frac{s}{0.353}+1\right]\left[\frac{s}{4.24}+1\right]\left[\frac{s}{218.05}+1\right]\left[\frac{s^2}{290.83}+\frac{1.46}{17.05}s+1\right]}$$

$$\frac{\beta}{\delta_a} = \frac{0.0060354\left[\frac{s}{0.0022}+1\right]\left[\frac{s}{7.79}+1\right]\left[\frac{s}{20.662}-1\right]}{\left[\frac{s}{0.353}+1\right]\left[\frac{s}{4.24}+1\right]\left[\frac{s}{218.05}+1\right]\left[\frac{s^2}{290.83}+\frac{1.46}{17.05}s+1\right]}$$

$$\frac{\varphi}{\delta_a} = \frac{8.4103\left[\frac{s}{0.35}+1\right]\left[\frac{s^2}{352.45}+\frac{0.80}{18.77}s+1\right]}{\left[\frac{s}{0.353}+1\right]\left[\frac{s}{4.24}+1\right]\left[\frac{s}{218.05}+1\right]\left[\frac{s^2}{290.83}+\frac{1.46}{17.05}s+1\right]}$$

$$\frac{\varphi}{\delta_r} = \frac{-0.015264\left[\frac{s}{0.057}+1\right]\left[\frac{s}{1.25}-1\right]\left[\frac{s}{9.70}+1\right]}{\left[\frac{s}{0.353}+1\right]\left[\frac{s}{4.24}+1\right]\left[\frac{s}{218.05}+1\right]\left[\frac{s^2}{290.83}+\frac{1.46}{17.05}s+1\right]}$$

CONTROL SYSTEMS GENERAL

An automatic control system is desirable if it enhances the accuracy of an action and reduces the amount of needed human attention. The preceding analysis of the towed body indicates stability for both longitudinal and lateral motion. An impulse elevator deflection in longitudinal motion, and impulse rudder or aileron deflections in lateral motion, all produce responses that return the body to its initial reference position with time in a stable manner. The towed body follows step-function inputs in both longitudinal and lateral motion with an error in the steady state. Automatic control systems should be installed if it is desired to tow the body in particular motion modes and if it is necessary to improve the dynamic responses. Some advantages that can be obtained with closed-loop feedback control systems are listed below:

1. Less attention is required.

2. The transient response can be improved, so that the body returns to the reference condition after a disturbance without excessive oscillations. Transient characteristics, such as the time to rise to maximum response after a step input, the overshoot above the steady-state value, and the time required to settle to the steady-state value, can be adjusted. Optimizing procedures, such as minimizing the integral of the product of time and the absolute value of error, can be used.

3. The response to specific inputs can be made to occur without error or with only a small error, in the steady state.

4. The design can be such as to afford good stability characteristics. The stability should not be affected by small changes in amplifier gains. After a disturbance, the system should return to the reference condition quickly.

5. The control ratio between the output and the input can be made less susceptible to undesired disturbances. The control system can be designed to adapt itself to changing conditions.

6. The control system can be designed such that the response to random statistical-type disturbances is minimum. A wide frequency bandwidth in the system increases the random disturbance power, but allows more accurate following of rapidly varying input signals and can improve the system's stability. The bandwidth should be large enough to pass the desired input frequencies, but should attenuate the higher frequencies. The system's resonant frequencies should not be near external resonant frequencies.

In a single-loop, feedback control system, part or all of the output is fed back to the input. (It can be fed back in any phase relationship to the input; negative feedback occurs when the feedback signal subtracts from the input; positive feedback when the feedback signal adds to the input.) The system error $E(s)$ is the difference between the reference input and the signal fed back, in negative feedback; and is the sum of these two in positive feedback. The control ratio between the Laplace transforms of the output and the input is related in the transfer functions:

$$\frac{C(s)}{R(s)} = \frac{G(s)}{1 + G(s)H(s)}$$

where $C(s)$ is the transfer function of the output

$R(s)$ is the transfer function of the input

$G(s)$ is the forward transfer function for the circuit connecting the output to the system error, $E(s)$

$H(s)$ is the feedback-circuit transfer function

For negative feedback, the algebraic sign of the $G(s)H(s)$ term is positive for real positive $G(s)$ and $H(s)$ values. In this case, the control ratio when $H(s)$ equals unity varies from 0 to 1 as the forward transfer function $G(s)$ varies from 0 to ∞. For positive feedback with $G(s)$ and $H(s)$ positive and real numbers, the control ratio with $H(s)$ equal to unity varies from 0 to ∞ as $G(s)$ varies from 0 to 1, and from $-\infty$ to -1 as $G(s)$ varies from 1 to ∞. The product $G(s)H(s)$ is known as the open-loop transfer function. When this is large compared to unity, the magnitude of the ratio between the output and the input becomes equal to $1/H(s)$.

The system error, $E(s)$, for negative feedback becomes equal to

$$\frac{E(s)}{R(s)} = \frac{1}{1 + G(s)H(s)}$$

The algebraic signs of the transfer functions $G(s)$ and $H(s)$ are assumed to be positive in the above equation.

The stability of closed-loop control systems is determined by the denominator, $1 + G(s)H(s)$, in these equations. Instability occurs when the open-loop transfer function, $G(s)H(s)$, is of unity magnitude and has an 180-degree phase. The open-loop transfer function can usually be written for linear systems as a ratio between factorable polynomials:

$$G(s)H(s) = \frac{K(s + a)(s + b)(s + c)\left(s^2 + 2\zeta_1 \omega_{n_1} + \omega_{n_1}^2\right)\ldots}{s^n(s + k)(s + l)(s + m)\left(s^2 + 2\zeta_2 \omega_{n_2} + \omega_{n_2}^2\right)\ldots}$$

where a,b,c are open-loop zeros

k,l,m are open-loop poles

K is the gain constant

ω_n is the natural frequency part of a complex pair

ζ is the damping ratio part of a complex pair

The form of the open-loop transfer function indicates the complexity of the control system. The denominator must be at least one degree higher in s than the numerator, for practical systems. When the denominator does not exceed the numerator by more than two degrees in s, the phase does not generally equal 180 degrees for finite frequencies unless there is an s^2 factor in the denominator. A factor, s^n, shifts the phase n times 90 degrees. Factors, $s+a$, approach 90-degree shifts as $s = j\omega$ increases in value. Quadratic factors approach 180-degree phase shifts as ω increases. Open-loop transfer functions with the denominator exceeding the numerator by one or two degrees in s usually indicate inherently stable control systems unless there are two open-loop poles at $s = 0$. When the denominator exceeds the numerator by more than two degrees in s, the control system still is usually stable over wide ranges of gain values, K. As the gain setting is increased from zero (the open-loop value), the closed-loop poles change (move along the root loci) and, eventually, instability occurs. It is desirable that the closed-loop poles (roots of the characteristic equation, $1 + G(s)H(s) = 0$) be

sufficiently far to the left in the complex plane to insure rapid transient decay (large negative roots and large negative real parts of the complex roots of the characteristic equation). Stated in another way, inherent stability occurs if the magnitude of the open-loop transfer function decreases at the most 20 dB per decade in frequency or 40 dB per decade with the s^n factor in the denominator having n equal to either 0 or 1. Each degree in s in the numerator causes the open-loop transfer function to increase by 20 dB per decade, while each degree in s in the denominator causes it to decrease by 20 dB per decade. The phase of the open-loop transfer function is always less than 180 degrees for inherent stability.

The steady-state error of the closed-loop systems depends on the form of the input functions in addition to the system's transfer functions. Control systems are classified into types by the power of the s^n factor of the denominator of the open-loop transfer functions. Type 0 has $n = 0$, Type 1 has $n = 1$, and so on. The final value Laplace theorem can be used to determine the steady-state error. The theorem states that if the Laplace transform of $f(t)$ is $sF(s)$, and if $sF(s)$ is analytic on the imaginary axis and the right-half plane, then the final value of the time function is given by

$$\lim_{t \to \infty} f(t) = \lim_{s \to 0} sF(s)$$

On the basis of the final value theorem, the steady-state-system following error becomes

$$e_{ss}(t) = e(t) = \lim_{t \to \infty} \lim_{s \to 0} \frac{sR(s)}{1 + G(s)H(s)}$$

For a Type 0 control and a step function input, the steady-state following error is a constant. For a Type 1 control and a step function input, the output follows the input without error in the steady state.

Control systems are usually modified from a preliminary design to improve the stability, the transient response, and the following error. Compensation consists of changing the forward transfer function, the feedback transfer function, or both by adding phase lead or phase lag networks. Networks added may include 90-degree phase leads such as differentiation circuits, 90-degree phase lags such as integration circuits, and RC filters which are integration and differentiation circuits in themselves.

The effects on the control systems of various compensation methods are examined below in a general manner. High damping usually indicates better stability characteristics. Transient damping is indicated by the time required to damp to half-amplitude for either simple roots or complex root pairs. The small roots (dominant roots) determine the least damped components. More stability is indicated by larger negative real roots or larger negative real parts of complex root pairs. The usual effects of compensation methods are:

1. *Integration in feedback path.* Adds a closed-loop pole and a 0.1 pole at zero. The steady-state error is less since the system is one type higher. The damping and the stability effects are usually not large since the effects on the dominant roots are generally small. The effects can be large for large dominant roots of the characteristic equation.
2. *Integration in forward transfer function* Adds a closed-loop pole. The system is one type higher and follows a more complicated input function

without error. Damping and stability effects are usually small for small roots.

3. *Differentiation in the feedback path.* Removes a closed-loop pole and adds an open-loop zero at zero. The system is one type lower and has a poorer steady-state condition. The damping and stability effects are usually small for small roots.
4. *Differentiation in forward transfer function.* Removes a closed-loop pole. The system is one type lower, and less complicated input functions can be followed without error. The damping and stability effects are usually small for small roots.
5. *Tachometer feedback (1 + b s feedback loop).* The steady-state-error constant is higher, and thus the steady-state error is higher. The damping and stability are both improved.
6. *High-pass filter added in series with the differentiation in tachometer feedback.* The steady-state error is improved over tachometer feedback. The damping and stability are both improved.
7. *Lead compensation in forward transfer function.* $\left[\frac{(1 + sT_1)T_2}{(1 + sT_2)T_1}\right]$.

   $T_1 > T_2$. Adds a closed-loop pole and a closed-loop zero. The steady-state error is the same as without the lead compensation. The damping and the stability are both improved.
8. *Lag compensation in the forward transfer function* $\left[\frac{1 + T_2 s}{1 + T_1 s}\right]$

   $T_1 < T_2$. Adds a closed-loop pole and a closed-loop zero. The steady-state error is not changed by this compensation. The damping and the stability are both improved.
9. *The addition of unity feedback.* This makes a Type 0 control out of any control type. Differentiation added to the feedback or the forward transfer function of a Type 0 control changes the closed-loop pole positions. The changed values of the poles usually improve the control-system stability and damping. If the differentiation is in the forward transfer function, it also adds a closed-loop zero.

The incorporation of a feedback control system into the towed body improves the body's dynamics and assists in the performance of the towing missions. Body A has been shown to be dynamically stable. It follows the elevator and cable tension step input functions in longitudinal motion with a constant steady-state error. In lateral motion, the body follows step input rudder or aileron variations with constant error in steady state. The towed body in itself is a Type 0 system in both longitudinal and lateral motion. For the complete longitudinal equations of motion, the transient solution consists of two damped exponentials with very short times to damp to half-amplitude and a damped sinusoid with a damping coefficient of 0.906. The time to damp to half-amplitude of the sinusoid is 0.544 second. For the short equations of longitudinal motion, the transient solution consists of two of the exponentials of the complete solution and another damped exponential with a longer damping time. The time to damp to half-amplitude of this longer-time term is 0.866 second. The dominant or long-time-to-damp transient term is largely determined by the cable tension and the pitch damping hydrodynamic coefficient, C_{mq}, for both the complete and the short longitudinal equations. The time to damp can be decreased by increasing the depression force and decreasing the magnitude of the pitch

damping coefficient. In the lateral equations of motion, the transient solution has a damped exponential with a very short time to damp to half-amplitude (corresponding to the roll subsidence mode), a damped sinusoid with 0.0552 second to damp to half-amplitude (corresponding to the Dutch Roll mode), a damped exponential with a time to damp to half-amplitude of 0.2075 second (corresponding to the spiral divergence mode), and a damped exponential with a damping time of 1.57 seconds (cable mode). The term with the largest damping time is determined by the cable tension and the yaw damping coefficient, C_{nr}. The damping time can be decreased by increasing the depression force and the body drag, and by decreasing the yaw damping coefficient. The critical long-time damping terms for both longitudinal and lateral motion can be lowered by increasing the depression force and decreasing the damping coefficients, C_{mq} and C_{nr}. A longitudinal control system can improve the damping and stability and provide a means of keeping the towed body at a constant commanded depth. In addition, a lateral control system can provide coordination so that turning can occur without skidding (side slipping). The lateral control system can also be used to orient the direction of motion.

LONGITUDINAL CONTROL SYSTEMS

It has been previously shown that Body A is a Type 0 system in that it follows a step input with an error. The longitudinal short solution indicates that the dominant cable mode damps to half-amplitude in 0.866 second. Here we shall describe a longitudinal control system designed to hold the towed body at commanded depths, in addition to improving the stability and damping. The control system parameters depend on the tow body with which the system operates, here assumed to be Body A (which could be improved). The effects of the elements in the control system are given by the transfer functions relating the output to the input of the elements as functions of s, the Laplace transform of time. The output/input conversion factors between angular and linear units in the elements is included in the transfer function constants. The components of the control system are assumed to be available. There are many commercial small-sized, accurate, and sensitive pressure gauges. It is assumed that a depth gauge converting depth to a proportional electrical signal is available. The elevator servo can be an electromechanical or a hydraulic unit, and is represented in the analysis by a simple time lag and a gain factor. Idealized gyroscopes without time lags are assumed. Commercial gyroscopes have been developed that are accurate and sensitive and are not much affected by vibrations, heat variations, or pressure variations. They are available as small, light units, weights being about 3 pounds, lengths about 5 inches, and diameters about 3 inches. The proposed control system should, of course, be a realistic design.

Figure 7 consists of three block diagrams of proposed depth control systems. The top diagram shows a basic feedback system to control depth. Basic controls can be adjusted by compensating networks such as minor loops and filters; in the middle diagram a damping minor loop is added to the basic control, and in the bottom diagram a filter is added to the outer feedback path. Three transfer functions indicated in the diagrams are related to the body dynamics. The transfer function relating the attitude angle rate with the elevator

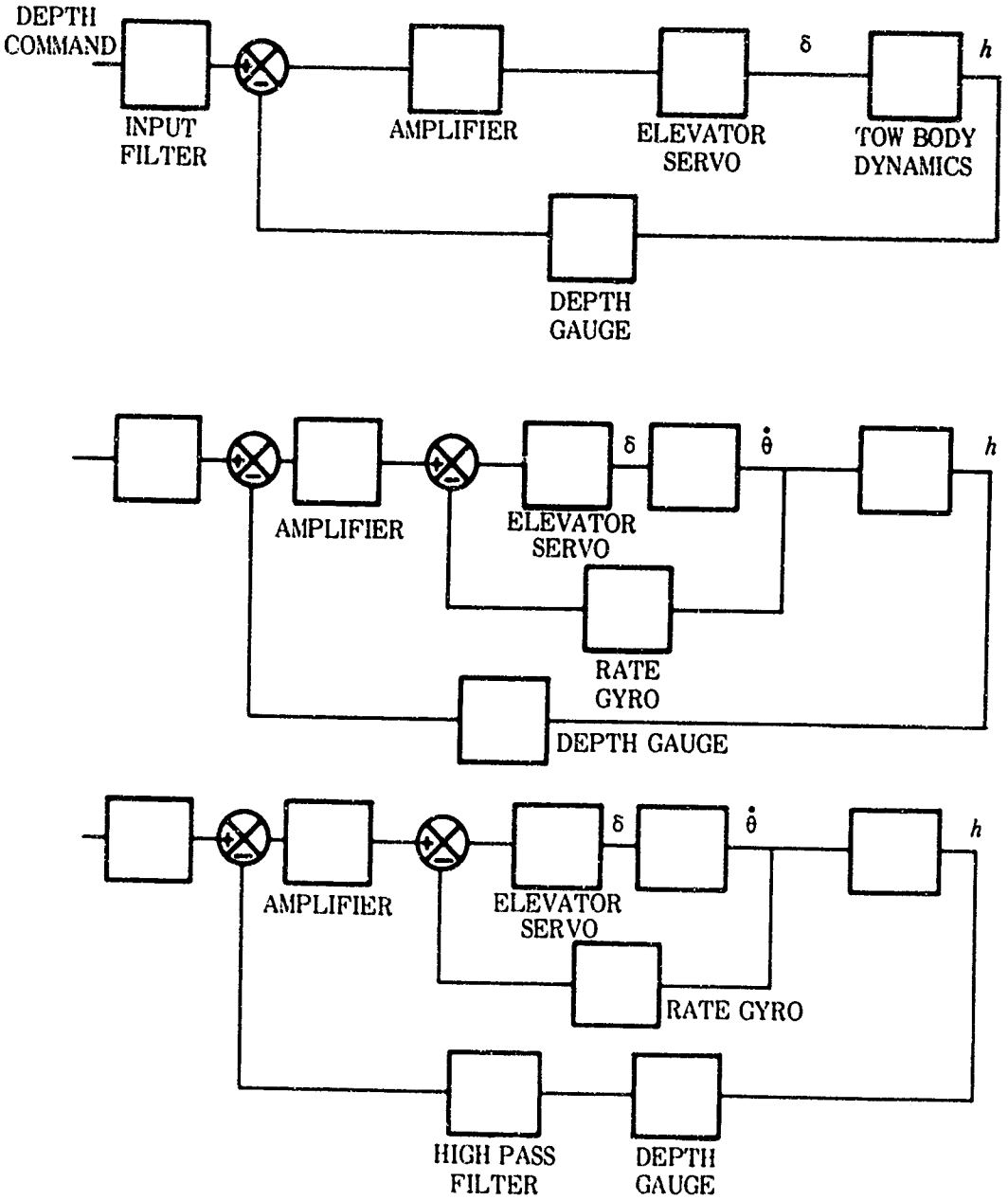

Figure 7. Depth control systems.

angle deflection, θ/δ_e, is directly obtained from the longitudinal equations of motion. The transfer function relating the depth with the attitude angle rate, $h/\dot{\theta}$, is obtained using the vertical acceleration, a_z:

$$\frac{h}{\dot{\theta}} = \frac{a_z}{\delta_e} \times \frac{\delta_e}{\theta} \times \frac{1}{s^3}$$

The vertical acceleration itself is calculated from the solution of the longitudinal equations of motion:

$$a_z = U\left[\frac{'\alpha}{\delta_e} - \frac{\theta}{\delta_e}\right] s$$

where U is the undisturbed forward velocity.

The transfer function relating the depth with the elevator angle deflection, h/δ_e, is given by the relationship

$$\frac{h}{\delta_e} = \frac{h}{\dot{\theta}} \times \frac{\dot{\theta}}{\delta_e}$$

The body dynamics transfer functions for Body A, based on the short-solution longitudinal equations of motion, are given by the equations:

$$\frac{\theta}{\delta_e} = \frac{-7.6558\left[\frac{s}{29.47} + 1\right] s}{\left[\frac{s}{51.18} + 1\right]\left[\frac{s}{18.82} + 1\right]\left[\frac{s}{0.80} + 1\right]}$$

$$\frac{h}{\dot{\theta}} = \frac{+73.674\left[\frac{s}{44.21} + 1\right]\left[\frac{s}{44.21} - 1\right]}{s^2\left[\frac{s}{29.47} + 1\right]}$$

$$\frac{h}{\delta_e} = \frac{-564.03\left[\frac{s}{44.21} + 1\right]\left[\frac{s}{44.21} - 1\right]}{s\left[\frac{s}{51.18} + 1\right]\left[\frac{s}{18.82} + 1\right]\left[\frac{s}{0.80} + 1\right]}$$

Feedback controls can be analyzed by many methods. The root locus method is convenient for repetitive analysis. System design usually requires several trial solutions that must be optimized. The root locus plots indicate damping and stability in the location of the roots of the characteristic equation

(closed-loop poles). They show, in graphical form, variations of the poles with system gains. The zeros and the poles of the open-loop transfer function are plotted on the complex plane, and root loci are obtained using the transfer function of the feedback control system:

$$\frac{C(s)}{R(s)} = \frac{G(s)}{1 + G(s)H(s)}$$

The roots of the denominator are the closed-loop poles. A plus sign in the denominator indicates negative feedback, and a minus sign indicates positive feedback. Positive feedback occurs when the algebraic sign of the open-loop transfer function is a plus and addition occurs at the error detector, or when the sign of $G(s)H(s)$ is a minus and subtraction occurs at the error detector. Negative feedback occurs when the product of the sign of $G(s)H(s)$ and the sign of the error detector operation is a minus. The open-loop transfer function must be of unit magnitude and of 0- or 180-degree phase at the closed-loop poles. The root loci are plots of the 0-degree phase requirement for positive feedback, and the 180-degree requirement for negative feedback. The magnitude requirement produces closed-loop poles on the root loci. A point on the root locus is a closed-loop pole when the open-loop transfer function is set equal in magnitude to unity:

$$G(s)H(s) = 1 = \frac{K(s - Z_1)(s - Z_2) \cdot \cdot \cdot \cdot \cdot}{(s - P_1)(s - P_2) \cdot \cdot \cdot \cdot \cdot}$$

The product of the distances to the open-loop poles from the point, divided by the product of the distances to the open-loop zeros from the point, is equal to the loop gain, K, corresponding to the closed-loop pole. Figure 8A shows the zero root locus for the basic depth control system corresponding to the upper block diagram of figure 7. Most of the right-hand locus is in the right half of the plane and corresponds to instability. The dominant closed-loop pole for the small stable part of the root locus has a negative real part less than 0.4. When a high-pass filter is added (fig. 8B), the root loci are shifted to the left increasing both the stability and the damping. The dominant root now has a negative real part of about 4. The time to damp to half-amplitude decreases from about 2 seconds for the basic control alone, to about 0.2 second for the basic control plus the high-pass filter. The electrical filter can be designed using common networks, for example:

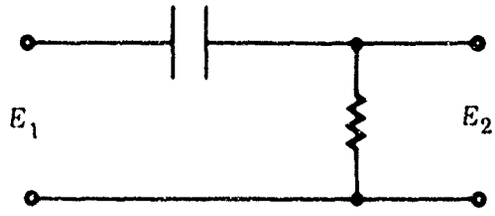

$$\frac{RCs}{1 + RCs} = \frac{E_2}{E_1}$$

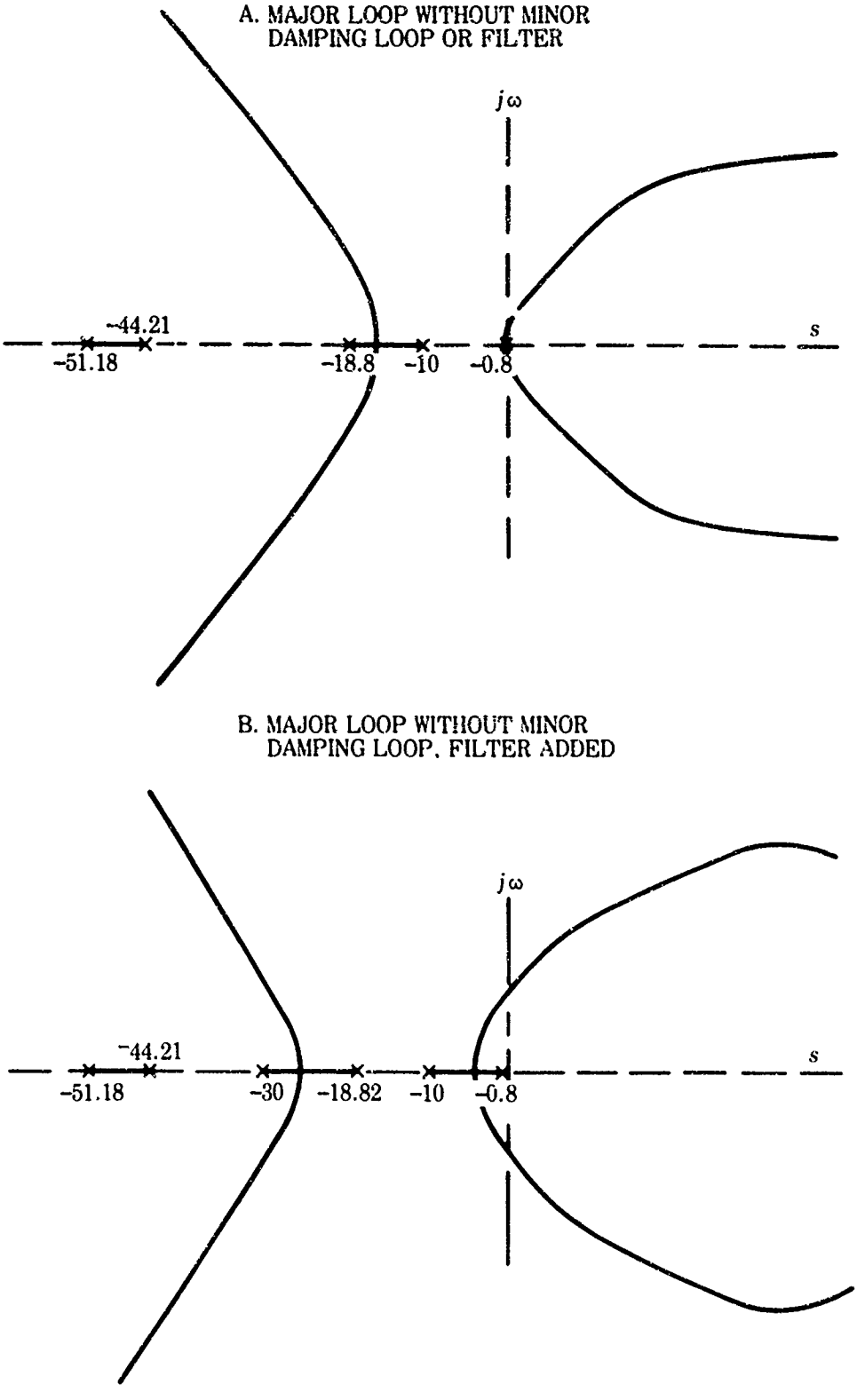

Figure 8. Longitudinal depth control – zero root loci.

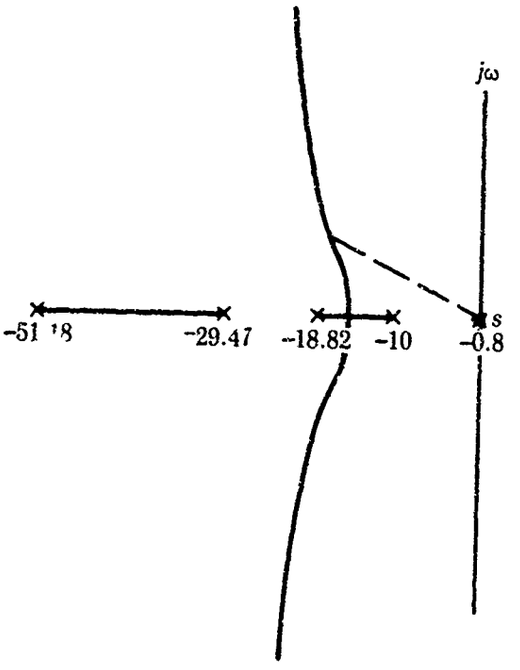

C. DAMPING MINOR LOOP ALONE

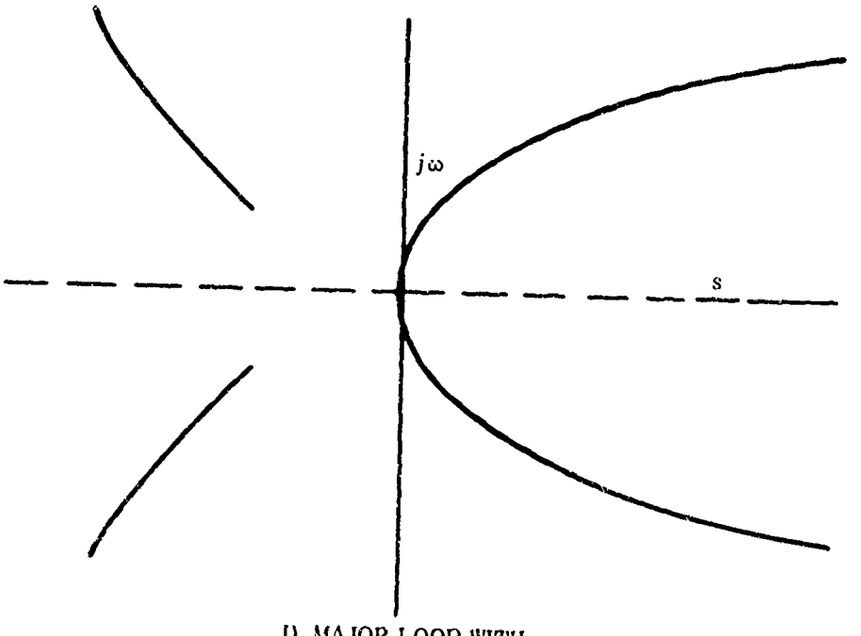

D. MAJOR LOOP WITH MINOR LOOP ADDED

Figure 8 (Continued).

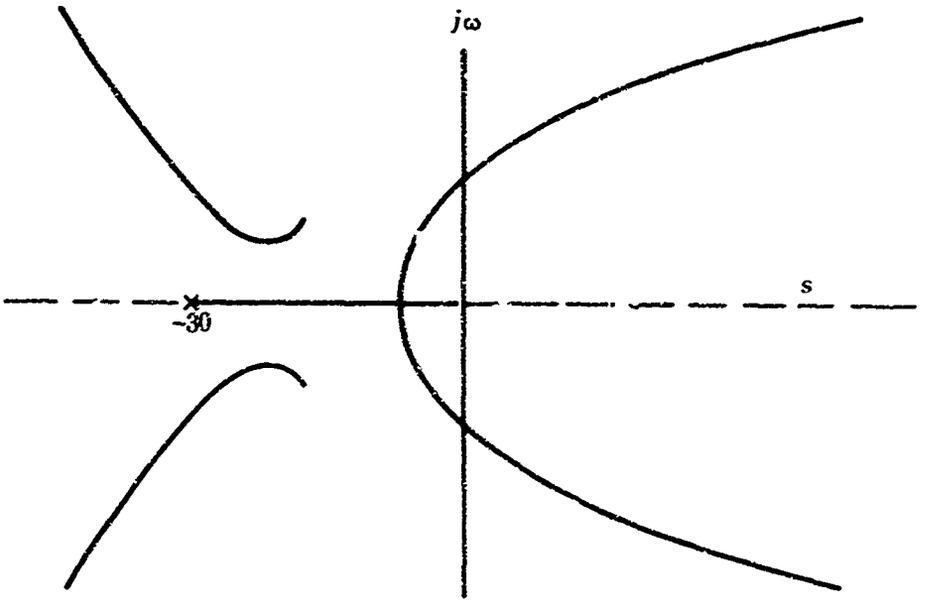

E. MAJOR LOOP, WITH MINOR LOOP AND FILTER ADDED

Figure 8 (Continued).

Figure 8C shows the root locus plot of the minor loop. The dominant root is determined by the locus on the real axis from –0.8 to 0. The value of gain constant of 320 produced a closed-loop pole at –44.21 and complex poles with a damping constant of 0.9. Figure 8D shows the zero angle root locus of the closed minor loop incorporated into the basic depth control system. The right-hand locus has a very small section in the stable left half of the complex plane. Figure 8E shows the effect of the addition of the same high-pass filter; the root loci are shifted to the left. The dominant pole can have a negative real part of about 7. The time to damp to half-amplitude can be about 0.1 second with the minor loop and the high-pass filter. Thus, compensation can change the control system considerably. The transient response to an input such as a step function depends on the chosen compensation. The rise time to design output, the overshoot above the design value, and the time to damp are characteristics having different damping requirements. The control system can be optimized according to several principles usually based on minimizing errors.

LATERAL CONTROL SYSTEMS

The towed body is inherently stable due to the stabilizing effect of the towing cable. Unlike an aircraft, it tends to return to its original heading after a disturbance. The cable root is dominant in the dynamics. For Body A, it has

been shown to have a half-amplitude damping time of 1.57 seconds. A control system can be used to reduce the damping times. It can be designed to coordinate the rudder and the aileron controls so that no side slip (skidding) occurs during a turn. Coordination can be obtained by feeding back to the rudder input a voltage proportional to the side-slip angle or the lateral acceleration. Here, a rudder coordination computer is discussed. It may be desirable to provide a method of orienting the yaw angle of the towed body by means other than the cable. A yaw-rate body orientation control is also discussed.

The top block diagram of figure 9 shows the closing of the rudder circuit through a rate gyroscope to form a closed feedback loop. The root locus plots of figures 10 (A through G) show that, for the feedback loop, the dominant closed-loop pole is very near the origin in all cases for either positive or negative values of the dihedral coefficient. When integration is added, for example, by use of an integrating gyro instead of the rate gyro, the root locus plots indicate that the closed-loop poles can have negative real parts considerably larger than the dominant cable root particularly for the body with the positive dihedral coefficient.

The middle block diagram of figure 9 shows connection of the aileron circuit to the rudder circuit through a coupling network called the rudder coordination computer. The method is based on keeping the side-slip angle at zero during turns by feeding back a required rudder input for a given aileron input. The total side-slip angle is related to the rudder and the aileron angles by the equation

$$\beta_T = TF(\beta/\delta_a)_a - TF(\beta/\delta_r)_r$$

where $TF(\beta/\delta_a)$ is the transfer function relating the side-slip angle with the aileron angle

$TF(\beta/\delta_r)$ is the transfer function relating the side-slip angle with the rudder angle

When the total side-slip angle is zero, the ratio between the perfectly coordinated rudder and aileron angles becomes

$$\frac{\delta_r}{\delta_a} = -\frac{TF(\beta/\delta_a)}{TF(\beta/\delta_r)} = TF_{rcc}$$

The middle block diagram of figure 9 shows that the negative of the transfer function ratios is equal to the transfer function of the rudder coordination computer, TF_{rcc}. Unlike an aircraft, positive rudder requires positive aileron, and a phase reversal is not required in the rudder computer circuit. The rudder-coordination-computer transfer functions for Body A ($C_{\ell\beta}$ –) and Body A' ($C_{\ell\beta}$ +) are given by the equations

Body A

$$TF_{rcc} = \frac{-0.012327\left[\frac{s}{0.0022}+1\right]\left[\frac{s}{7.79}+1\right]\left[\frac{s}{20.66}-1\right]}{\left[\frac{s}{0.42}+1\right]\left[\frac{s}{4.05}+1\right]\left[\frac{s}{19.38}+1\right]\left[\frac{s}{738.82}+1\right]}$$

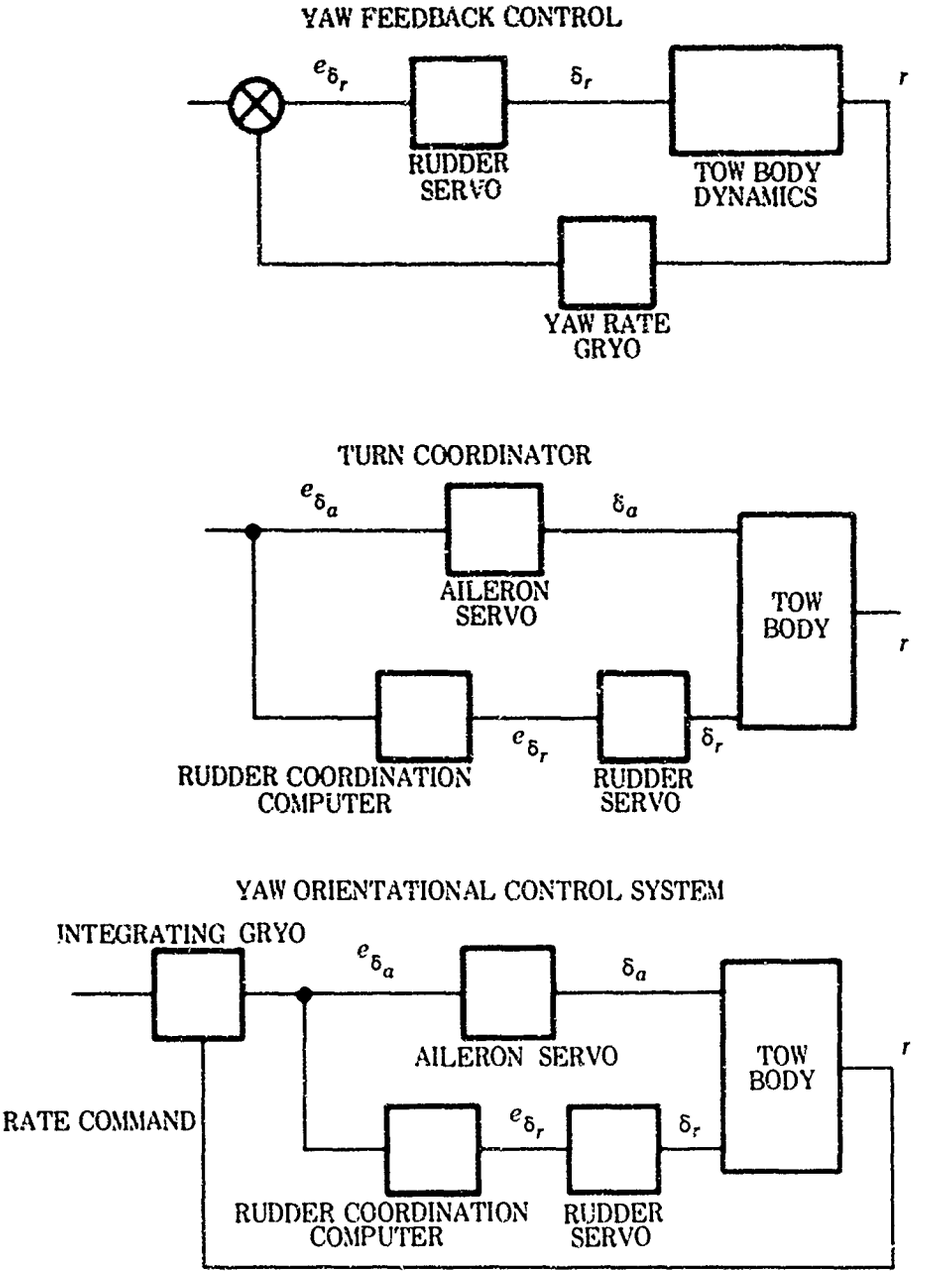

Figure 9. Lateral control systems.

Body A'

$$TF_{rcc} = \frac{-0.012077\left[\frac{s}{0.0022}+1\right]\left[\frac{s}{7.79}+1\right]\left[\frac{s}{20.66}-1\right]}{\left[\frac{s}{0.35}+1\right]\left[\frac{s}{3.75}+1\right]\left[\frac{s^2}{19,122}+\frac{0.539}{138.28}s+1\right]}$$

Values of transfer functions that are a decade in frequency away from a reference frequency are 20 dB apart for first-order functions. Thus, the rudder-coordination transfer functions can be approximated for angular frequencies from about 1 to 10 radians per second by the equations

Body A ($C_{\ell\beta}-$)

$$TF_{rcc} = \frac{2.353\left[\frac{s}{7.79}+1\right]}{\left[\frac{s}{4.05}+1\right]}$$

Body A' ($C_{\ell\beta}+$)

$$TF_{rcc} = \frac{1.9213\left[\frac{s}{7.79}+1\right]}{\left[\frac{s}{3.75}+1\right]}$$

The transfer function between the total yaw rate and the input voltage of the rudder-coordination-computer circuit, e_{δ_a}, is given by the equation

$$\frac{r}{e\delta_a} = TF_{as} \times TF(\dot{\Psi}/\delta_a) + TF_{rs} \times TF_{rcc} \times TF(\dot{\Psi}/\delta_r)$$

where TF_{as} is the transfer function of the aileron servo

TF_{rs} is the transfer function of the rudder servo

As the equation above indicates, the two applied inputs of the aileron and rudder angles add algebraically in the yaw-angle effects. The bottom block diagram of figure 9 shows a yaw orientation system with rudder coordination. An integrating yaw-rate gyroscope is included. The open-loop transfer functions for Bodies A and A' are given by the approximate equations:

$$\frac{\Psi}{e_{\delta_a}} = \frac{0.44081\left[\frac{s}{7.79}+1\right]\left[\frac{s}{0.0623}-1\right]\left[\frac{s}{70.01}+1\right]}{\left[\frac{s}{0.44}+1\right]\left[\frac{s}{3.34}+1\right]\left[\frac{s}{217.63}+1\right]\left[\frac{s^2}{288.01}+\frac{1.536}{16.97}s+1\right]}$$

$$\frac{\Psi}{e_{\delta_a}} = \frac{0.94481\left[\frac{s}{7.79}+1\right]\left[\frac{s}{2.84}+1\right]\left[\frac{s}{114.14}+1\right]}{\left[\frac{s}{0.353}+1\right]\left[\frac{s}{3.75}+1\right]\left[\frac{s}{218.05}+1\right]\left[\frac{s^2}{290.83}+\frac{1.46}{17.05}s+1\right]}$$

The open-loop transfer functions are based on the approximate rudder-coordination transfer functions. The rudder produces the principal effects on yaw. The orientation system can be checked on analog computers. The more complete rudder-coordination-computer transfer functions can be used if necessary. The approximate transfer functions can be represented by the common network below:

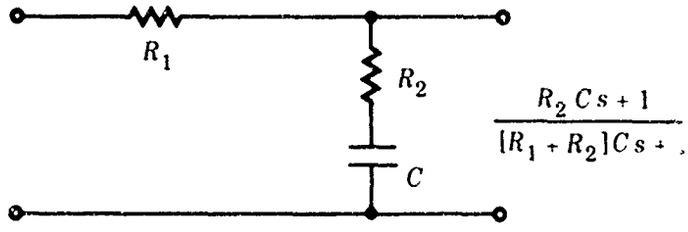

The root locus plots for the approximate transfer functions are shown in figure 10 for the yaw orientation system. It can be seen, at least at lower gains, that both Bodies A and A' are stable. The dominant closed-loop-pole damping time for the positive dihedral body is about 0.244 second. For the negative dihedral body, the damping time is at the best about 0.7 second. Additional networks can be added to improve the transient response if desired. Phase-lead differentiating networks tend to narrow the system bandwidth while phase-lag integrating networks tend to broaden the bandwidth.

The control systems help reduce possible coupling between the longitudinal and lateral equations of motion. The presence in the equations of the two terms listed below causes intercoupling:

$$\left[I_{xx}-I_{zz}\right]PR \qquad\qquad \left[I_{yy}-I_{xx}\right]PQ$$

where I_{xx} is the body's moment of inertia about the longitudinal axis

I_{zz} is the body's moment of inertia about the vertical axis

I_{yy} is the body's moment of inertia about the lateral axis

The roll rate P is not large in the tow bodies due to the cable. The addition of control systems reduces the yaw rate R and the pitch rate Q.

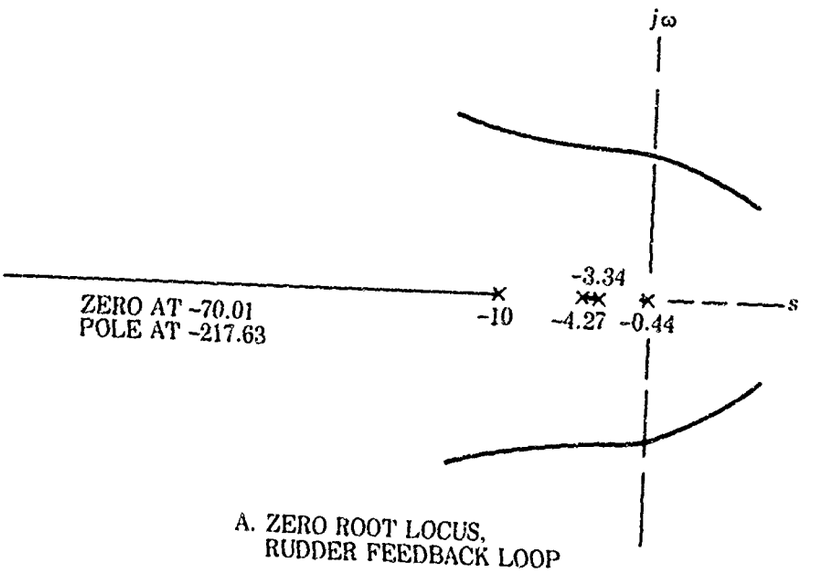

A. ZERO ROOT LOCUS,
RUDDER FEEDBACK LOOP

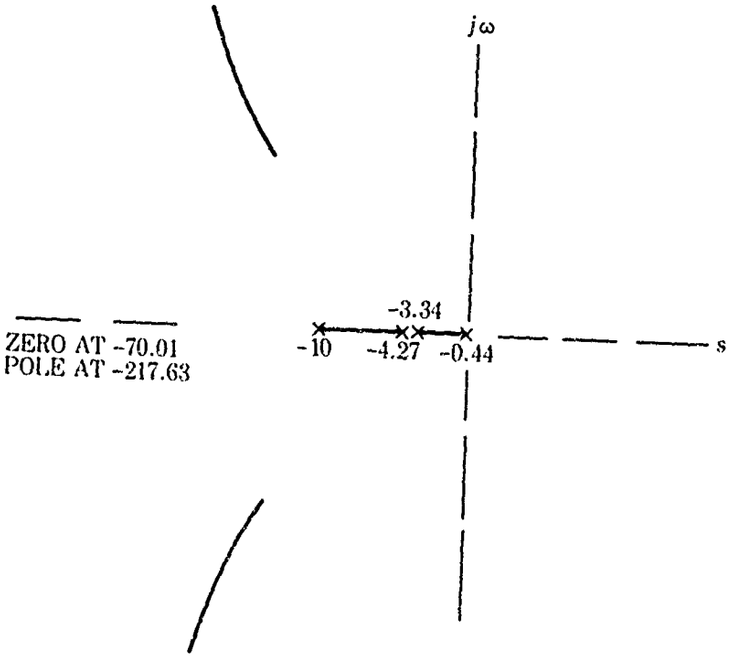

B. 180° ROOT LOCUS,
RUDDER FEEDBACK LOOP,
$C_{\ell\beta}$

Figure 10. Lateral motion root loci -- yaw orientation system.

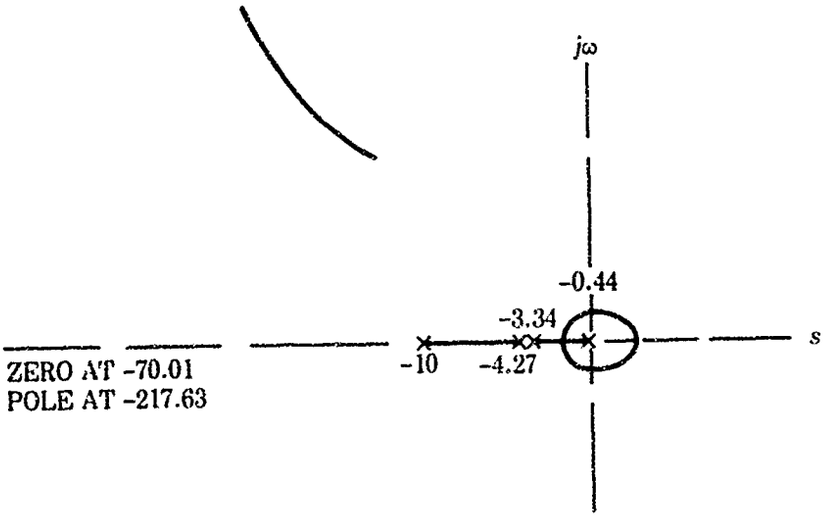

C. ZERO ROOT LOCUS, RUDDER FEEDBACK LOOP, INTEGRATION ADDED, $C_{\ell\beta}$

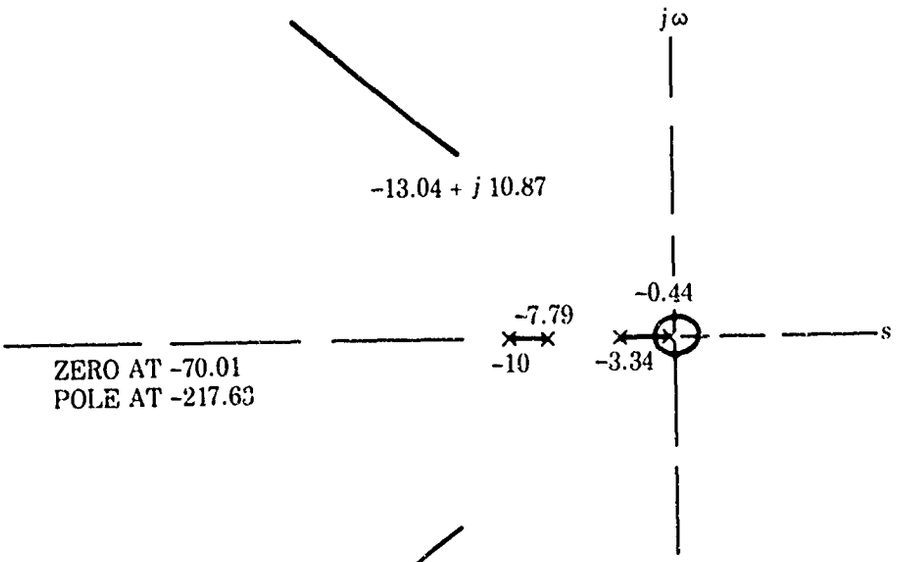

D. ZERO ROOT LOCUS, WITH RUDDER COORDINATION COMPUTER AND INTEGRATING GYROSCOPE, $C_{\ell\beta}$

Figure 10 (Continued)

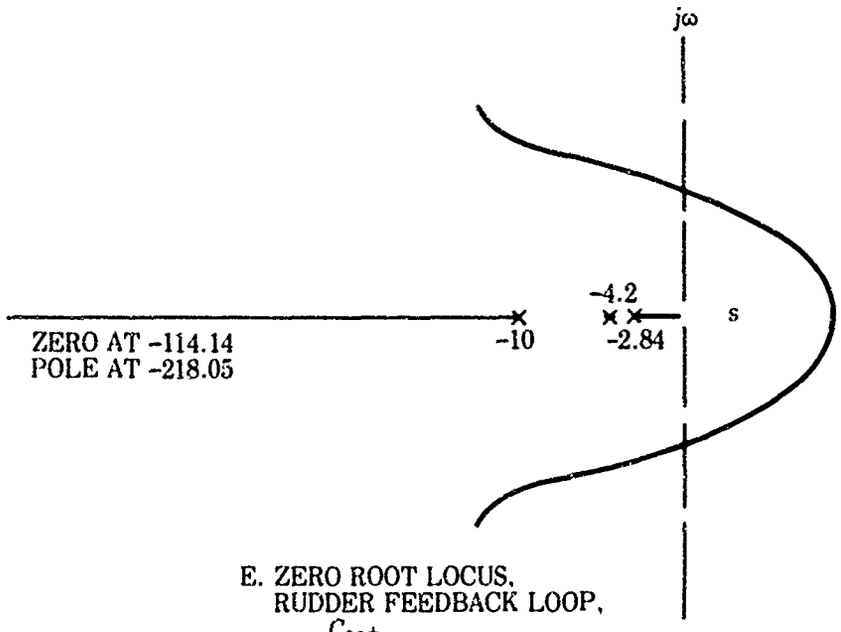

E. ZERO ROOT LOCUS,
RUDDER FEEDBACK LOOP,
$C_{\ell\beta^+}$

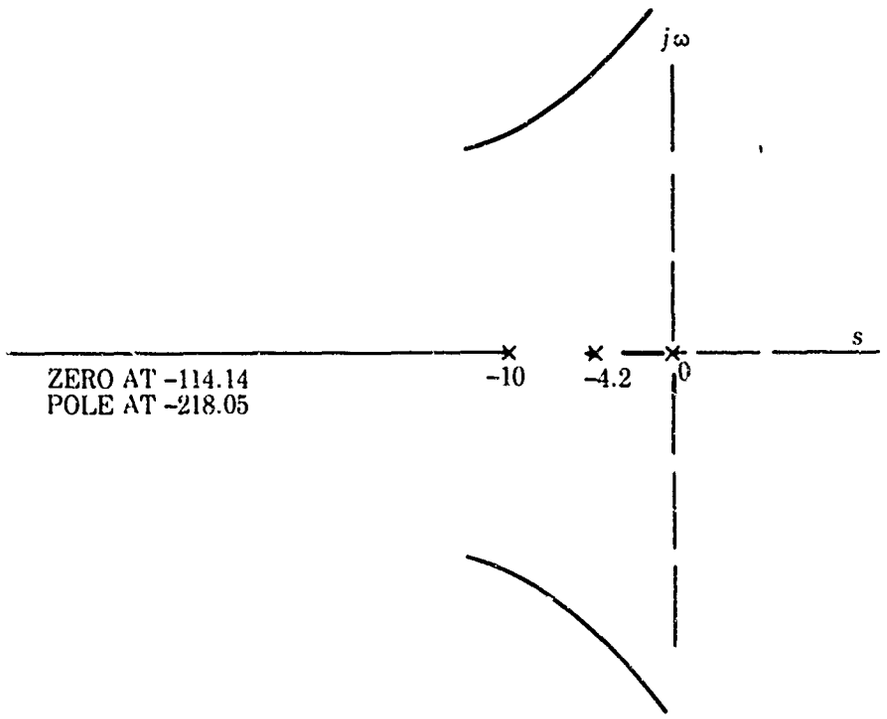

F. 180° ROOT LOCUS,
RUDDER FEEDBACK LOOP,
INTEGRATION ADDED, $C_{\ell\beta^+}$

Figure 10 (Continued).

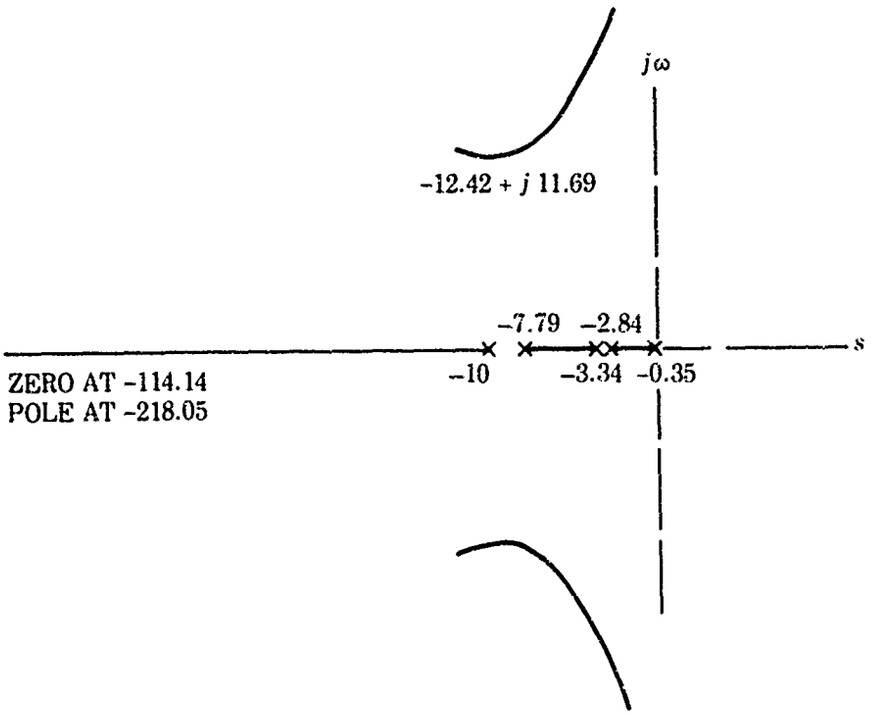

G. 180° ROOT LOCUS, WITH RUDDER COORDINATION COMPUTER INTEGRATING GYROSCOPE, $C_{\ell\beta}$

Figure 10 (Continued).

In summary, in reference to closed-loop feedback systems, it can be said that a control system output follows the input better, and with less disturbance effects, and with high forward-transfer-function gains. The output-input transfer function becomes

$$\frac{GG_b}{1 + GG_bH}$$

If the gain G is large and the gains G_b and H are not too small, the output-input transfer function becomes $1/H$.

The disturbance output for the network shown below is given by

$$\frac{G_b}{1 + GG_bH}$$

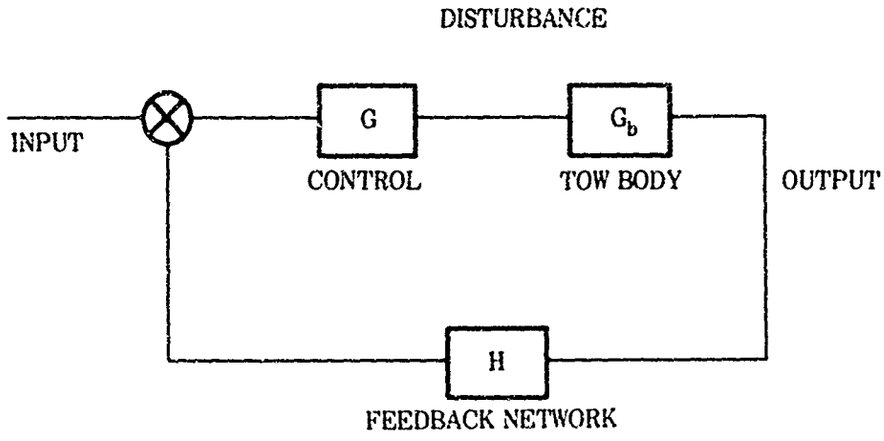

This becomes equal to the small value $1/GH$ when the gain G is large. An input filter called a model can be added. For a high gain, G, the output follows the model output. Adaptive control systems usually have high-variable-gain circuits and still retain stability. They can have electronic counting devices which measure the gain and adjust to a maximum stable value. In the case of Body A' (C_{ℓ_β} +), the cable σ pole on the real axis approaches the zero at very high gains. The Dutch Roll closed-loop pole then becomes dominant at high gains and approaches the imaginary axis; it must be limited for stability.

TOW BODY DESIGN

Preliminary design analysis has been performed mainly with three bodies, designated Body A, Body I, and Body II. Detailed analysis was made in both longitudinal and lateral motion of Body A which has a negative dihedral coefficient, of Body A' which has a positive dihedral coefficient of the same magnitude, and of Body A'' which is of the same form but has a zero dihedral coefficient. In addition to the depressor angle, the wing location and the tail-center-of-pressure location in relation to the body axis affect the dihedral coefficient, producing equivalent dihedral angles of about 3 degrees or more depending on the lateral area.

All the bodies studied have the same 30-inch maximum diameter, but they differ in other respects. Some important design considerations are the drag; the hydrodynamic coefficients, particularly the damping coefficients, C_{nr} and C_{mq}; and the depression force. All the bodies are axisymmetrical, streamlined forms with depressor and control surface appendages. We designed the axisymmetrical forms using the David Taylor Model Basin method originated by Landweber and Gertler. The bodies have a length/diameter ratio of about 2.7 for minimum drag. Drag has an important effect on the required towing horsepower and the attainable depths. It has a beneficial effect on the damping time of the dominant cable

mode in lateral motion. A considerable portion of the required towing horsepower is needed to counteract the body drag. For a 2000-pound drag, 276 horsepower is required to tow the body at 45 knots, while for a 600-foot towing cable with a drag of 15 pounds per foot 1530 horsepower is required. The attainable depth is 405 feet at 45 knots with a depression force of 14,000 pounds and a 2000-pound drag.

The total body drag depends considerably on the depressor and tail surfaces. Additional drag arises from the interference between components and from imperfections on the surfaces. Hoerner shows how to estimate the total drag on such bodies as aircraft. by adding together all the drags of the components in drag areas. A drag area is the product of the drag coefficient and the area that it is defined for:

$$\frac{D}{\bar{q}} = C_d S$$

where $\bar{q}$ is the dynamic pressure

$C_d S$ is the drag area

Here, the total drag is considered to be the sum of the depressor drag, the tail drag, the depressor-induced drag, and the main body drag. The imperfection and interference drags are neglected since they are small percentages of the others and can be lessened by careful design. The drag area of the induced drag is approximated by

$$\frac{C_L{}^2}{AR\pi} = C_{i_n}$$

where AR is the aspect ratio b^2/S

S is the wing area

The main-body drag coefficient can be based on wetted area, or cross-sectional area as it is here. The drag coefficient for an axisymmetrical body is approximated by Hoerner as follows:

$$C_{D0} = C_f \left[3\left(\frac{\ell}{d}\right) + 4.5\left(\frac{d}{\ell}\right)^{1/2} + 21\left(\frac{d}{\ell}\right)^2 \right]$$

where C_f is the skin-friction drag coefficient of the body

C_{D0} is the drag coefficient defined for the frontal area

The wing and tail drags are based on the plan area. The profile drag is assumed to be nearly zero. The sectional drag coefficient is based on the skin friction for the upper and lower surfaces modified by factors that account for the section thickness. The coefficient is given by the equation

$$C_{Ds} = 2\, C_f \left[1 + \left(\frac{t}{c}\right) + \left(\frac{t}{c}\right)^2 \right]$$

where C_{Ds} is the sectional drag coefficient

t is the section thickness

c is the section chord

The wing and tail thickness-to-chord ratios were taken to be 0.2 in the calculations. The skin-friction coefficient was assumed to be 0.0025. The average skin-friction coefficient is about 0.0025 for the body Reynolds number of 3.5×10^7 which corresponds to fully developed turbulence over an 81-inch body at 45 knots in 50°F water. The transition to neutral turbulence occurs on the body at about 15 inches back of the nose. Transition to self-excited turbulence occurs at about 22 inches back of the nose. Based on these approximations, the tow body drag areas are:

		Drag Area
Main Body	$13.72 \times C_f \times 4.90874$	0.1498
Depressor	$2.48 \times C_f \times 6$	0.0372
Tail	$2.48 \times C_f \times 4$	0.0248
Induced	0.1188	0.1188
Total Drag Area		0.3306

The frontal-area drag coefficient is obtained by dividing the drag area by the frontal area, 4.90874 square feet. The frontal-area coefficient for the values listed above is 0.0673. The body drag at 45 knots equals 1910 pounds. The skin-drag coefficient may be less than the chosen average value of 0.0025 under ideal conditions, but the interference and imperfection drags and the drag at the tie point have been omitted. The body is in fully developed turbulence at points further back than about 25 inches from the nose at 45 knots. For fully developed turbulence, the broadband pressure at the boundary is about 80 dB above 1 dyne cm^2. It is desirable to build the body surface of soft rubber from about 10 inches back of the nose, to delay turbulence to the self-excited value. The outer portion of the body should be made of a low-elastic-modulus material (such as urethane foam) of sufficient structural strength, in order to present a filter to the flow-noise pressure. Flow noise is present over bodies of the tow body size at 45 knots. It can be minimized by delaying the points of transition and by energy absorption.

The depressor wing must be large enough to produce a large depression load at low lift coefficients. A depression force of nearly 14,000 pounds is required to attain depths of about 400 feet with a body drag of 2000 pounds and a 500-foot cable with a drag of 15 pounds per foot. Because of induced drag, the lift coefficient should be limited to values of about 0.4. The aspect ratio should be large for low induced drag. The wing and tail section should be thin for small drag, but must also be structurally strong enough. Symmetrical wing and tail sections with a thickness-to-chord ratio limited to about 0.2 should be used. The NACA four digit numbering system number for this symmetrical section is 0020.

The horizontal and vertical tail surfaces determine the damping coefficients, C_{mq} and C_{nr}. These coefficients affect all the roots for both longitudinal and lateral motion favorably, except the dominant cable roots for both longitudinal and lateral motion. The values are proportional to the square of the distance from

the c.g. to the surface quarter-chord point, and proportional to the surface area of either the horizontal or the vertical tail areas. The damping coefficients should be large but not so large as to make the cable roots too small.

The dihedral angle affects the roots of the characteristic equation and hence the transient response. Positive dihedral coefficients adversely affect the dominant cable root. The response in yaw control systems appears to be better for positive dihedral coefficients. A negative dihedral coefficient is required to pull up the low wing in lateral gusts if the tie point is connected at the c.g. of the body. If the tie point occurs above the c.g., no dihedral is required due to the stabilizing effect of the towing cable. The diagrams below indicate the top view and front view of a tow body with positive side slip and a negative dihedral coefficient.

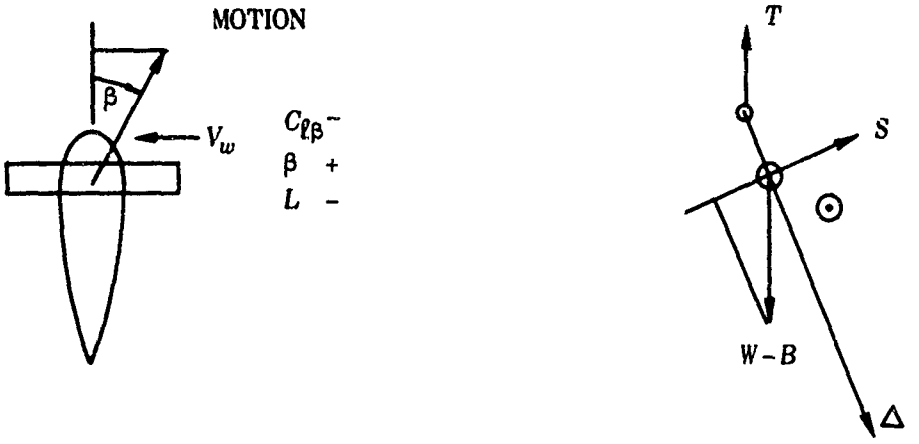

The control surfaces are the standard aircraft type: an elevator, ailerons, and a rudder. A down elevator is assumed positive, and it produces a negative moment. Figure 11 shows the effectiveness factors of the control surfaces. A 0.5 effectiveness factor, $d\alpha_t/d\,\delta_e$, is provided by an elevator area of about 0.35 for an aspect ratio of 7. The factor depends somewhat on the gap and the type of seal in addition to the aspect ratio. In general, the variations are not large. The lateral controls are the ailerons and the rudder. Positive aileron, defined as motion that lowers the right wing, corresponds to right aileron up. The ailerons operate differentially in that when the right aileron is up, the left aileron is down. Positive rudder, defined as rudder to the left, produces a force in the positive Y direction. The ailerons extend over 0.7 of the depressor wing span, the ratio of the chord of the aileron to the chord of the wing being 0.3. This produces a value of 0.6 for $C_{\ell\delta a}$, the aileron moment coefficient. The values of this coefficient vary from zero to about 0.7. The ratio of rudder chord to vertical-tail-surface chord is chosen to be about 0.35 for a 0.5 effectiveness factor. The tail surfaces should have aspect ratios of about 3.

For a left turn, the tow body with positive or left rudder requires positive ailerons to balance the centrifugal force. Positive aileron lowers the right wing and requires positive or left rudder. For Body A' (positive dihedral coefficient), $C_{\ell\delta r}$, the rolling moment coefficient due to rudder, opposes the proper bank angle; and $C_{n\delta a}$, the yawing moment coefficient due to aileron angle, helps the

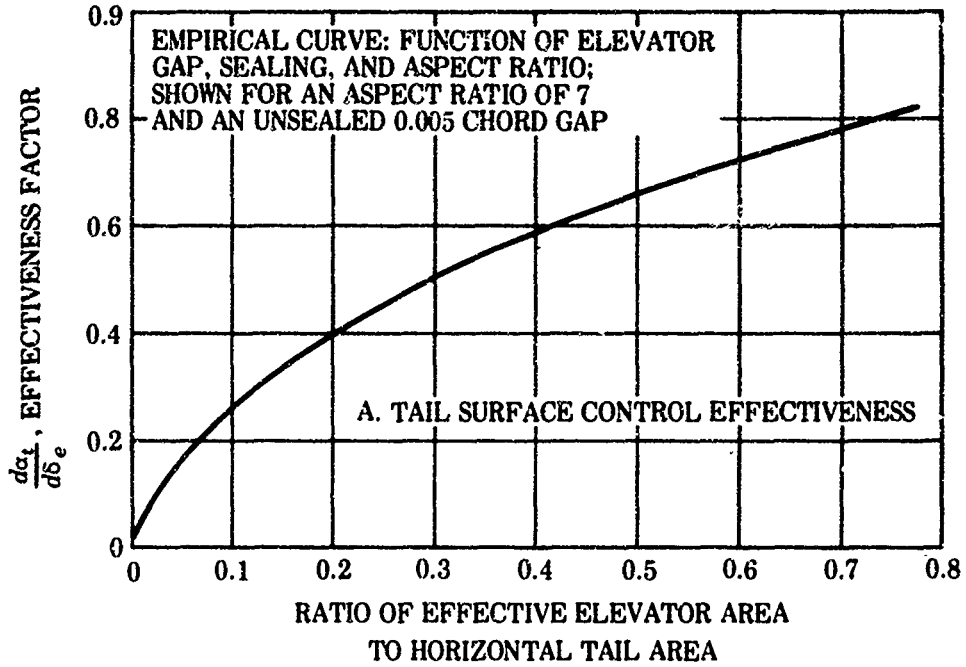

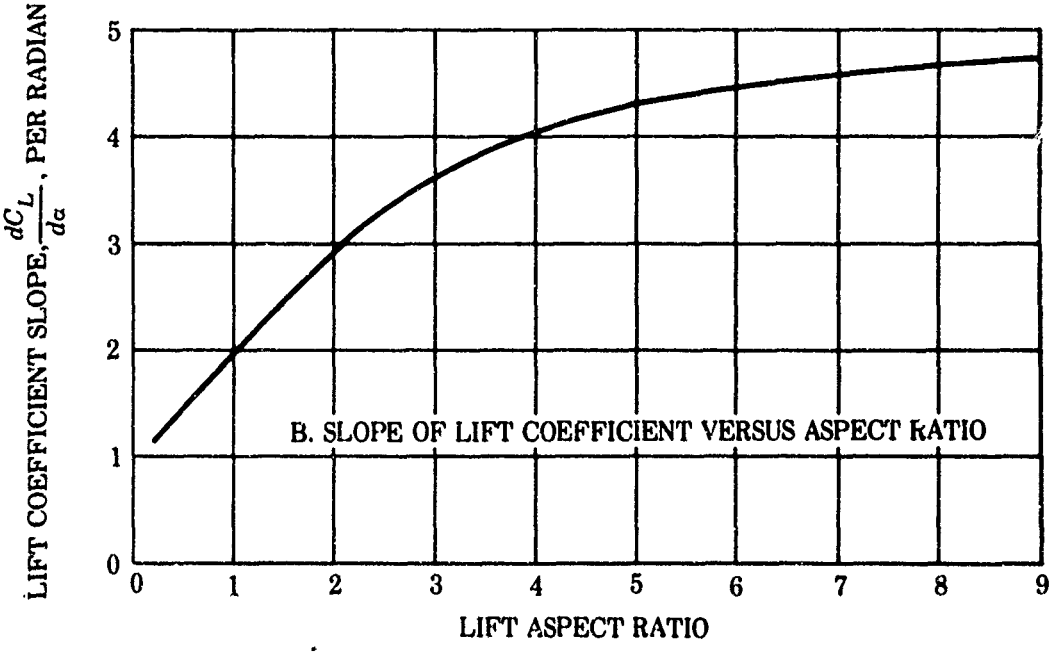

Figure 11. Effectiveness of control surfaces.

proper turn. For Body A (negative dihedral coefficient), $C_{\ell_{\delta r}}$ helps the proper bank angle while $C_{n\delta a}$ helps complete the turn. For a 300-foot turn radius of Body A, the centrifugal force is about 1155 pounds and requires a bank angle of about 4.73 degrees.

In addition to Bodies A, A', and A'', a light body designated Body I and a heavy body designated Body II were analyzed for a towing speed of 45 knots and a straight, level path. The numerical parameters of Body I are:

U	76 ft-sec	S	3 ft^2	m	10 slugs
I_{yy}	20 slug ft^2	T_0	8400 lb	ℓ_t	6 ft
S_t	1 ft^2	dz	1 ft	dx	0 ft
$\bar{q}$	5776 lb/ft^2	c	81.85 degrees	W-B	0 lb

The hydrodynamic coefficients for longitudinal motion of Body I are:

$C_{z\alpha} - 4$	$C_{zq} - 2$	$C_{z\delta_e}$ –0.125
$C_{m\alpha}$ –0.3	$C_{m\dot{\alpha}} - 3$	$C_{m\delta_e}$ –0.5
$C_{z\dot{\alpha}} - 1$	$C_{mq} - 8$	

The transfer functions for Body I are shown in Appendix C. For Body II, the numerical parameters and the hydrodynamic coefficients are:

U	76 ft/sec	S	6 ft^2	m	60 slugs
I_{yy}	1330 slug ft^2	T_0	14,000 lb	ℓ_t	6 ft
S_t	3 ft^2	dz	0 ft	dx	0 ft
$\bar{q}$	5776 lb/ft^2	c	81.85 degrees	W-B	0 lb

$C_{z\alpha} - 4$	$C_{m\dot{\alpha}} - 54$	$C_{z\delta_e} - 0.375$
$C_{m\alpha} - 2$	$C_{zq} - 9$	$C_{m\delta_e} - 2.25$
$C_{z\dot{\alpha}} - 4.5$	$C_{mq} - 108$	

The short-solution longitudinal equations of motion indicate the times to damp to half-amplitude for Body I with the tie point at the c.g. to be 8.295, 0.01752, and 0.007255 seconds. With the tie point 1 foot above the c.g., the damping times of Body I become 0.05584, 0.02436, and 0.007342 seconds. For Body II with the tie point at the c.g., the half-amplitude damping times are 18.15, 0.02128, and 0.04667 seconds. (The damping times for the short solution of Body A were 0.866, 0.0368, and 0.0135 seconds.) These results show the significant influence of the tie location on the dominant cable root. The light Body I damps very rapidly for the dominant cable root because of the low value of the coefficient C_{mq}, with the tie point above the c.g. The weight and the inertia are (optimistically) too small. The moment of inertia of Body II was chosen to be very large. This affects the values of the nondominant roots, increasing their value to about double those of Body A. Figure 12 shows the analog computer solution setup for the longitudinal equations of motion for Body II.

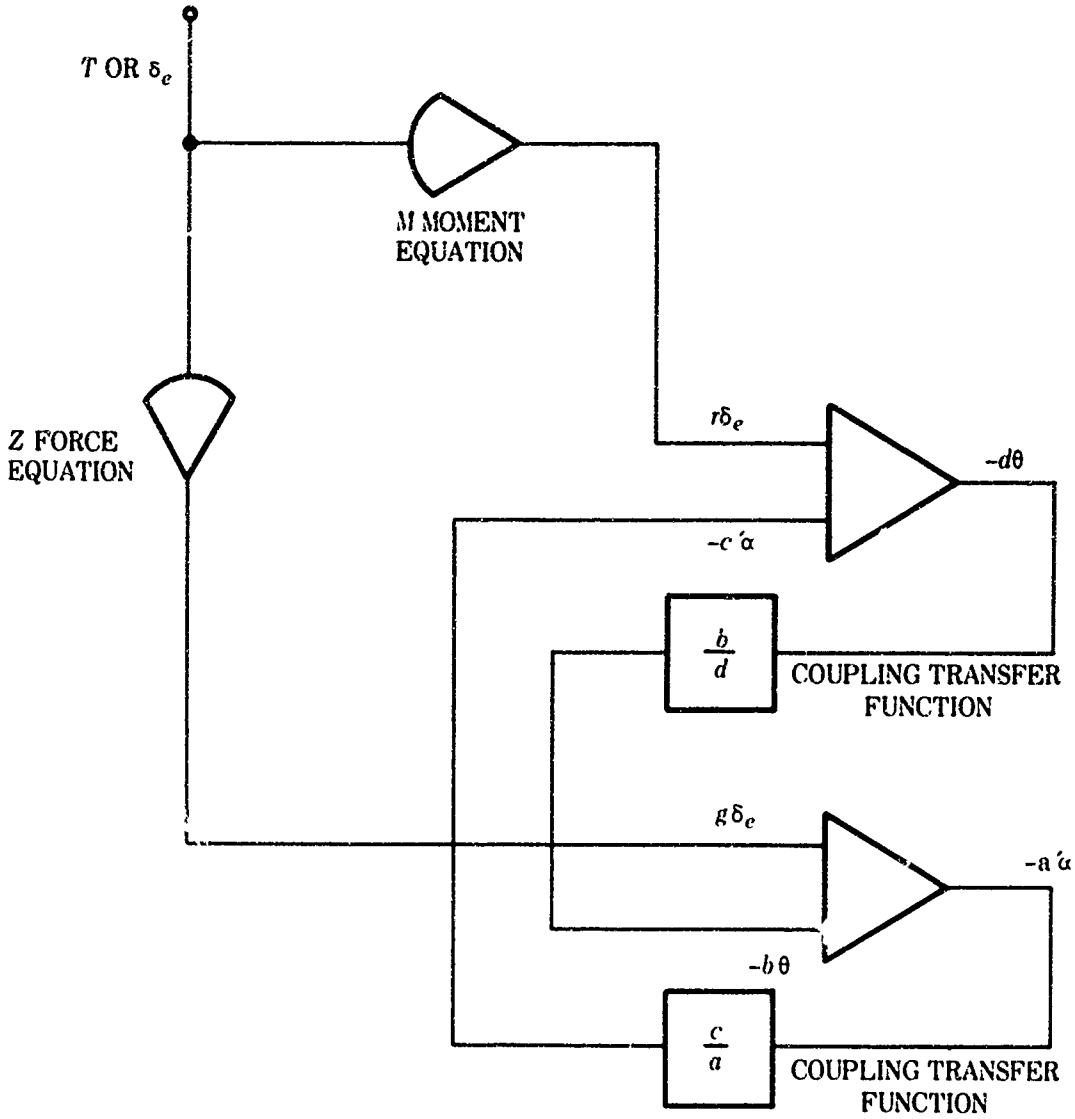

SHORT SOLUTION LONGITUDINAL EQUATIONS

$$a\,\dot{\alpha} + b\theta = g\delta_e$$
$$c\,\dot{\alpha} + d\theta = r\delta_e$$

BODY II FACTORS

$a = 4(1 + 0.04035s)$
$b = -0.0572\,(1 + 1.2666s)$
$c = 2(1 + 0.17763s)$
$d = 0.7105(1 + 0.002439s)s$
$g = 0.02858\,T - 0.375\,\delta_e$
$r = -2.25\,\delta_e$

T IS IN THOUSANDS OF POUNDS
δ_e IS IN RADIANS

Figure 12. Analog computer setup for the longitudinal equations of motion (Body II).

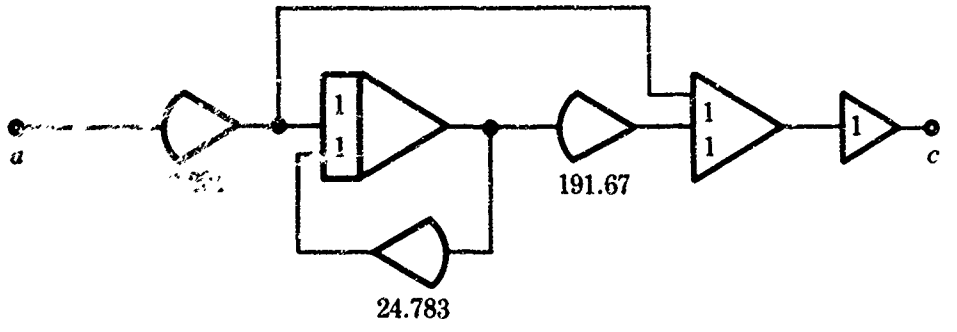

TRANSFER FUNCTION FROM Z FORCE TO M MOMENT EQUATION

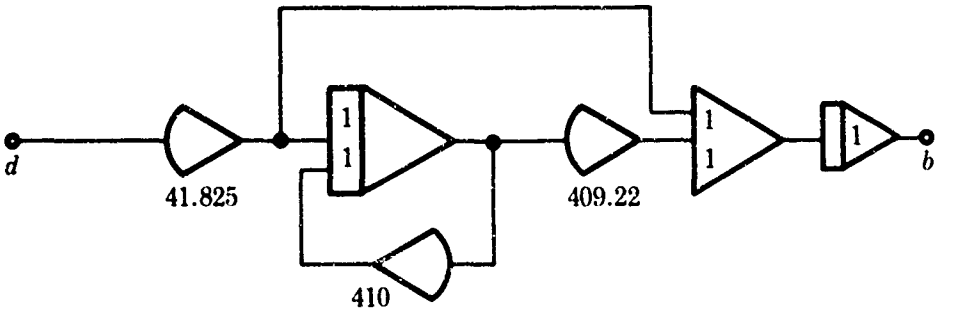

TRANSFER FUNCTION FROM M MOMENT TO Z FORCE EQUATION

NUMBERS ARE VOLTAGE RATIOS IN DB

Figure 12 (Continued).

TOW CABLE

Tow cables have been investigated by many, particularly M.C. Eames. Figures 13 through 15, showing cable characteristics, are from a previous study by the author. Figure 13 indicates that, at a ratio of thickness to chord of 0.25,

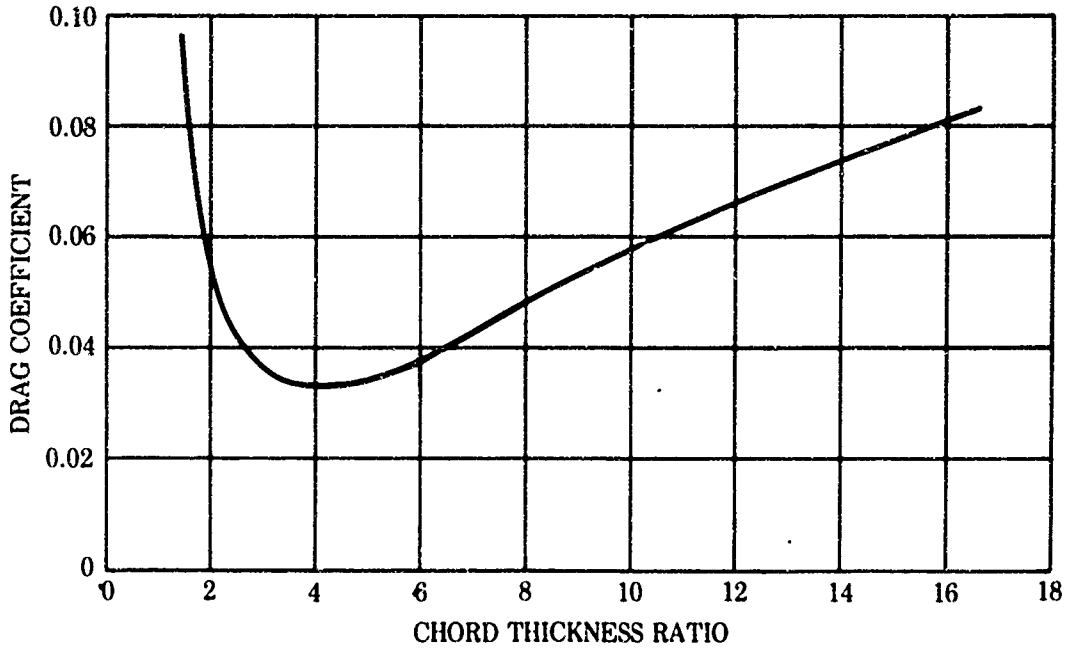

Figure 13. Cable cross-section (frontal) area coefficient versus chord thickness ratio, fully turbulent flow.

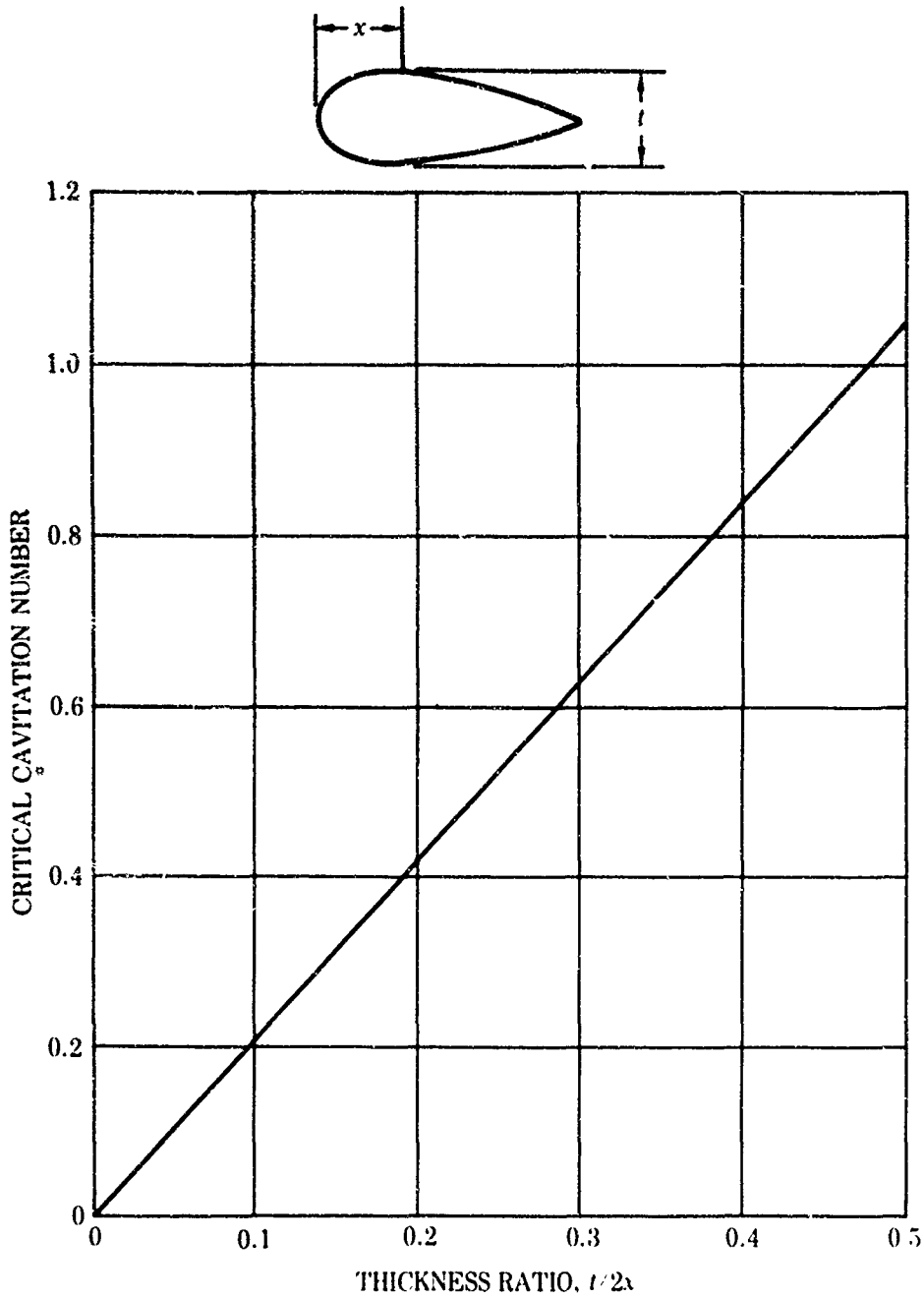

Figure 14. Critical cavitation number versus thickness ratio

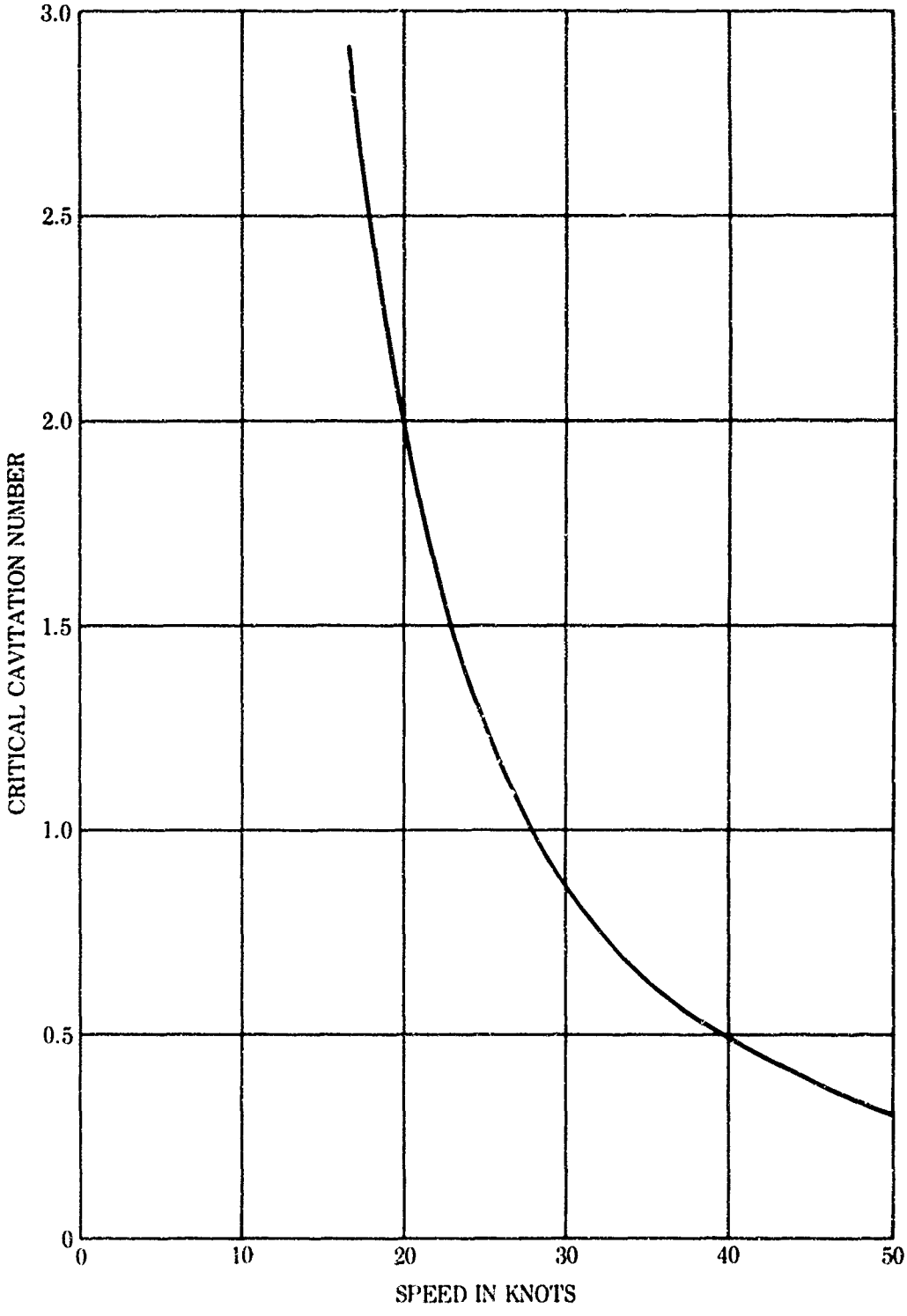

Figure 15 Critical cavitation number versus speed

the cable drag coefficient based on the frontal area is 0.033. Table 3 shows the cable drag per foot at 45 knots for three drag coefficients and three cable thicknesses.

TABLE 3. FRONTAL AREA DRAG OF CABLES

Cable Thickness (Inches)	Cable Drag for a Frontal Area Drag Coefficient of:		
	0.033	0.035	0.040
0.375	5.51	5.84	6.68
0.600	9.53	10.11	11.56
0.700	11.12	12.79	13.48

The drag coefficients are based on a Reynolds number of 10^6 at normal incidence. The drag under the varying conditions of actual motion will not attain the values shown in the table. For a 0.6-inch thickness of optimum shape, the drag per foot under operating conditions may be 11 pounds per foot or more. A 0.375-inch thick, optimum-shape cable with dynamic stabilizers under operating conditions probably produces a drag of 8 pounds per foot or more.

Figure 16 (A through H) shows the body depth plotted against depression force for three depression force/drag ratios, for cable lengths from 500 to 900 feet, and for cable drags of 7 and 15 pounds per foot. For a cable drag of about 11 pounds per foot, a depth exceeding 400 feet is attainable with a 600-foot cable length at 45 knots for a depression force of 14,000 pounds and a 2000-pound body drag. The attainable depth increases with the depression force, but the required horsepower to pull the body increases with the depression force (fig. 17). About 1560 horsepower is required to pull a body with 2000-pound drag at 45 knots if one uses a 600-foot cable with a drag of 11 pounds per foot. Laminar flow cables are required for minimum drag and cavitation-free operation at all depths at this speed.

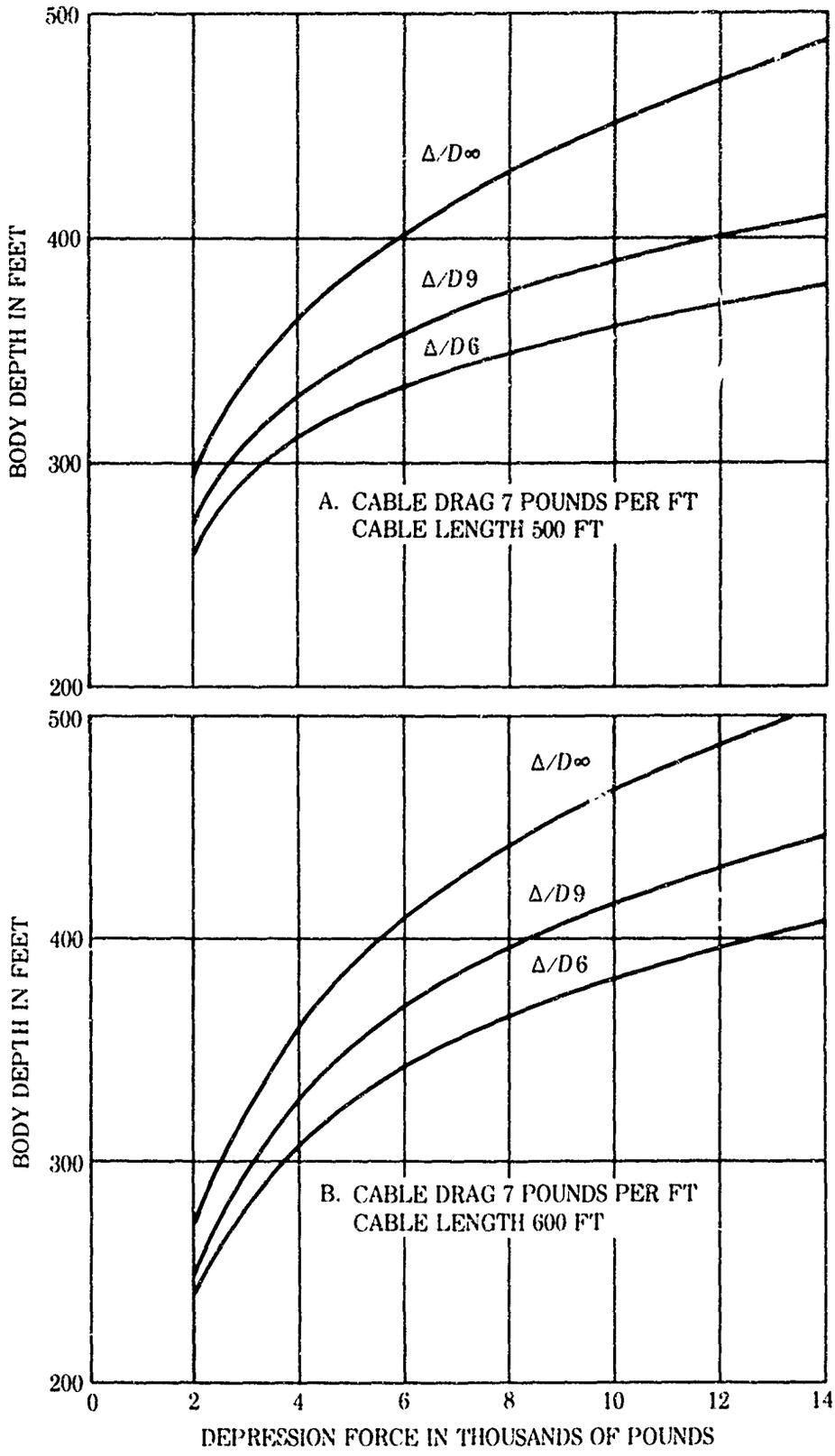

Figure 16. Depression force versus body depth, speed 45 knots.

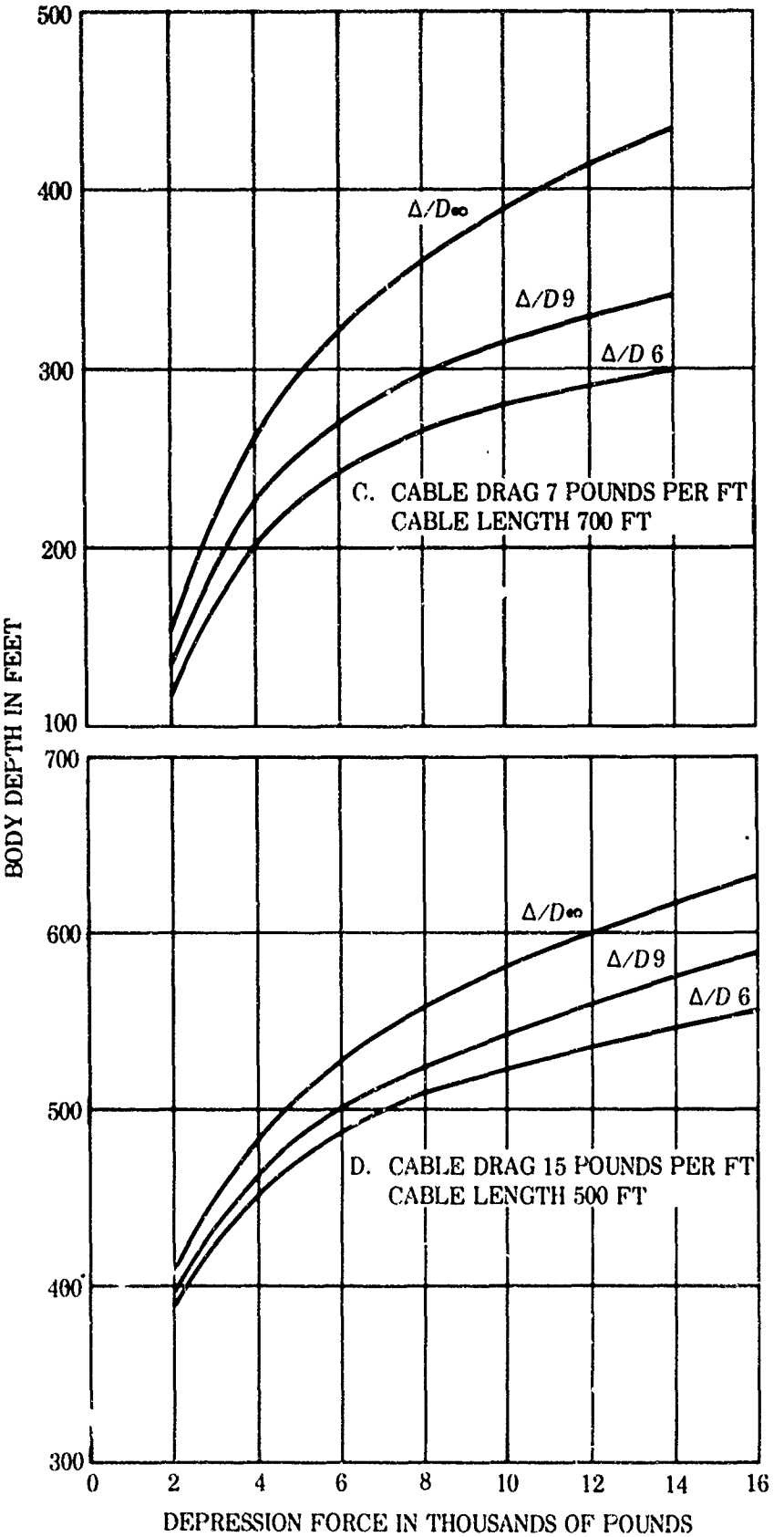

Figure 16 (Continued).

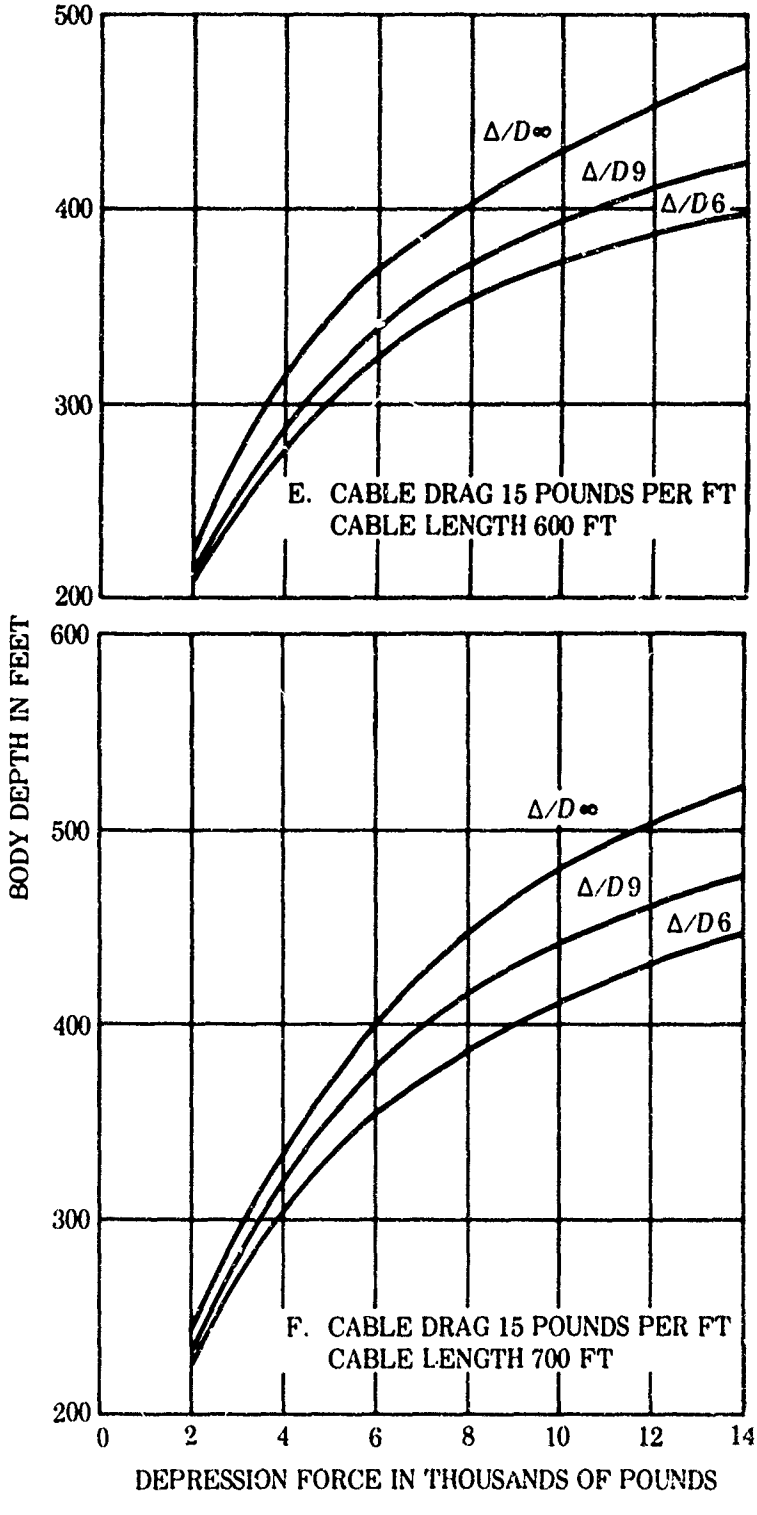

Figure 16 (Continued).

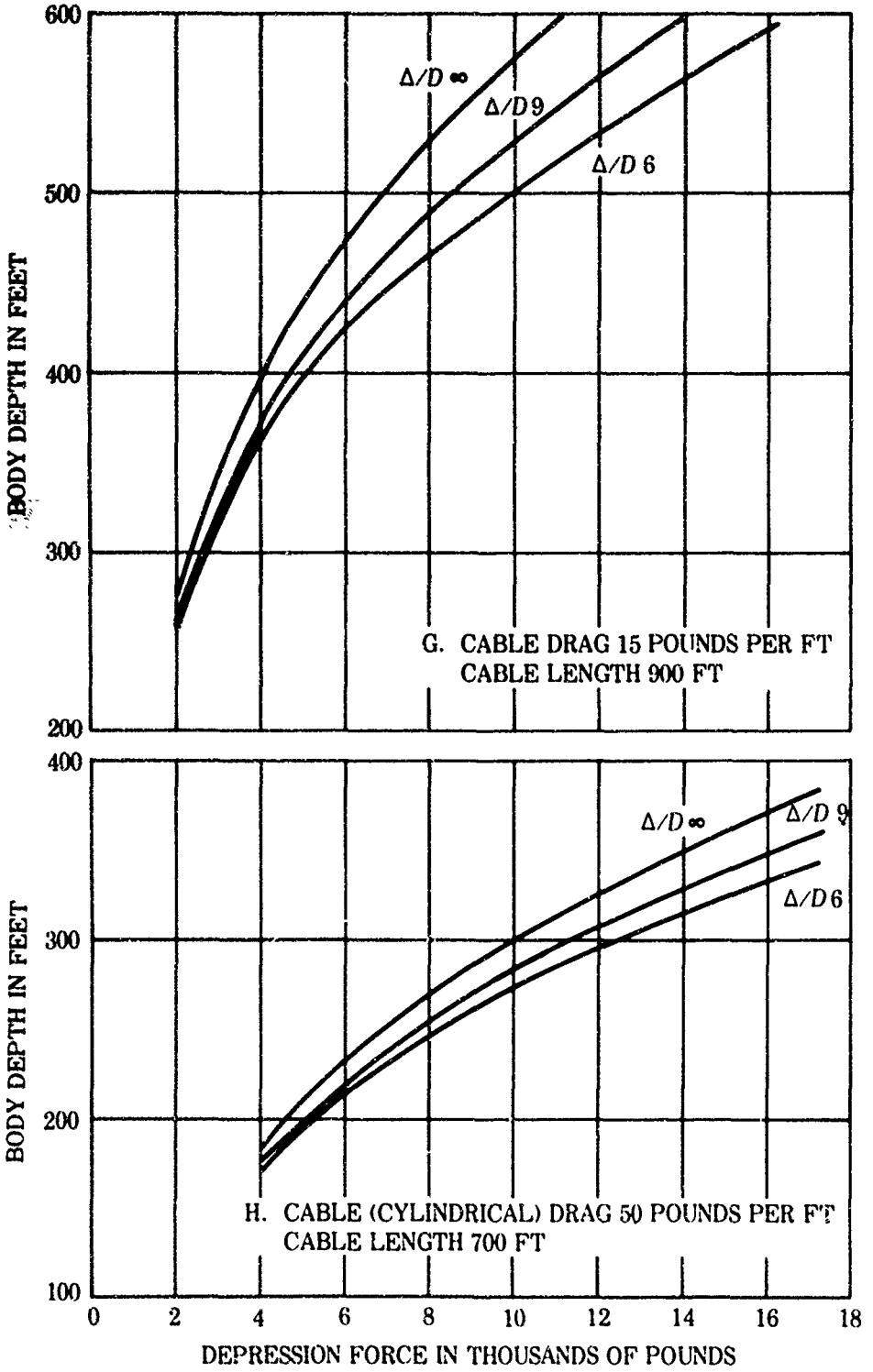

Figure 16 (Continued).

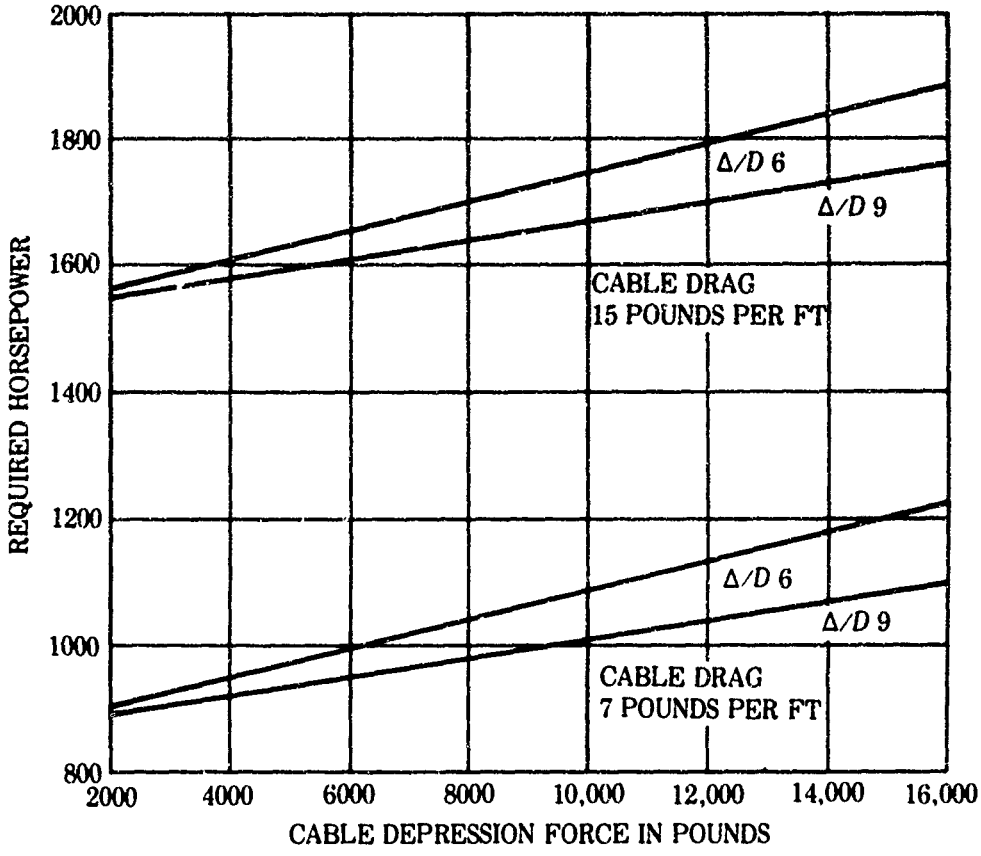

Figure 17. Required horsepower versus cable depression force; 600-foot cable, 2000-pound body drag, 45-knot speed.

NOISE CONSIDERATIONS

The tow body design must consider the random, statistical-type disturbances that are generated by surface activity and by the turbulent tow-body boundary. The recommended tow cable design features small, streamlined cross sections. The random energy generated in such a cable should be small, since the boundary layer is laminar and no cavitation should occur.

Most of the tow body surface has a turbulent boundary at 45 knots. The point of neutral transition to turbulence occurs at about 15 inches back of the nose, while the self-excited transition point occurs at about 22 inches back of the nose. The value of the broadband pressure for fully developed turbulence at the surface can be estimated. The ratio of the broadband pressure to the dynamic pressure of the flow is approximately constant at 0.0035 in most flow conditions in both air and water. The power spectrum of this flow-noise energy peaks at a particular value of the Strouhal number for both air and water at

normal speeds. The broadband flow-noise pressure expected at 45 knots is 79.72 dB above 1 dyne per square centimeter. Figure 17 shows a flow-noise power spectrum curve obtained from pipe flow. The nondimensional power spectrum is plotted against the nondimensional Strouhal number. The Strouhal number used is given by

$$\frac{\omega\delta}{U}$$

where U is the flow velocity

δ is the boundary layer thickness

ω is the angular frequency in radians per second

The power spectrum peaks at an angular frequency of 5618 radians per second or 894.12 cycles per second at 45 knots for a 0.5-inch boundary layer thickness.

The boundary layer thickness can be approximated by the nomograms of figures 19 and 20. Figure 19 gives the boundary layer thickness for both laminar

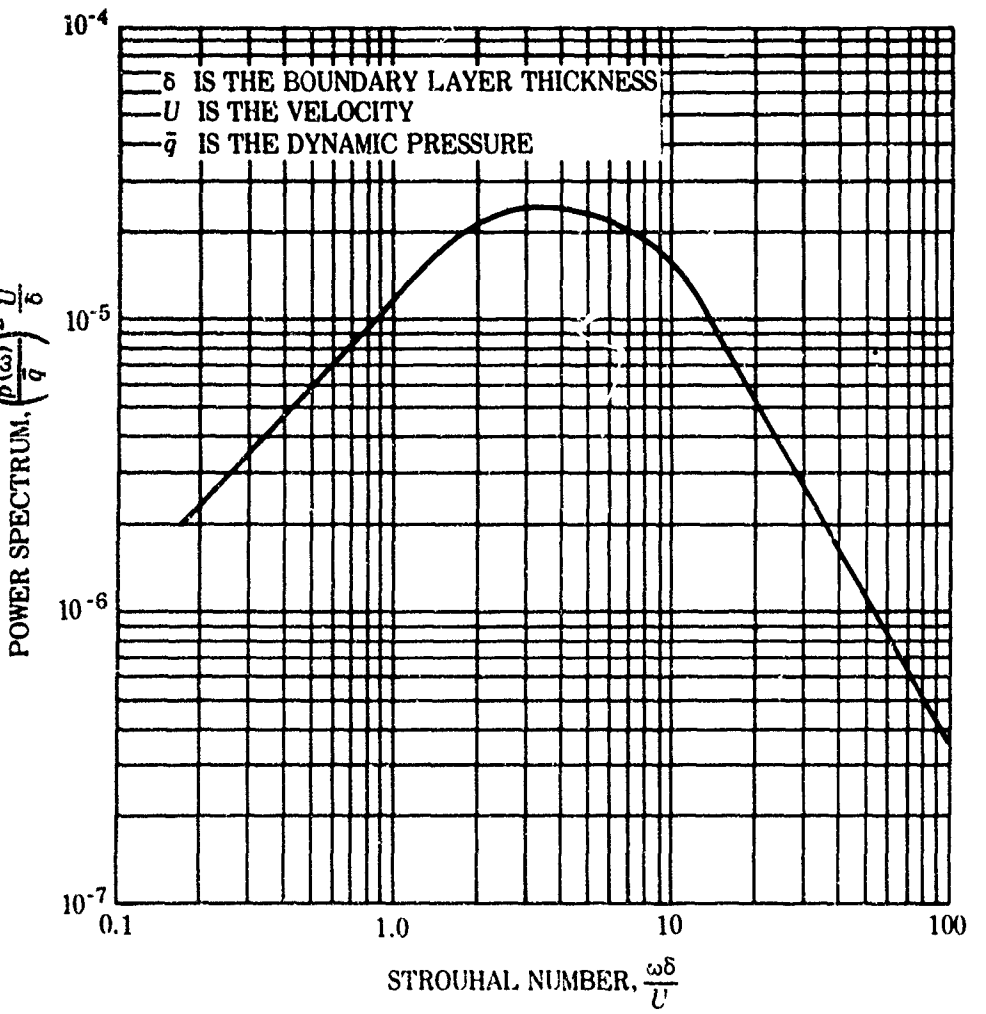

Figure 18. Flow noise power spectrum versus Strouhal number.

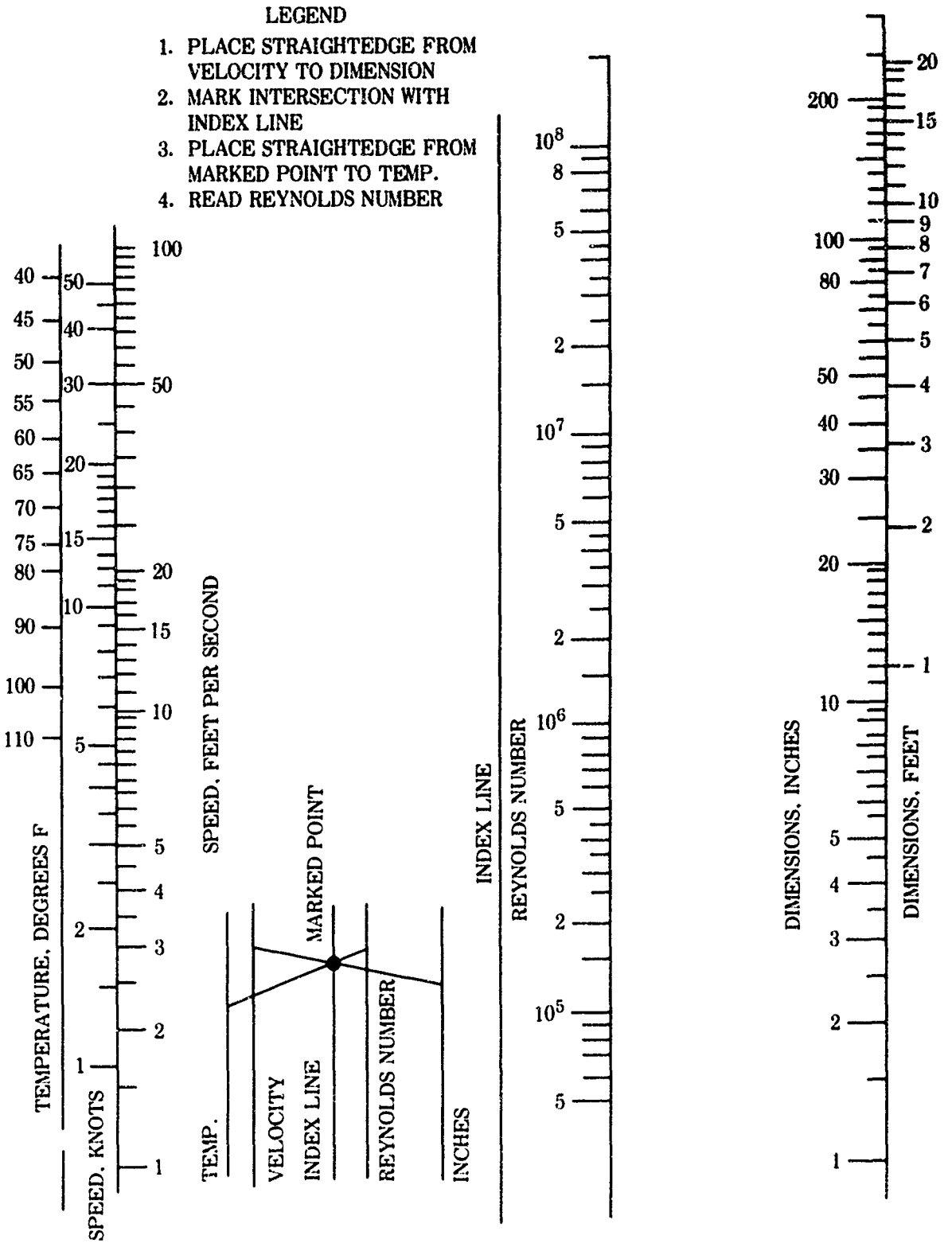

Figure 19. Nomogram giving Reynolds number in water at normal temperatures.

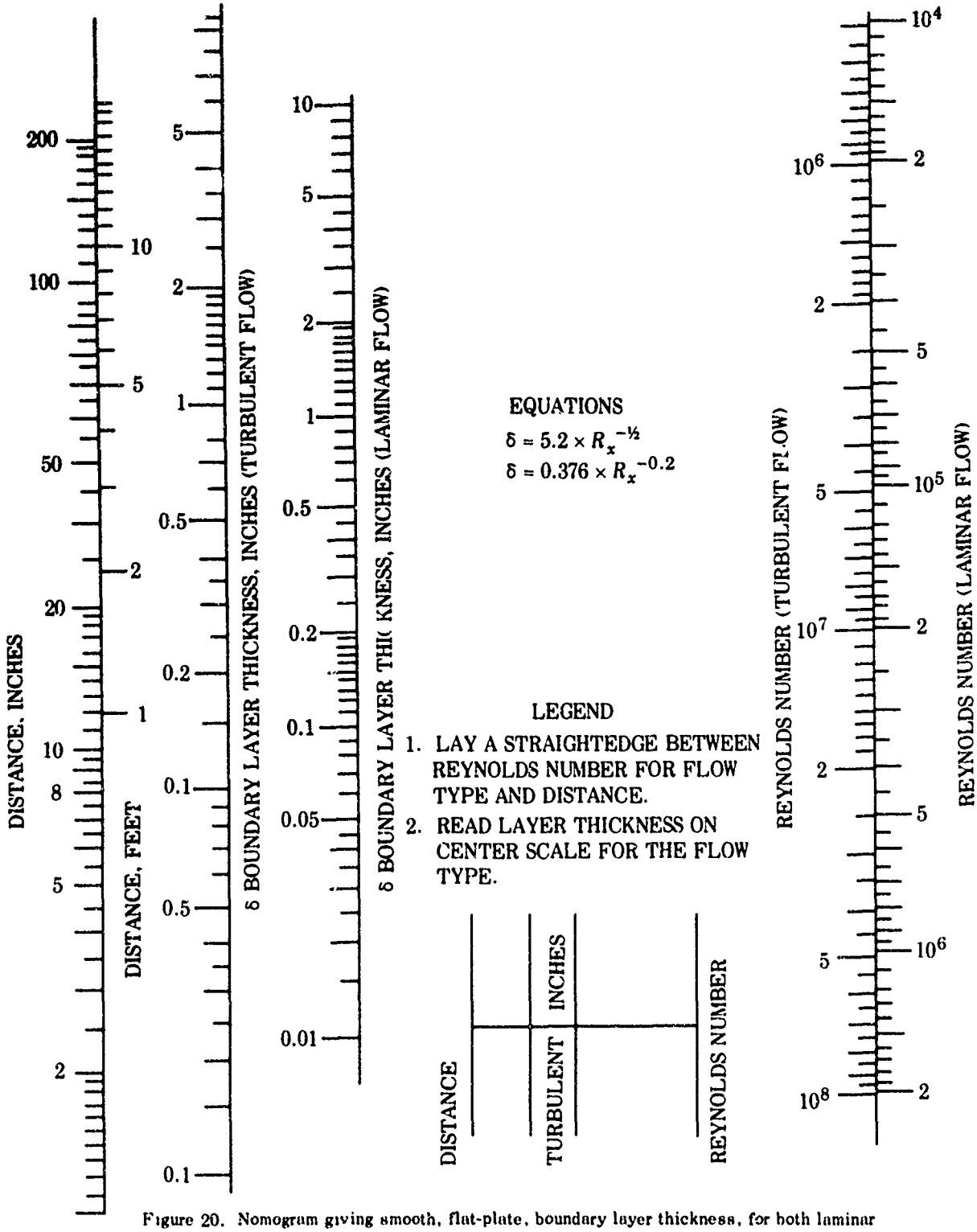

Figure 20. Nomogram giving smooth, flat-plate, boundary layer thickness, for both laminar and turbulent flow

and turbulent flow over a flat plate corresponding to the Reynolds number at the point; the Reynolds number can be obtained from figure 18. As an example, assume the distance is 10 inches at 45 knots for 50°F water. The Reynolds number becomes 4.4×10^6. The boundary layer thickness is 0.17 inch. The peak of the power spectrum should occur at 16,523 radians per second or 2629.8 cycles per second. A representative boundary layer thickness for Body A is about 0.5 to 0.7 inch.

Random energy generated at the surface by ship's motion and wave motion applies an input to the towing cable. The spectrum of this energy is probably fairly wide-band. The towing cable conducts some of this energy down the cable in the form of compressional and transverse waves, the cable acting as a filter. The average input power to the cable is given by

$$P_i = \frac{1}{2\pi} \int_{-\infty}^{\infty} \Phi(\omega) d\omega$$

where $\Phi(\omega)$ is the input power spectrum.

The power output from the cable is given by

$$P_0 = \frac{1}{2\pi} \int_{-\infty}^{\infty} |G_c|^2 \Phi(\omega)\, d\omega$$

where G_c is the transfer function of the cable.
If the cable is represented by a simple low-pass filter with a transfer function of

$$\frac{1}{1 + RCs}$$

and the input power spectrum is white noise, the output power becomes

$$\frac{K}{2RC}$$

where K is the constant white-noise spectrum.

The towing cables probably filter out much of the input surface energy even at frequencies below 1000 cycles per second.

RESULTS AND CONCLUSIONS

The following results and conclusions are based on a mathematical analysis of the motion of underwater towed bodies:

1. A practical tow body, designated Body A, was designed. The maximum diameter is 30 inches, and the main-body length/diameter ratio is 2.7.
2. The tie-point location was shown to be important to the body's stability. It should be forward and above the body's center of gravity.

3. The hydrodynamic coefficients can be predetermined to a fair degree of accuracy. A mathematical model can be set up which can be checked on analog or digital computers.
4. The most important parameters determining the dominant, characteristic equation roots for both longitudinal and lateral motion are the cable tension and the damping coefficients, C_{mq} and C_{nr}. The root values determine the body's stability and transient response.
5. The body drag is an important parameter determining the required towing horsepower and the attainable depth. The total body drag is the sum of the drags due to the main body, the depressor wing, the tail surfaces, and induced drag. Induced drag is a considerable portion of the total drag. The minimum attainable drag under idealized conditions is probably about 1750 pounds at 45 knots.
6. Tow bodies can be easily designed to have longitudinal and lateral dynamic stability. The hydrodynamic coefficients have the major influence on the roots of the characteristic equations.
7. The tow bodies without automatic controls are "Type 0" systems. They follow step inputs of the control surfaces with a following error.
8. The depressor wing area should be sufficient to produce high depression forces at low value of lift coefficients. Low lift coefficients and high aspect ratios reduce the induced drag.
9. A depressor-wing dihedral angle is required if the tie point is at the body's center of gravity. A negative dihedral coefficient is more favorable than a positive coefficient in its effect on the dominant cable root. A better lateral control system can be obtained with a positive coefficient.
10. In choosing the tow body construction materials, one should consider the pressure fluctuations of random flow noise.
11. The control surfaces can be designed with sufficient area to provide an acceptable degree of control effectiveness.
12. Control systems greatly improve the transient characteristics. The stability and damping can be favorably changed.
13. A longitudinal control system is presented. This system, in addition to holding the tow body at a commanded depth, improves the damping and stability.
14. A lateral control system is presented. This system improves the stability and damping, coordinates the rudder and ailerons so that no skidding occurs during turns, and provides a yaw-rate directional control for the tow body.
15. Intercoupling of the longitudinal and lateral motion is very small even without automatic controls. Roll damping of the tow body itself is excellent.
16. Turning is considerably aided by the introduction of turn coordination. The required bank angle is less than 5 degrees for a 300-foot-radius turn for Body A at 45 knots.
17. Flow noise study indicates a broadband pressure of 80 dB above 1 dyne per cm^2 in the turbulent boundary layer of the tow body. A nondimensional power spectrum curve is presented. The frequency at which the power spectrum peaks depends on the speed and the boundary layer thickness. Nomograms are presented which can be used to estimate the boundary layer thickness.
18. The streamlined towing cable attenuates much of the higher-frequency random energy travelling down the cable, particularly for transverse modes.
19. The attainable depths and required horsepower depend primarily on the towing cable. The tow body's depression force/drag ratio must be large. Small-cross-section, laminar-flow streamlined cables are required for the low drag per foot, and for the prevention of cavitation at all depths.

BIBLIOGRAPHY

Blakelock, J. H., Automatic Control of Aircraft and Missiles, Wiley, 1965

David Taylor Model Basin Report 719, Mathematical Formulation of Bodies of Revolution, by L. Landweber and M. Gertler, September 1950

David Taylor Model Basin Report 752, A Method For the Calculation of the Turbulent Boundary Layer in a Pressure Gradient, by P. S. Granville, May 1951

Dommasch, D. O. and others, Airplane Aerodynamics, Pitman, 1951

Etkin, B., Dynamics of Flight: Stability and Control, Wiley, 1959

Hansen, H. M. and Chenea, P. F., Mechanics of Vibration, Wiley 1952

Hoerner, S. F., Fluid-Dynamic Drag; Practical Information on Aerodynamic Drag and Hydrodynamic Resistance, 3d ed., Midland Park, New Jersey, 1965

Navy Electronics Laboratory Report 1223, Flow Noise Study of Water Flowing Through Pipes, by P. O. Laitinen, 13 May 1964

Perkins, C. D. and Hage, R. E., Airplane Performance Stability and Control, Wiley, 1949

Shinners, S. M., Control System Design, Wiley, 1964

Williams, J. E. F., "The Noise of High Speed Missiles," Chapter 6 in v.2 of Crandall, S. H., Random Vibration, 2v., Technology Press of the Massachusetts Institute of Technology, 1958-1963

Willmarth, W. W., "Wall Pressure Fluctuations in a Turbulent Boundary Layer," Acoustical Society of America, Journal, v.28, p.1048-1053, November 1956

APPENDIX A: BODY A TRANSFER FUNCTIONS

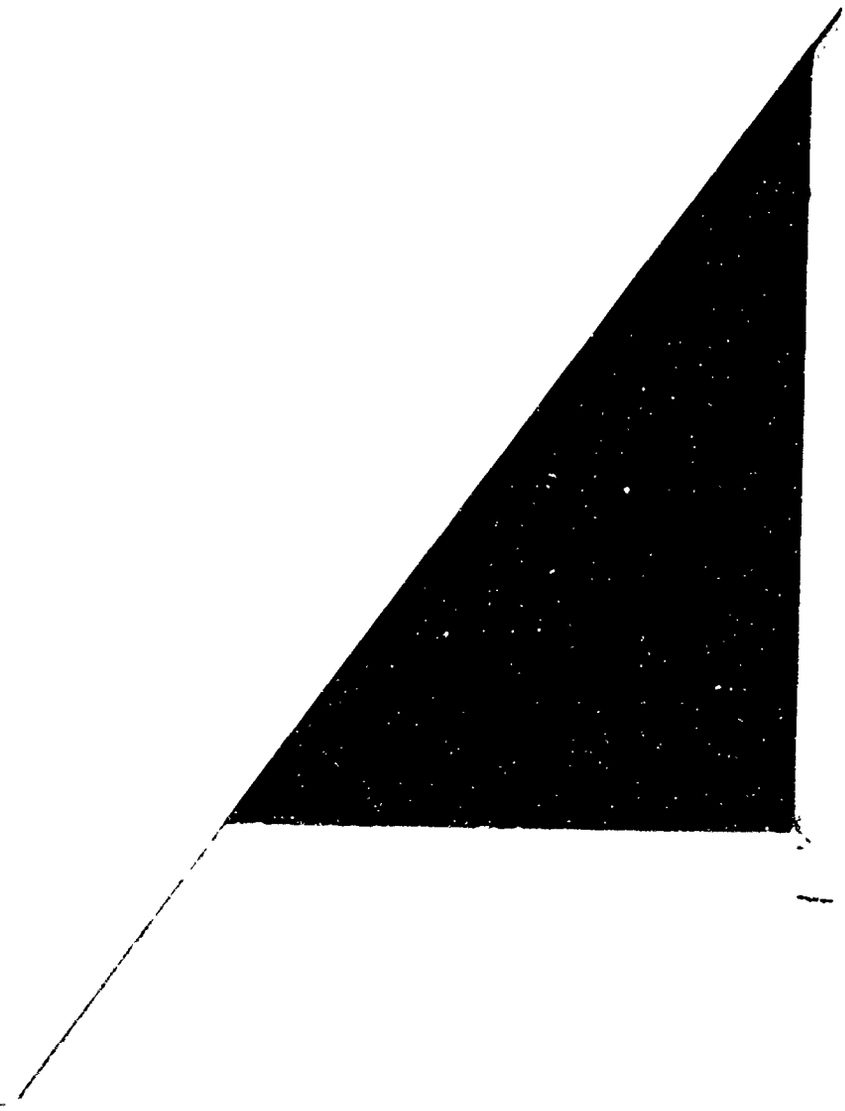

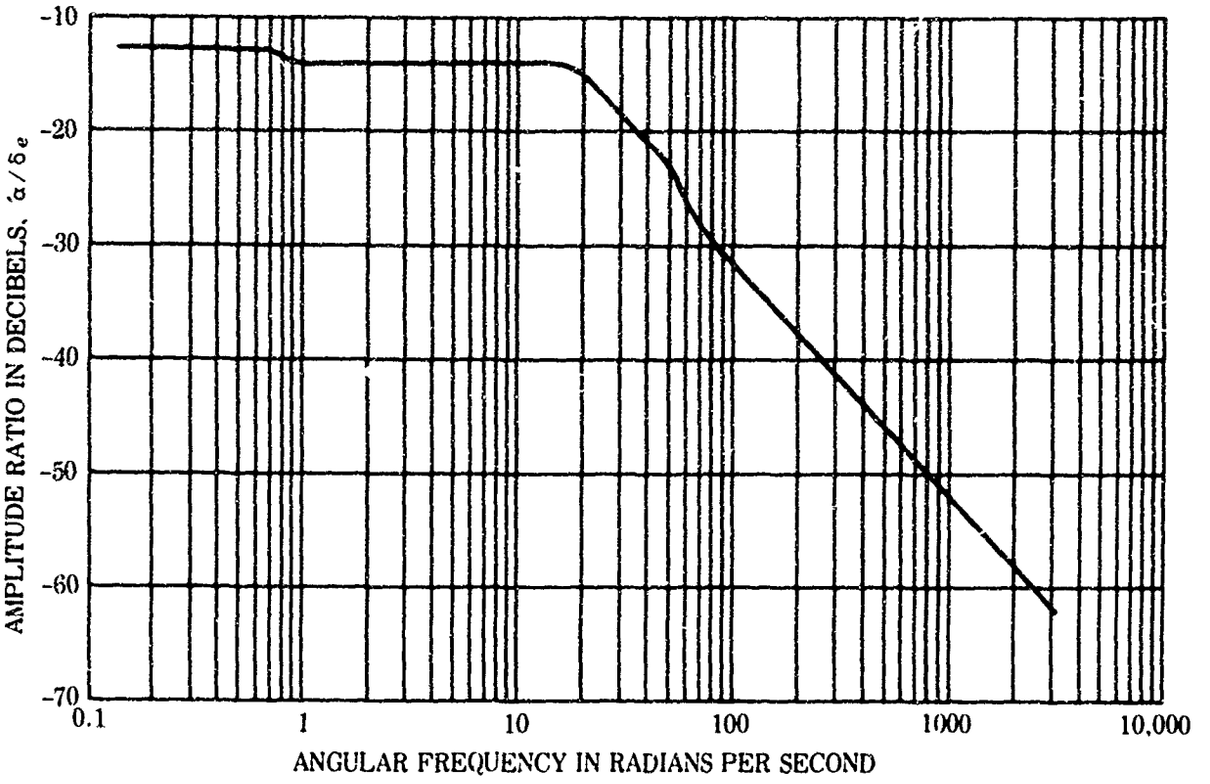

Figure A-1. Angle of attack – elevator angle; short solution.

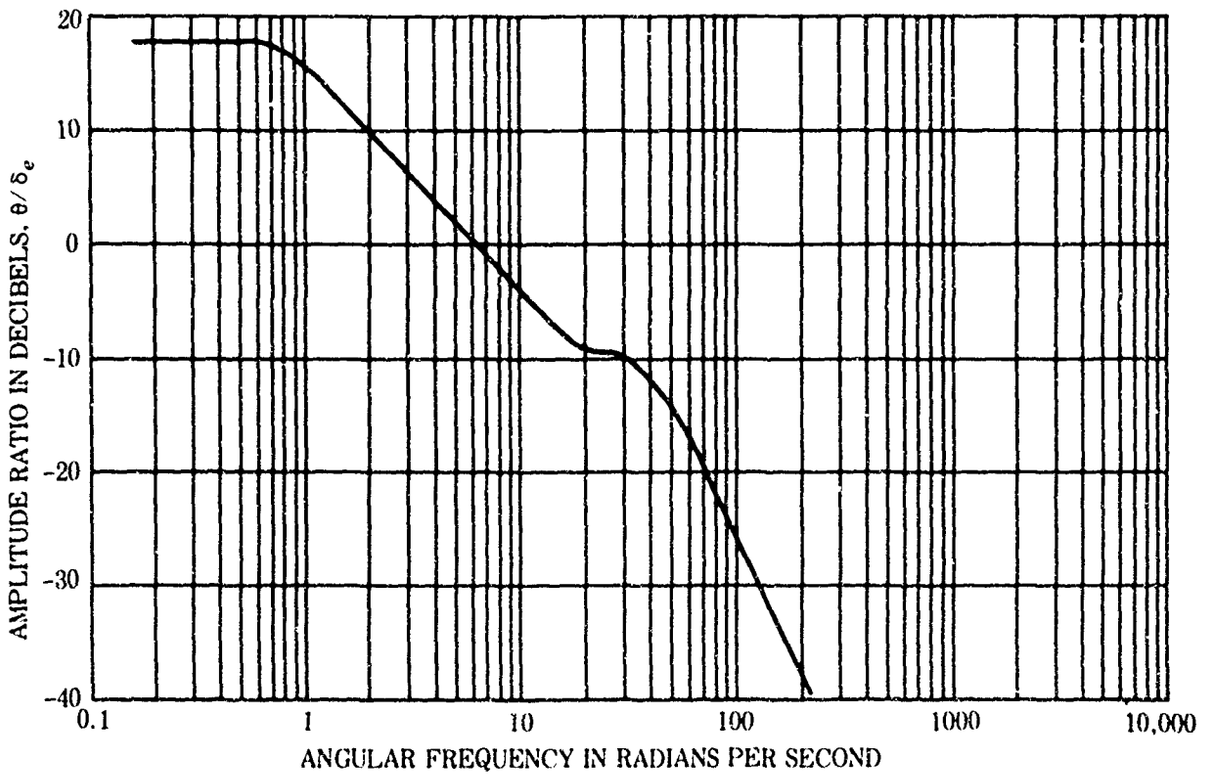

Figure A-2. Attitude angle – elevator angle; short solution.

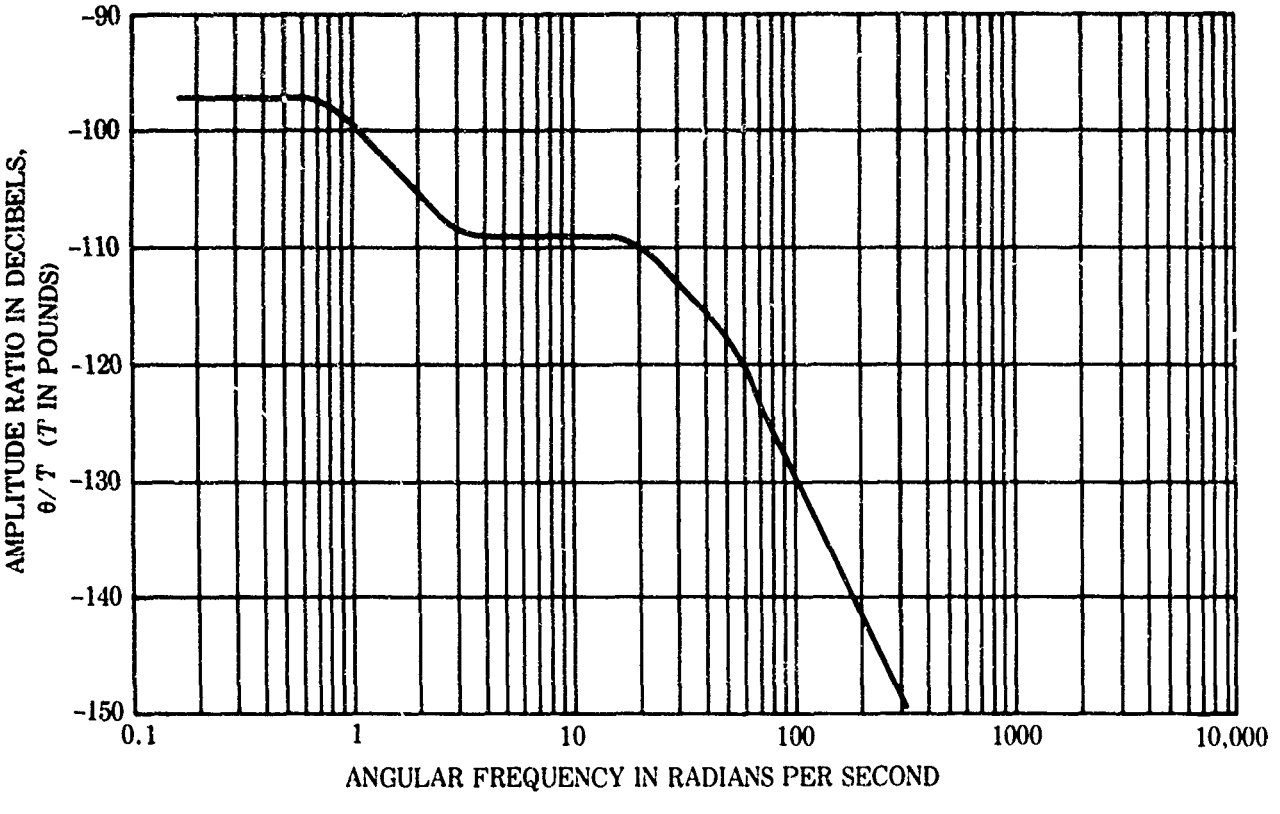

Figure A-3. Attitude angle – cable tension; short solution.

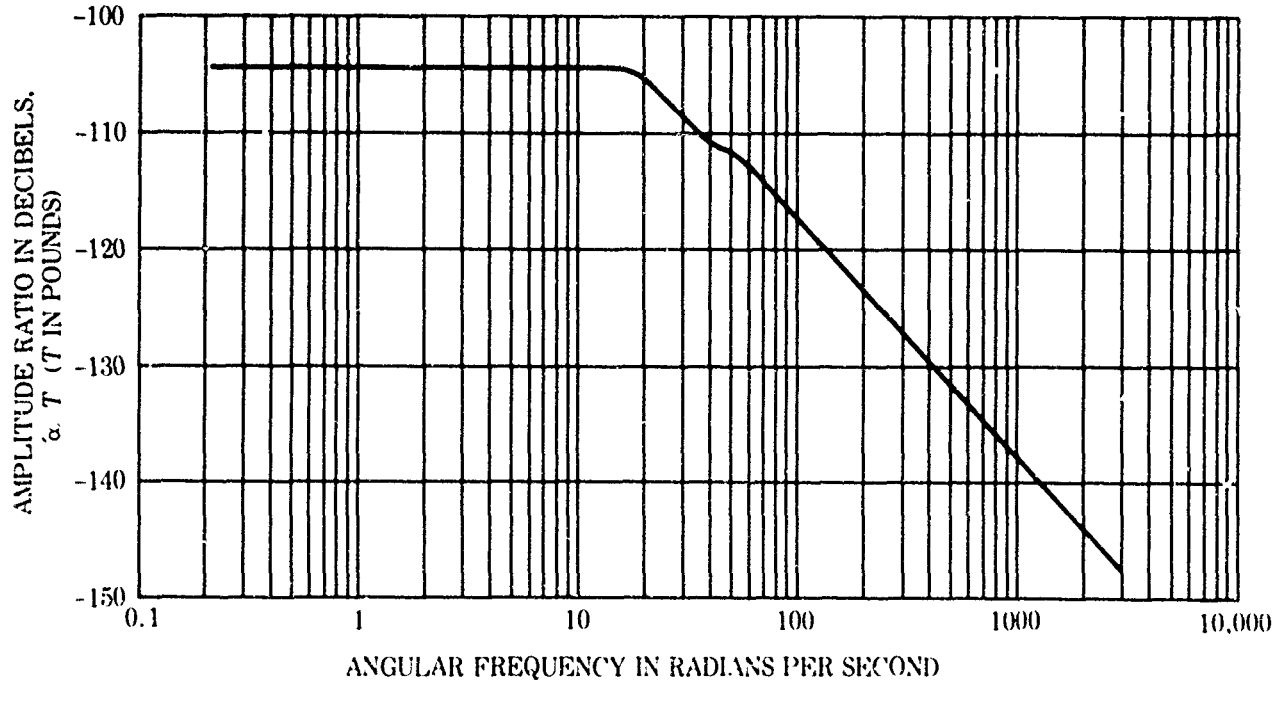

Figure A-4 Angle of attack – cable tension; short solution.

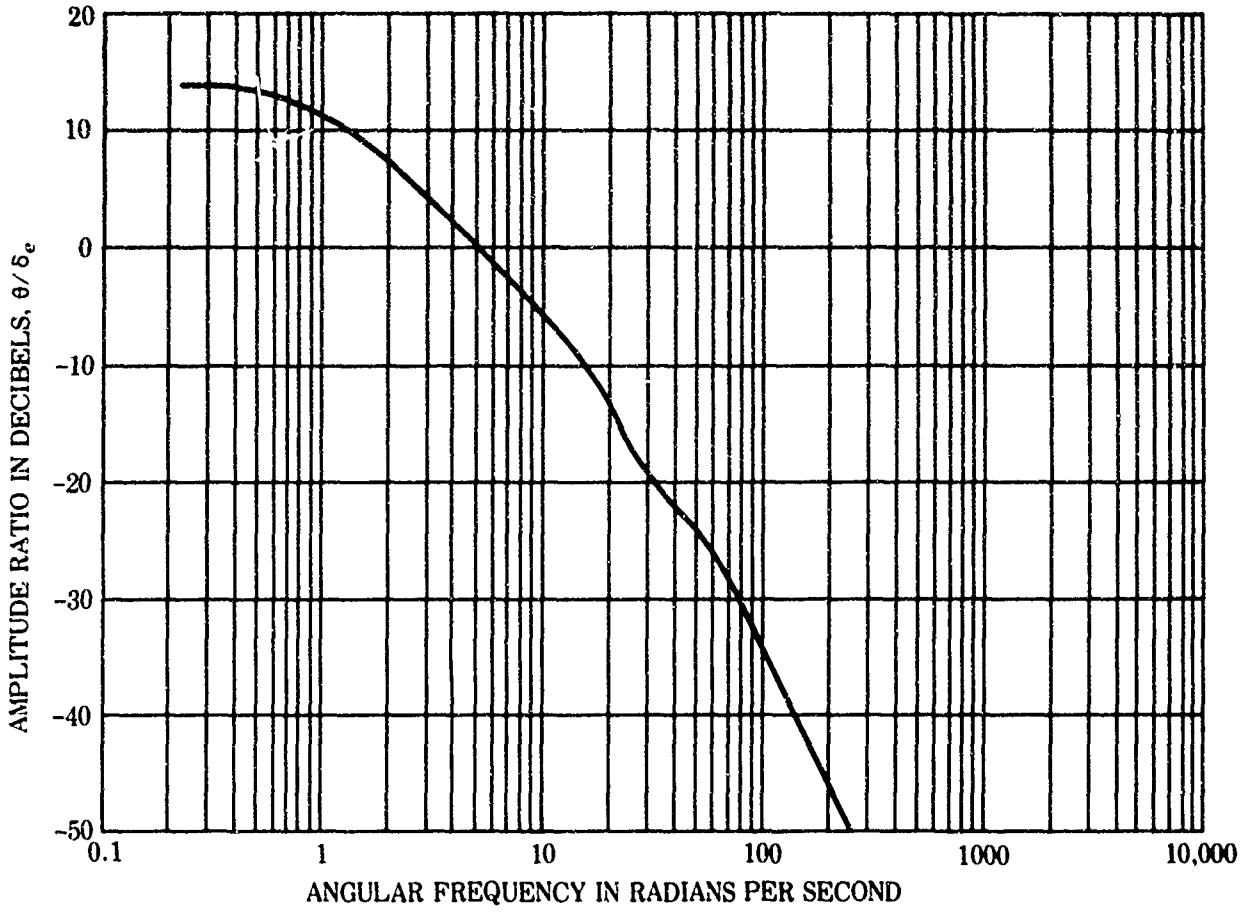

Figure A-5. Attitude angle – elevator angle; complete longitudinal solution.

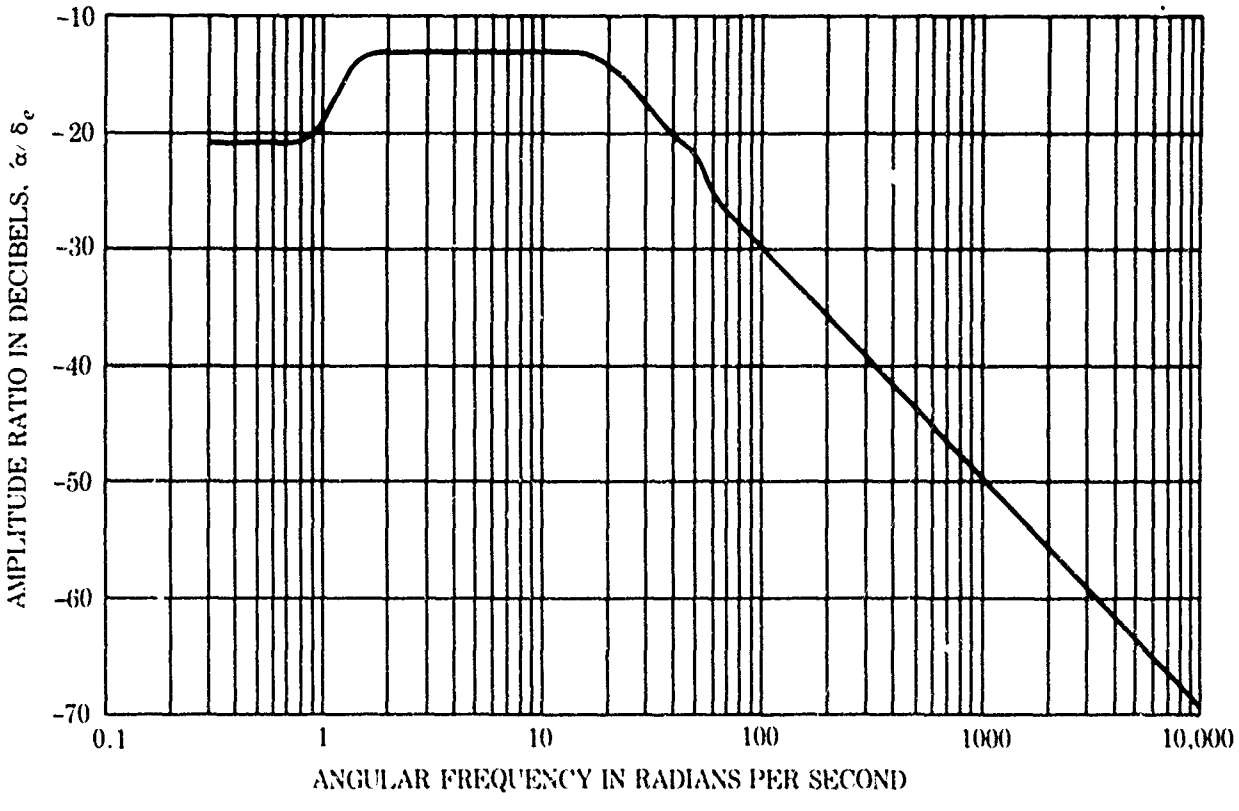

Figure A-6 Angle of attack – elevator angle; complete longitudinal solution.

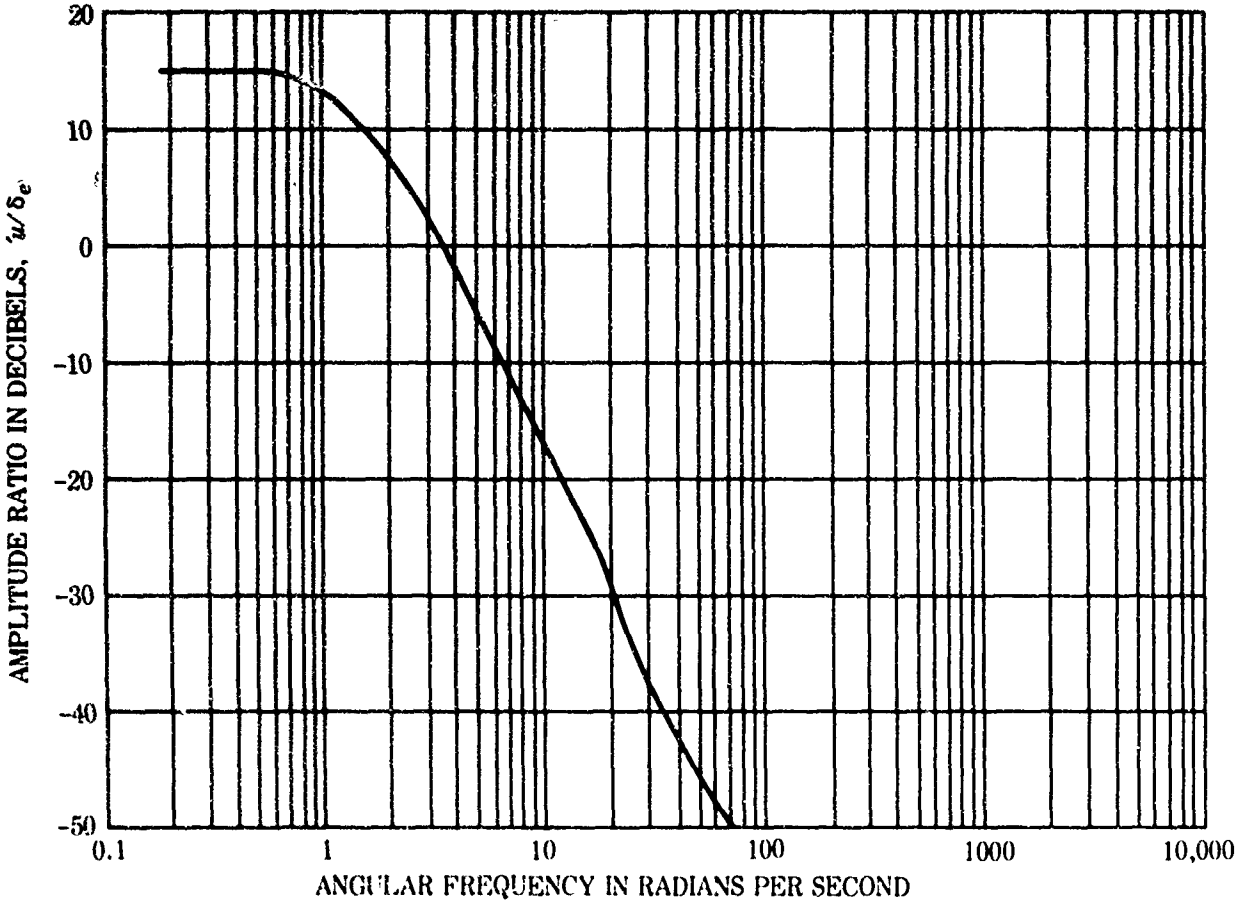

Figure A-7. Forward velocity – elevator angle; complete longitudinal solution.

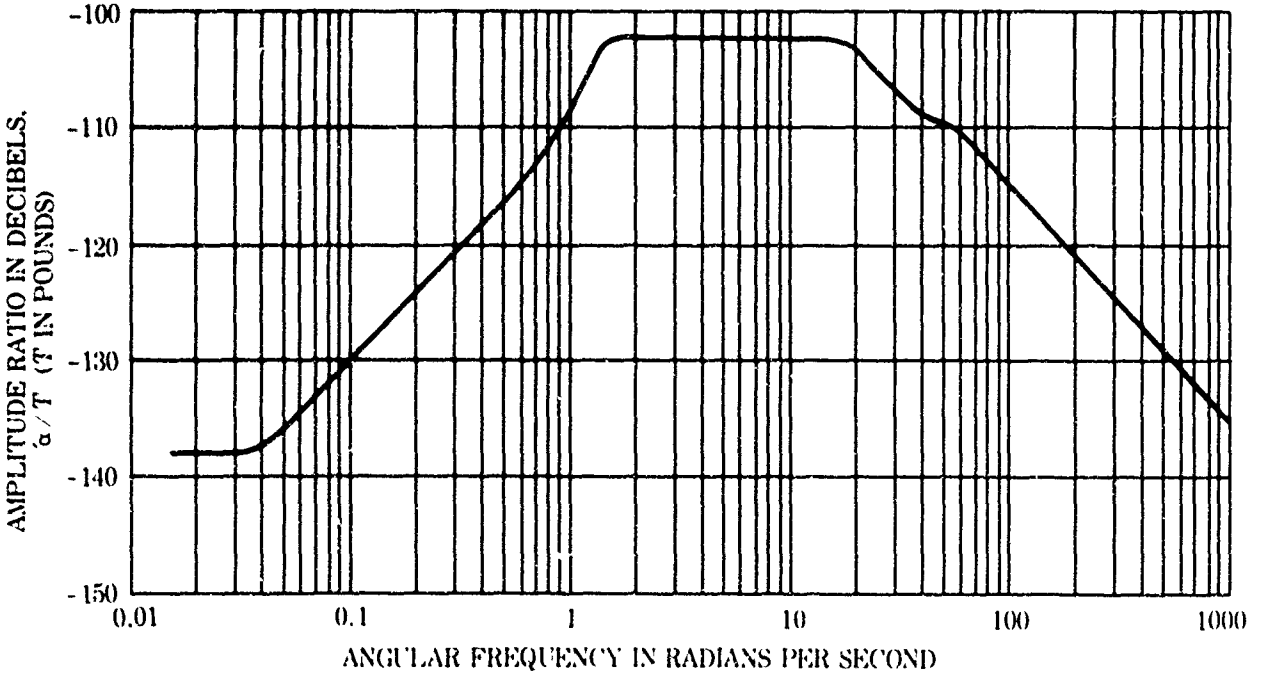

Figure A-8. Angle of attack – cable tension; complete longitudinal solution

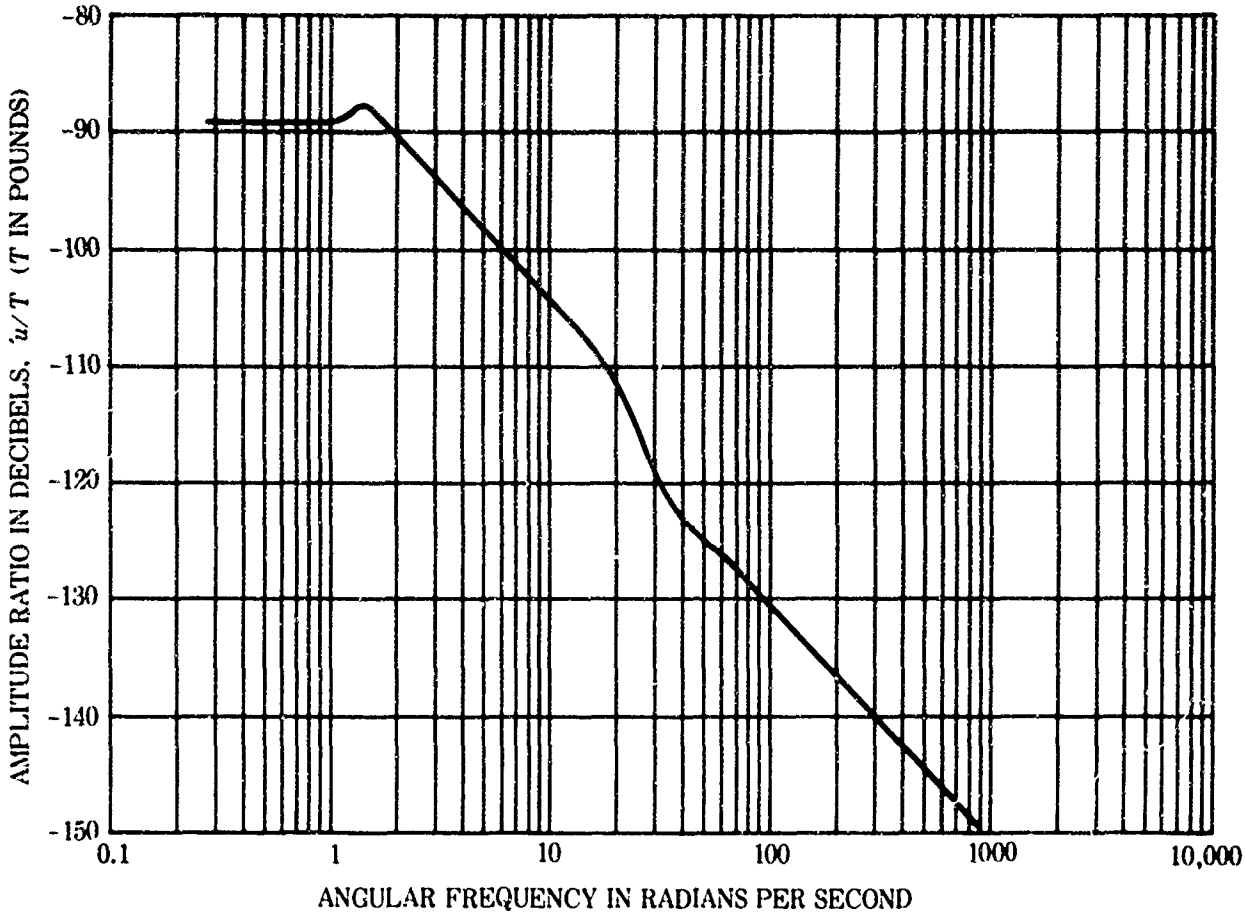

Figure A-9. Forward velocity – cable tension; complete longitudinal solution.

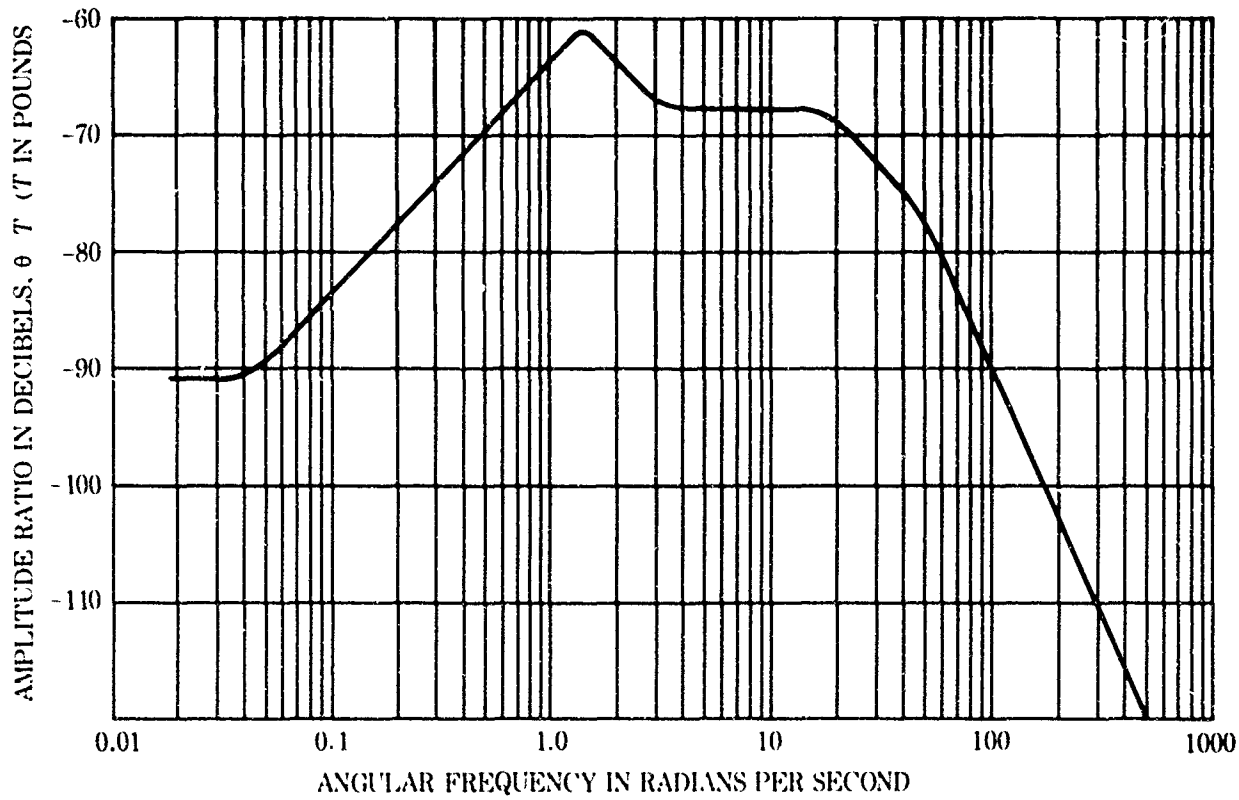

Figure A-10. Attitude angle – cable tension; complete longitudinal solution

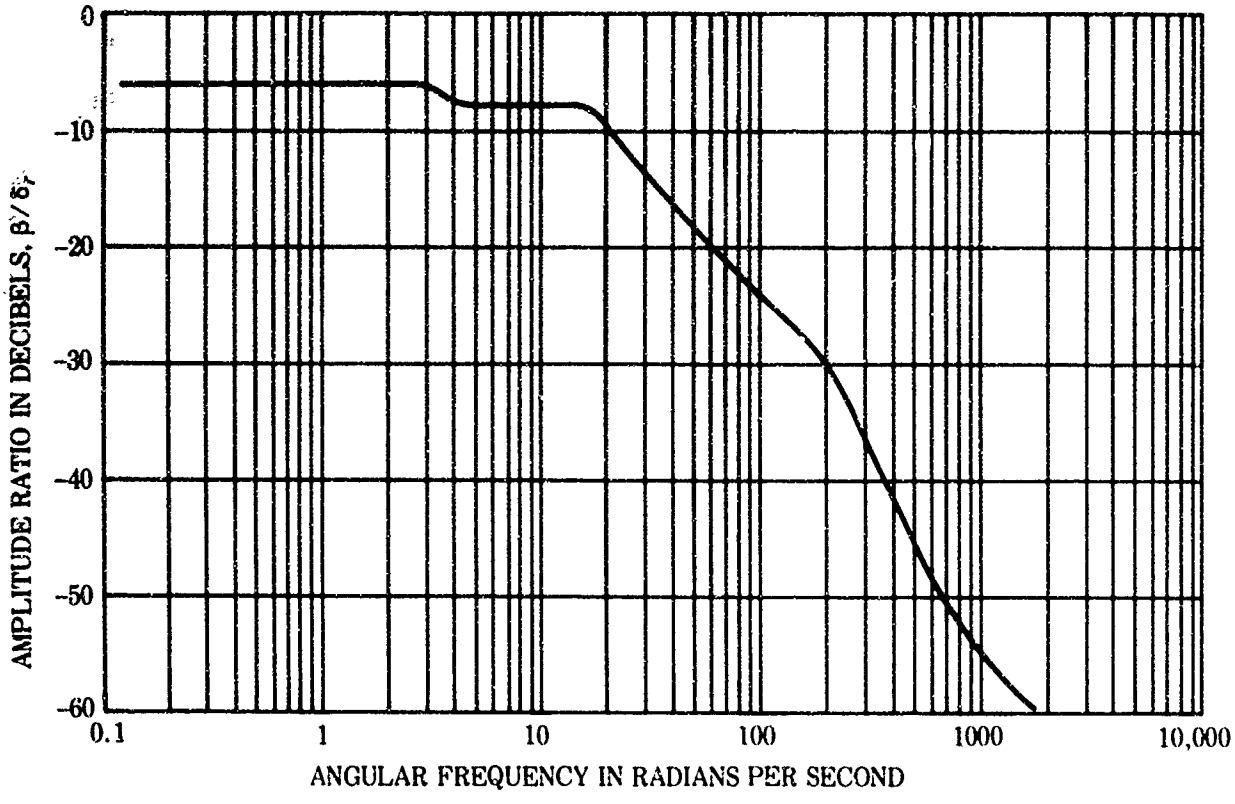

Figure A-11. Side-slip angle – rudder angle.

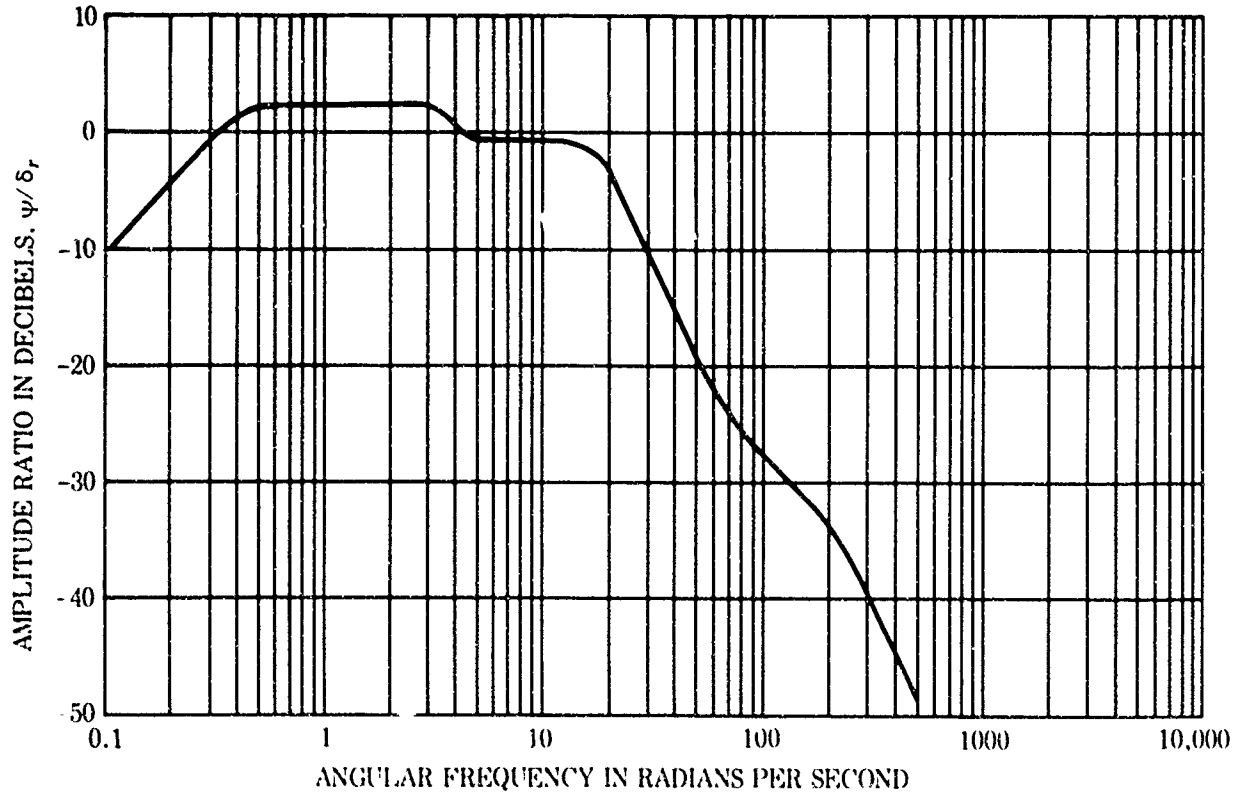

Figure A-12. Yaw angle – rudder angle.

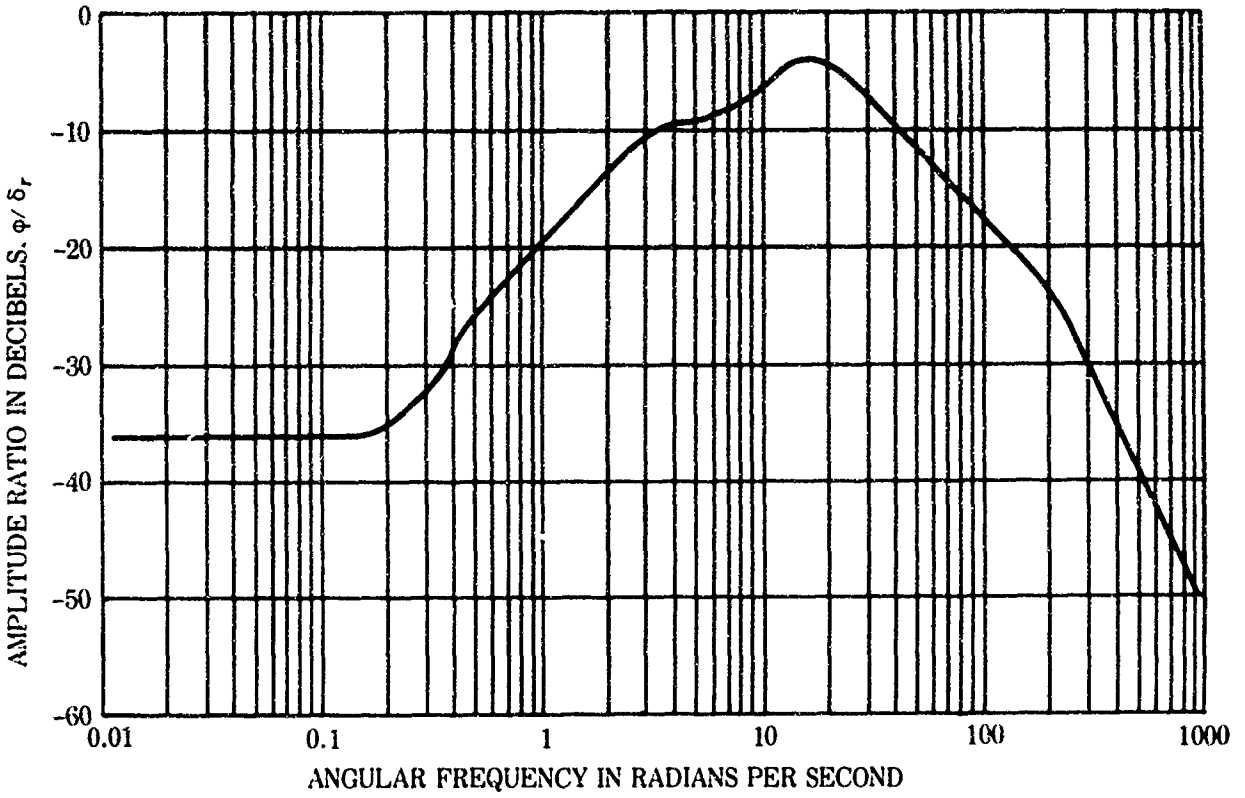

Figure A-13. Roll angle – rudder angle.

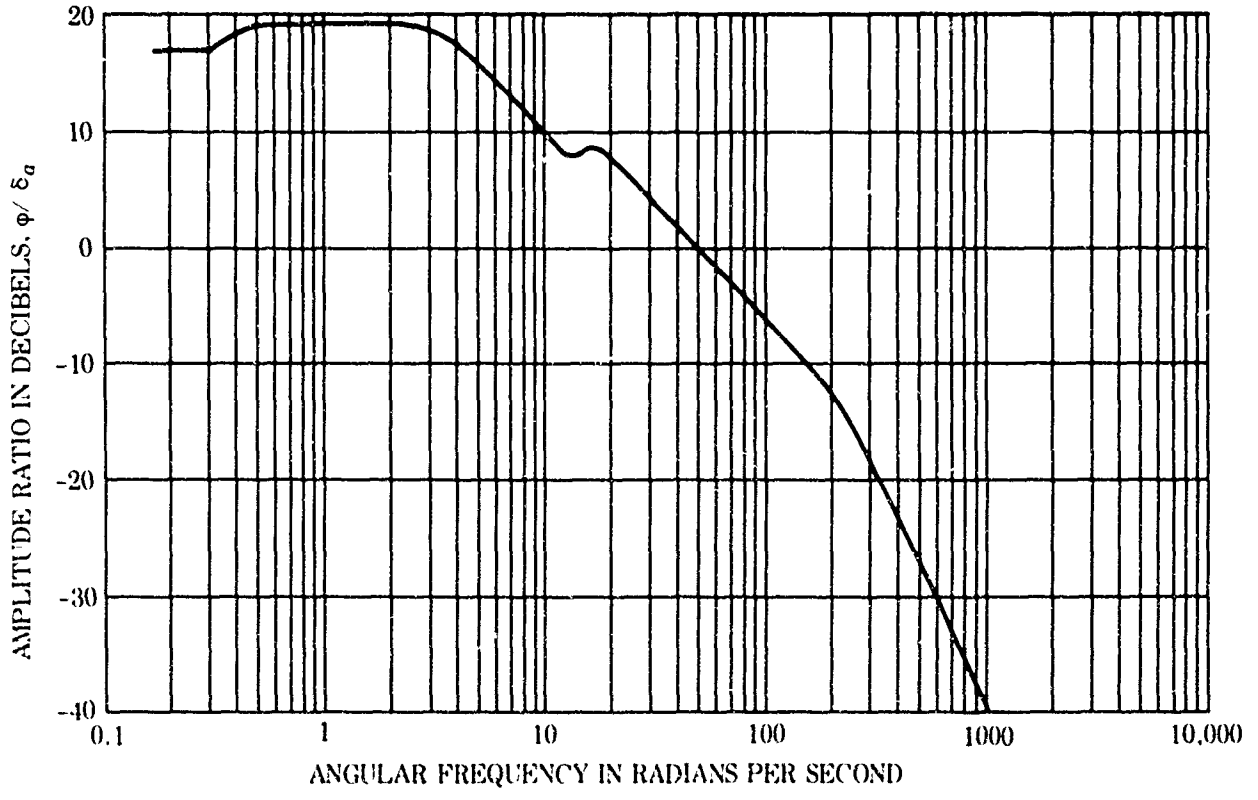

Figure A-14. Roll angle – aileron angle

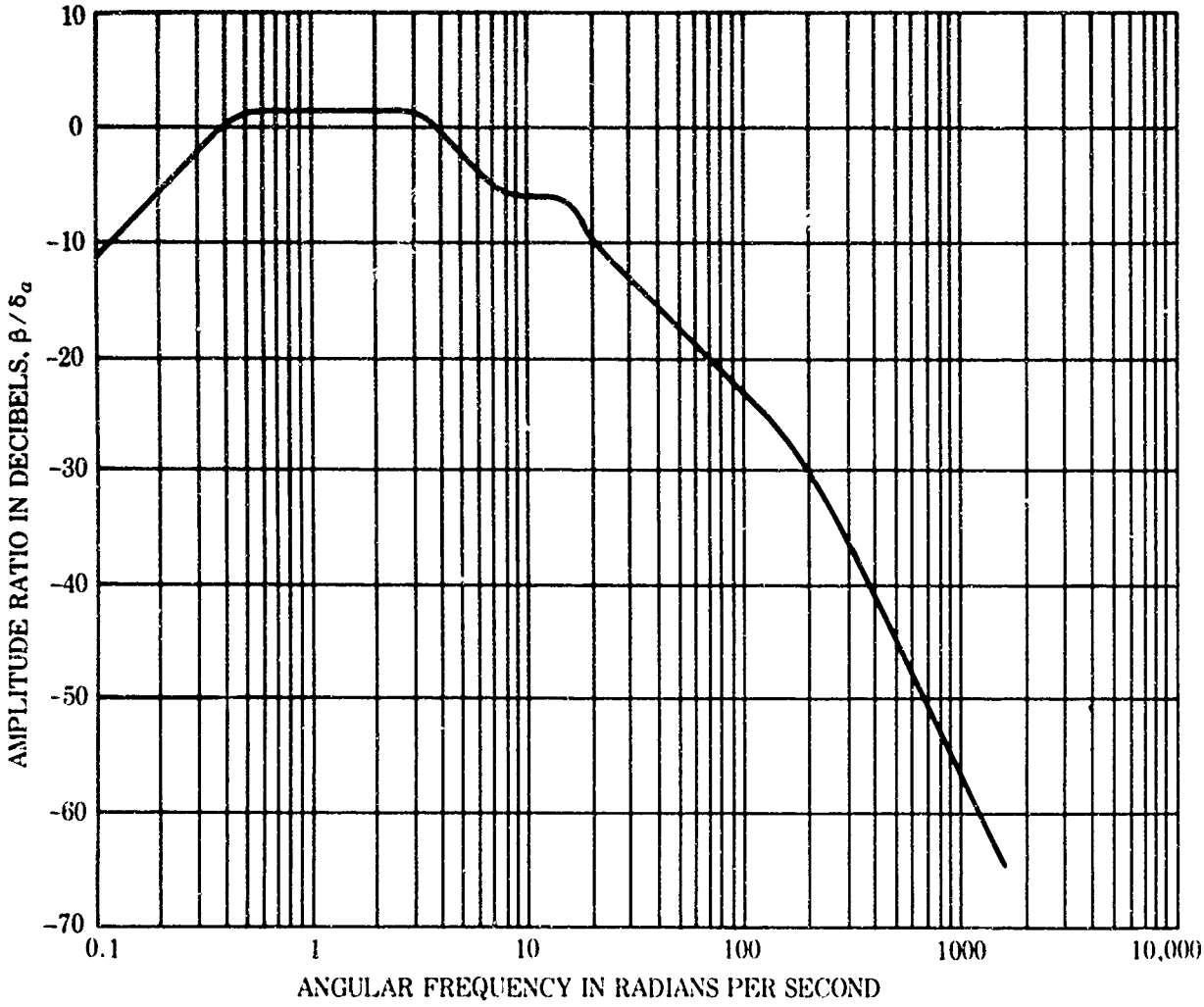

Figure A-15. Side-slip angle – aileron angle.

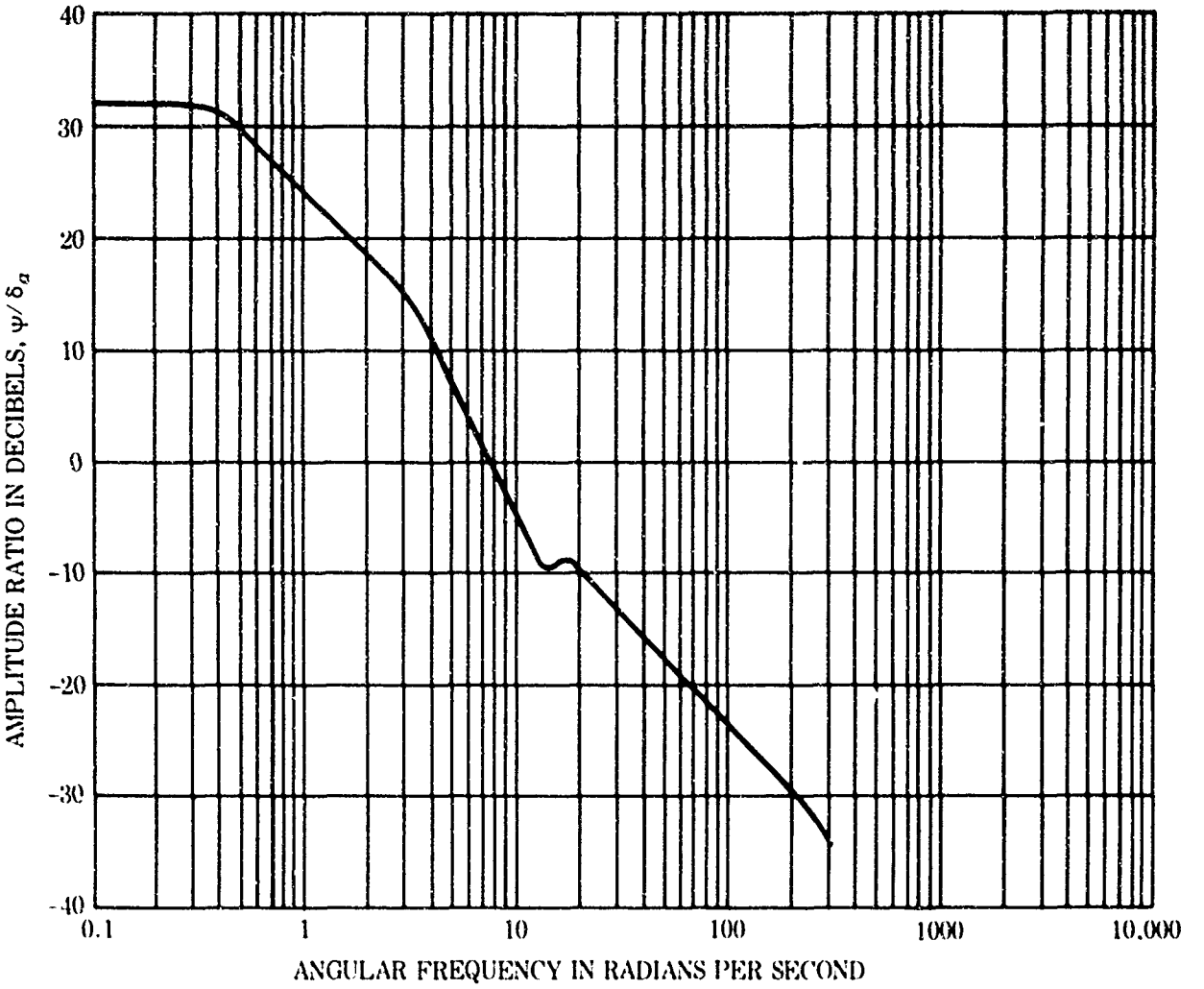

Figure A-16. Yaw angle – aileron angle.

REVERSE SIDE BLANK

APPENDIX B: BODY A TRANSFER FUNCTIONS

B

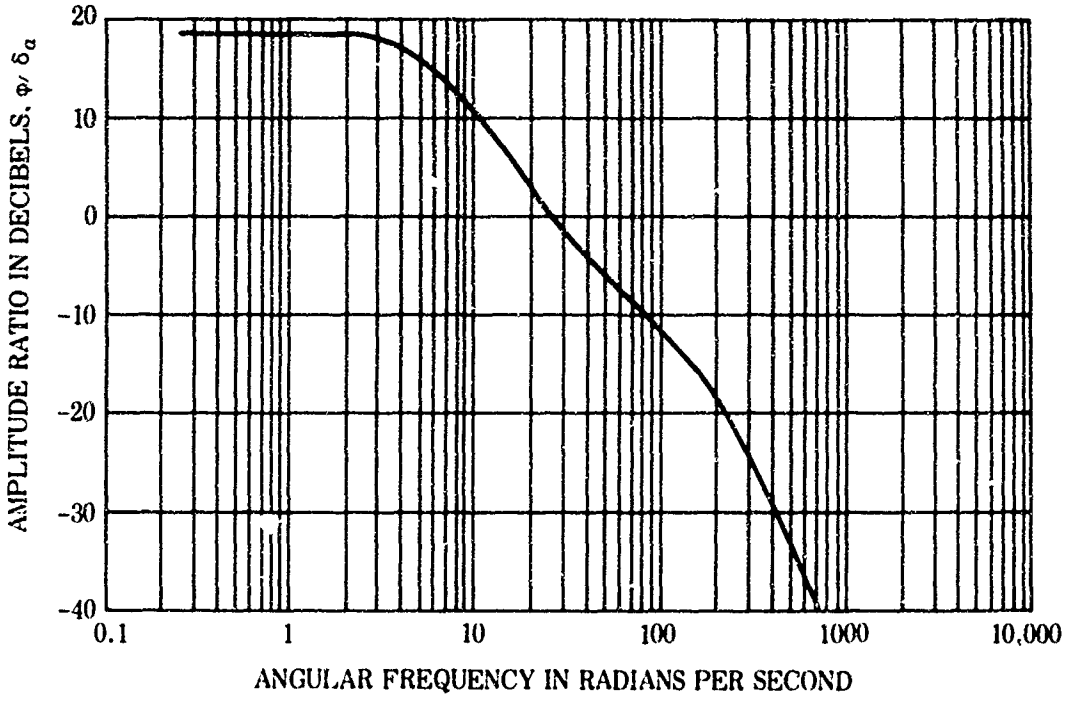

Figure B-1. Roll angle – aileron angle; $C_{\ell\beta}$

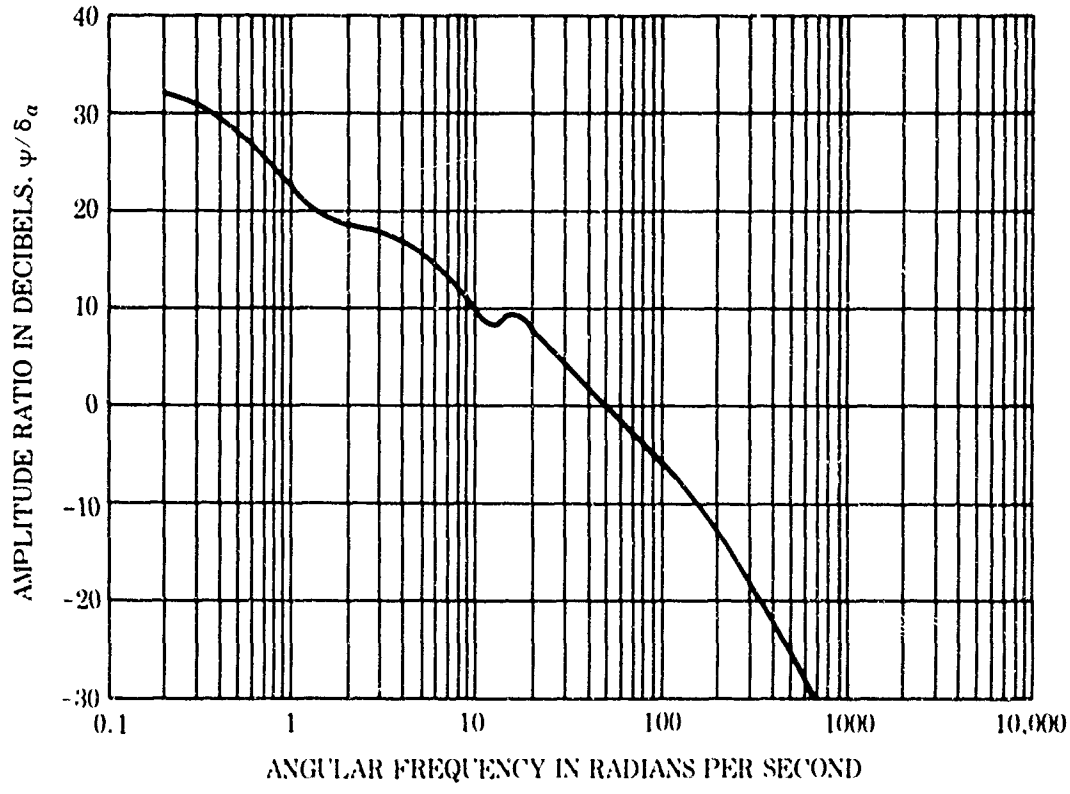

Figure B-2 Yaw angle – aileron angle, $C_{\ell\beta}$

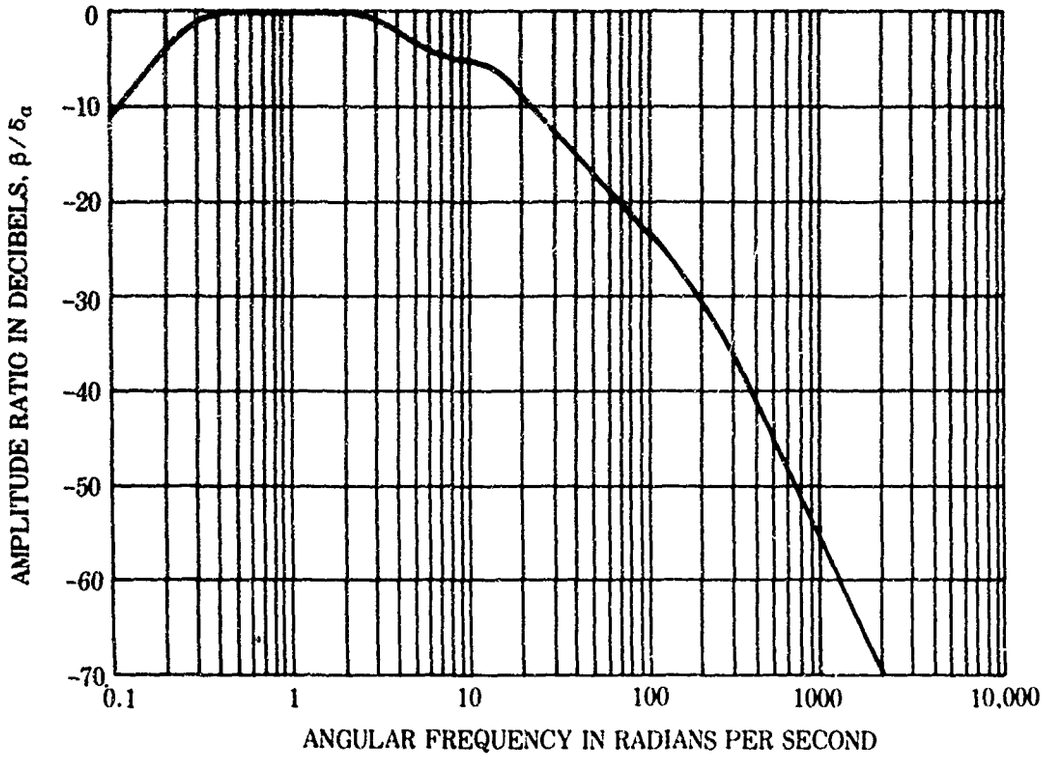

Figure B-3. Side-slip angle – aileron angle; $C_{\ell\beta}$

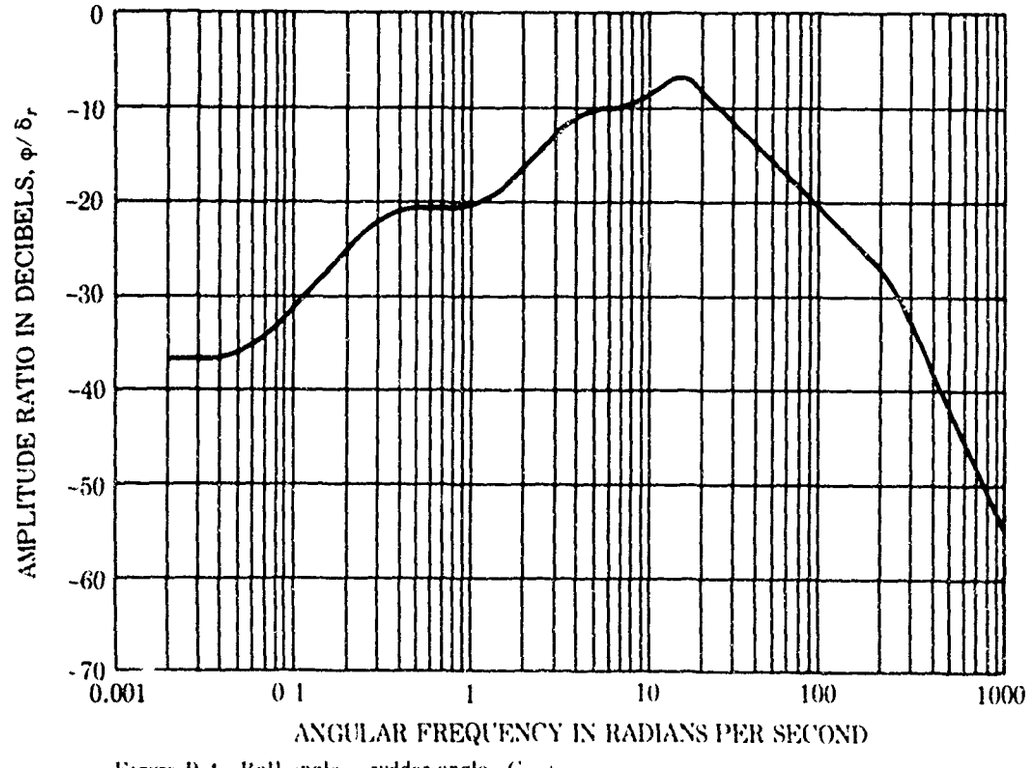

Figure B-4 Roll angle – rudder angle, $C_{\ell\beta}$

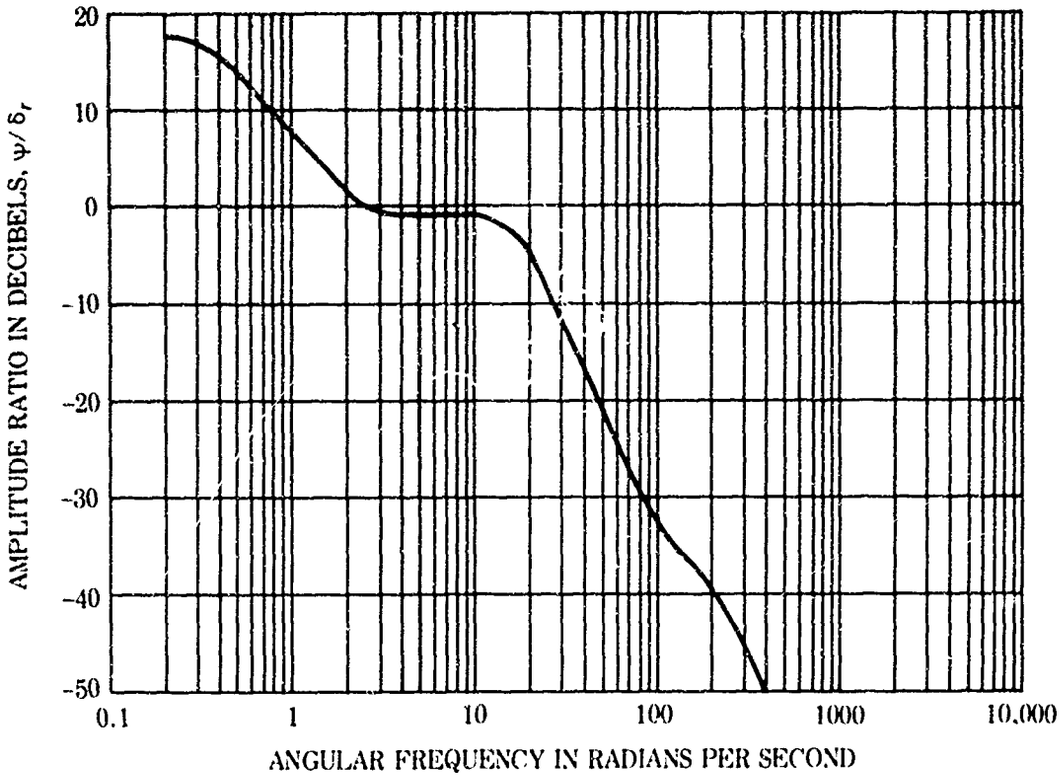

Figure B-5. Yaw angle – rudder angle; $C_{\ell\beta}$

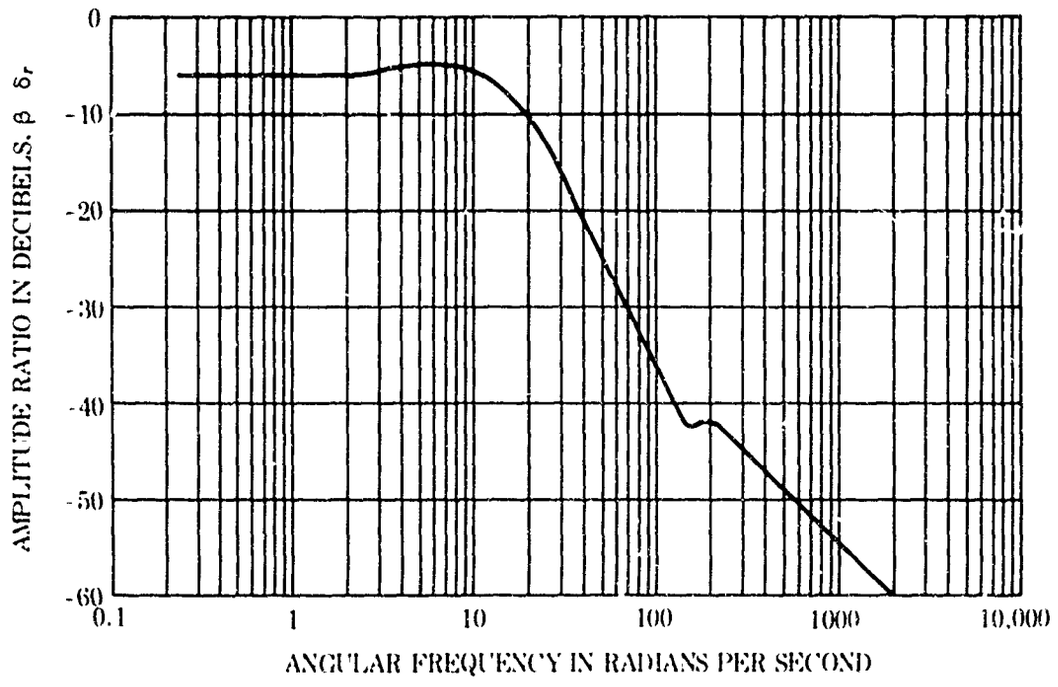

Figure B-6. Side-slip angle – rudder angle, $C_{\ell\beta}$

REVERSE SIDE BLANK

APPENDIX C: BODY I TRANSFER FUNCTIONS

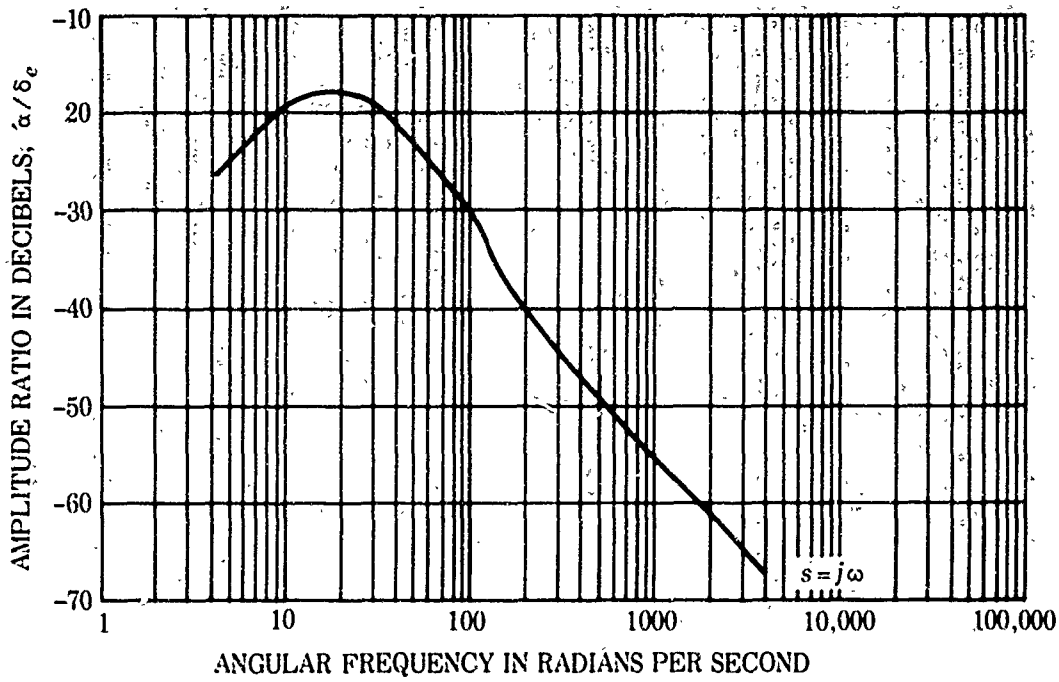

Figure C-1. Angle of attack – elevator angle; tow point 1 ft above C.G.

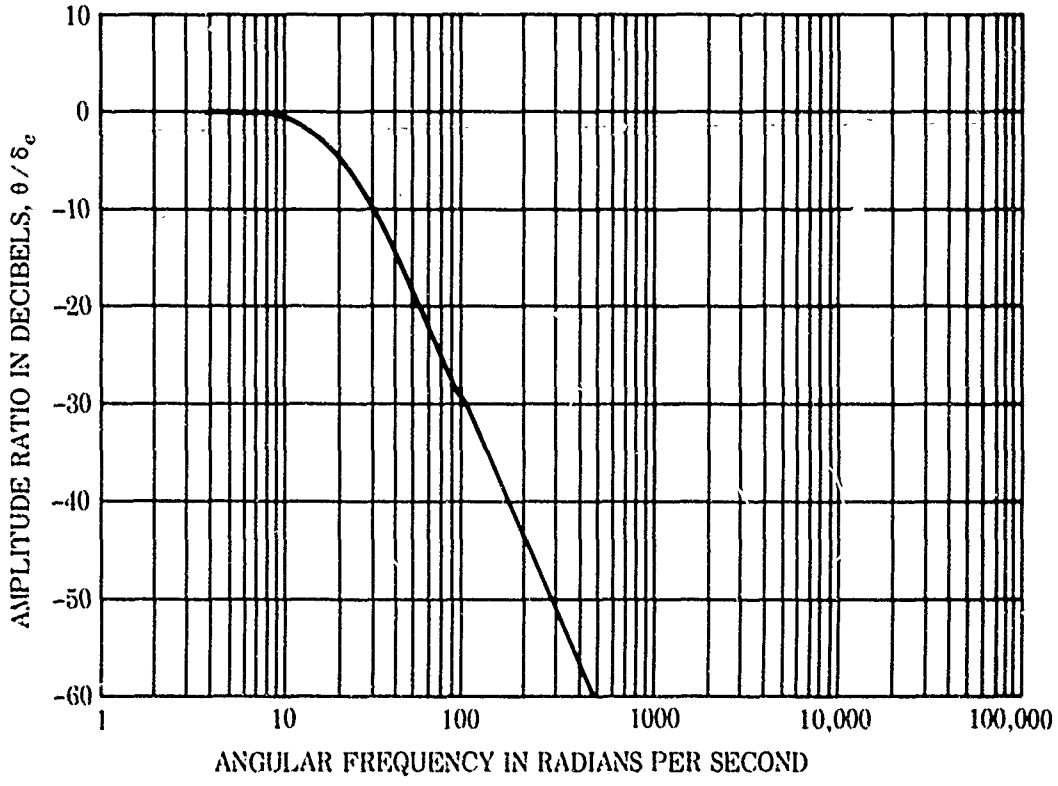

Figure C-2. Body attitude angle – elevator angle; tow point 1 ft above C.G.

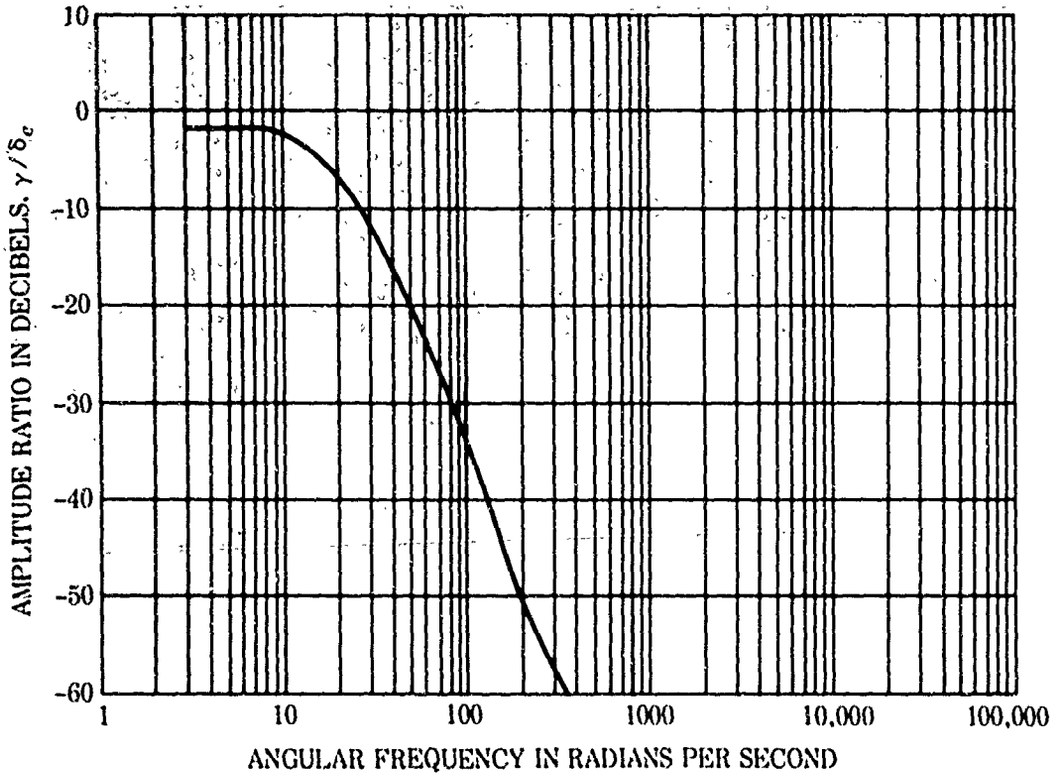

Figure C-3. Path angle – elevator angle; tow point 1 ft above C.G.

UNCLASSIFIED
Security Classification

DOCUMENT CONTROL DATA - R & D

Security classification of title, body of abstract and indexing annotation must be entered when the overall report is classified)

1 ORIGINATING ACTIVITY (Corporate author) Navy Electronics Laboratory San Diego, California 92152	2a. REPORT SECURITY CLASSIFICATION UNCLASSIFIED 2b. GROUP

3 REPORT TITLE

CABLE-TOWED UNDERWATER BODY DESIGN

4) DESCRIPTIVE NOTES (Type of report and inclusive dates)

Research and Development Report September 1965 - December 1966

5 AUTHOR(S) (First name, middle initial, last name)

P.O. Laitinen

6. REPORT DATE	7a. TOTAL NO. OF PAGES	7b. NO. OF REFS
17 April 1967	94	12

8a. CONTRACT OR GRANT NO.	9a. ORIGINATOR'S REPORT NUMBER(S)
b. PROJECT NO S46-06 Task 1723 c. (NEL J60172) d.	1452 9b. OTHER REPORT NO(S) (Any other numbers that may be assigned this report)

10 DISTRIBUTION STATEMENT

Distribution of this document is unlimited

11 SUPPLEMENTARY NOTES	12 SPONSORING MILITARY ACTIVITY
	Naval Ship Systems Command Department of the Navy

13 ABSTRACT

A general design procedure was originated for towed underwater bodies, based on the longitudinal and lateral dynamics. A practical design was worked out for a specific body to be towed at 45 knots. Characteristics that have a major influence on towed underwater body design are the hydrodynamic coefficients, the damping coefficients, the body drag, the cable tension, and the cable tow-point. The attainable depth and required horsepower depend primarily on the cable, which should be of small-cross-section, laminar-flow streamlined type. Automatic longitudinal and lateral control systems are desirable.

DD FORM 1 NOV 65 1473 (PAGE 1)

S/N 0101-807-6801

UNCLASSIFIED
Security Classification

14 KEY WORDS	LINK A		LINK B		LINK C	
	ROLE	WT	ROLE	WT	ROLE	WT
Towed Bodies - Hydrodynamic Characteristics Towed Bodies - Design						